Laminin-Functionalized Polyethylene Glycol Hydrogels for Nucleus Pulposus Regeneration

by

Aubrey Therese Francisco

Department of Biomedical Engineering
Duke University

Date:_____

Approved:

_____
Lori A. Setton, Supervisor

_____
Jun Chen

_____
Stephen L. Craig

_____
Farshid Guilak

_____
Kam W. Leong

Dissertation submitted in partial fulfillment of the requirements for the degree of Doctor of Philosophy in the Department of Biomedical Engineering in the Graduate School of Duke University

2013

ABSTRACT

Laminin-Functionalized Polyethylene Glycol Hydrogels for Nucleus Pulposus Regeneration

by

Aubrey Therese Francisco

Department of Biomedical Engineering
Duke University

Date:_____
Approved:

_____
Lori A. Setton, Supervisor

_____
Jun Chen

_____
Stephen L. Craig

_____
Farshid Guilak

_____
Kam W. Leong

An abstract of a dissertation submitted in partial fulfillment of the requirements for the degree of Doctor of Philosophy in the Department of Biomedical Engineering in the Graduate School of Duke University

2013

Abstract

Intervertebral disc (IVD) disorders and age-related degeneration are believed to contribute to low back pain. There is significant interest in cell-based strategies for regenerating the nucleus pulposus (NP) region of the disc; however, few scaffolds have been evaluated for their ability to promote or maintain an immature NP cell phenotype. Additionally, while cell delivery to the pathological IVD has significant therapeutic potential for enhancing NP regeneration, the development of injectable biomaterials that retain delivered cells, promote cell survival, and maintain or promote an NP cell phenotype in vivo remains a significant challenge. Previous studies have demonstrated NP cell – laminin interactions in the NP region of the IVD that promote cell attachment and biosynthesis. These findings suggest that incorporating laminin ligands into biomaterial scaffolds for NP tissue engineering or cell delivery to the disc may be beneficial for promoting NP cell survival and phenotype. In this dissertation, laminin-111 (LM111) functionalized poly(ethylene glycol) (PEG) hydrogels were developed and evaluated as biomaterial scaffolds for cell-based NP regeneration.

Here, PEG-LM111 conjugates with functional acrylate groups for crosslinking were synthesized and characterized to allow for protein coupling to both photocrosslinkable and injectable PEG-based biomaterial scaffolds. PEG-LM111 conjugates synthesized using low ratios of PEG to LM111 were found support NP cell

attachment and signaling in a manner similar to unmodified LM111. A single PEG-LM111 conjugate was conjugated to photocrosslinkable PEG-LM111 hydrogels, and studies were performed to evaluate the effects of hydrogel formulation on immature NP cell phenotype in vitro. When primary immature porcine NP cells were seeded onto PEG-LM111 hydrogels of varying stiffnesses, softer LM111 presenting hydrogels were found to promote cell clustering and increased levels of sGAG production as compared to stiffer LM111 presenting and PEG-only gels. When cells were encapsulated in 3D gels, hydrogel formulation was found to influence NP cell metabolism and expression of proposed NP phenotypic markers, with higher expression of N-cadherin and cytokeratin 8 observed for cells cultured in softer (<1 kPa) PEG-LM111 hydrogels.

A novel, injectable PEG-LM111 hydrogel was developed as a biomaterial carrier for cell delivery to the IVD. PEG-LM111 conjugates were crosslinked via a Michael-type addition reaction upon the addition of PEG-octoacrylate and PEG-dithiol. Injectable PEG-LM111 hydrogel gelation time, mechanical properties, and ability to retain delivered cells in the IVD space were evaluated. Gelation occurred in approximately 20 minutes without an initiator, with dynamic shear moduli in the range of 0.9 – 1.4 kPa. Primary NP cell retention in cultured IVD explants was significantly higher over 14 days when cells were delivered within a PEG-LM111 hydrogel carrier, as compared to cells in liquid suspension.

The studies presented in this dissertation demonstrate that soft, LM111 functionalized hydrogels may promote or maintain the expression of specific markers and cell-cell interactions characteristic of an immature NP cell phenotype. Furthermore, these findings suggest that this novel, injectable laminin-functionalized biomaterial may be an easy to use and biocompatible carrier for delivering cells to the IVD.

Dedication

To my mother, for her unparalleled love and encouragement, and for instilling in me both an inquisitive spirit and a passion for improving the lives of others. And to my father, for teaching me to always consider the big picture, and for being a constant source of strength and calm during this sometimes trying journey.

Contents

List of Tables

List of Figures

Acknowledgements

The completion of dissertation would not have been possible without the contributions of numerous individuals. First, I would like to thank my advisor, Dr. Lori Setton, for her guidance and support, both professional and personal. I am thankful for her insight, constructive criticism, knowledge and patience. My time spent under Dr. Setton's direction allowed me to develop as a researcher, mentor, and collaborator, and I am grateful to have had to opportunity to work with her. I would also like to appreciatively acknowledge and thank my committee members, Dr. Jun Chen, Dr. Stephen Craig, Dr. Farshid Guilak, and Dr. Kam Leong, for their helpful guidance and for sharing their enthusiasm for this work.

I have had the privilege to collaborate with an incredible group of talented individuals, who provided significant effort and intellectual contributions towards this work. I'd like to thank Dr. Robby Bowles for his assistance with all bioluminescence imaging aspects of the studies contained herein, and for his willingness to continually lend his expertise and advice. Jonathan Brunger was instrumental in the successful generation of luciferase expressing primary NP cells for cell tracking experiments, and I am extremely grateful for his efforts. I would also like to thank Robert Mancino for his assistance with mechanical testing and organ culture studies. Priscilla Hwang, Dr. Claire Jeong and Liufang Jing also provided valuable contributions to this work, for which I am very thankful. Finally, I'd like to express my appreciation for the

contributions of several colleagues who assisted with in vivo experiments, including Dr. Yi-Te Chen, Steve Johnson, David Tainter, and Devin Bridgen.

I am grateful for the advice, encouragement and support provided by both former and present members of the Setton lab. Dr. Chris Gilchrist, who laid the groundwork for our labs interest in developing laminin-functionalized biomaterials, has been an incredible source of personal and professional encouragement throughout my time at Duke. I have also gained a great deal from my interactions with Dr. Michael Sinclair, Tim Mwangi, Dr. Kyle Allen, Dr. Isaac Karikari, and Dr. Dana Nettles, who have all graciously offered their advice, support and expertise.

Lastly, I'd like to express my deepest appreciation for the love, strength and encouragement I have received from so many family members and friends throughout my graduate career, particularly during this past year of unforeseen challenges. I am forever grateful for the understanding and support from my parents, Don and Therese, my sisters, Brianne and Bridget, and my fiancé, Eric.

1. Introduction

The human intervertebral disc (IVD) is a fibrocartilaginous tissue that undergoes significant changes in cell population, matrix composition and structure during growth, and with aging-related degeneration. IVD disorders including herniation, stenosis, spondylolysis, and degeneration resulted in more than 663,000 inpatients stays for back surgery or other back disorder treatments in the US in 2008 alone, costing more than $9.5 billion and making back problems the ninth most expensive condition treated in US hospitals [1] . IVD degeneration is associated with a loss of disc height and hydration, diminished blood supply in the endplates, and anulus fibrosus (AF) tears [2-4]. Current therapies for treating disc degeneration include conservative non-surgical approaches and surgical intervention such as discectomy, spinal fusion, and total disc replacement; however, these therapies do not restore the structure and function of the native IVD.

Disc degeneration is believed to originate in the nucleus pulposus (NP) region of the disc [4]; therefore, there is significant interest in tissue engineering strategies to regenerate the NP. The native NP is composed primarily of water, proteoglycans and collagen type II. Degeneration of the NP is characterized by decreased water content, decreased cellularity, loss of proteoglycans in the extracellular matrix (ECM), and increased matrix stiffness [5, 6]. Aging itself is associated with an early loss of the juvenile NP cell population that is originally derived from the embryonic notochord [7-9], and disappears from the human disc within the first decade of life. These large, highly

vacuolated [9, 10] notochordal-like NP cells organize in cell clusters [9, 11], and have been shown to produce a proteoglycan-rich matrix [12], and are therefore thought to be involved in generating and maintaining the highly hydrated NP tissue. Furthermore, these cells have been shown to secrete soluble mediators that regulate proteoglycan synthesis by other cell types [13-16]. Therefore, the aging associated loss of this notochordal-like NP cell population has been hypothesized to be a contributing factor to IVD degeneration [17], and suggests that promoting or maintaining a notochordal-like NP cell phenotype may be useful for NP tissue regeneration.

Cell-based strategies for IVD regeneration rely on three main components: an appropriate cell source, a biomaterial or scaffold, and differentiation conditions suitable for generating an NP-like matrix [18]. Strategies for NP regeneration have utilized one or more of these components, including cells cultured within scaffolds in vitro and in vivo [19-21], and cells delivered either alone or within an injectable biomaterial carrier [22]. Cell delivery alone would limit damage to the adjacent AF tissue [23], however, calcification of the cartilaginous end plates severely limits diffusion of glucose and oxygen into the disc that is believed to create a hostile extracellular environment not well suited to maintain cell viability or matrix synthesis [3, 24, 25]. Therefore, it is likely that functional regeneration of NP tissue will require an appropriate scaffold and biological signals that promote cell survival and maintain or promote an NP cell phenotype and matrix production. A variety of synthetic, natural, and composite materials have been

investigated for NP regeneration (see Section 1.4), mainly in the form of hydrogels due to the highly hydrated nature of the native NP. Unlike biomaterials for other tissue engineering applications [26, 27], few peptide and protein functionalized scaffolds to direct biological responses of NP cells have been developed [28]. Furthermore, scaffold biochemical and physical properties that promote or maintain an immature NP cell phenotype are currently unknown.

The ECM environment, including ECM ligand and mechanical stiffness, are known to be key regulators of cell behaviors such as adhesion, survival, phenotype and organization. Previous work in our laboratory suggests immature NP cells reside in an environment rich in laminin ECM proteins and that these cells highly express numerous laminin receptors as compared to cells of the adjacent AF [29-32]. Additionally, soft (< 0.7 kPa), laminin-containing basement membrane extract substrates have been shown to promote immature NP cell rounded morphology, cell-cell interactions, and proteoglycan production [33]. These findings suggest that NP cell phenotype is dependent upon both ECM ligand and mechanical properties.

The central hypothesis of this research was that a laminin presenting hydrogel scaffold with matrix elasticity similar to that of the native NP would support cell adhesion, survival and maintenance of phenotype. In the studies presented here, a poly(ethylene glycol)-laminin (PEG-LM111) conjugate with functional acrylate groups for crosslinking was synthesized and characterized (Chapter 2), to allow for protein coupling to both

photocrosslinkable and injectable PEG-based biomaterial scaffolds. PEG hydrogels were chosen since they readily allow for incorporation of biological signals derived from the native ECM [26, 34], and, due to their non-fouling properties, PEG hydrogels provide a suitable environment for studying cell-ligand interactions. Studies were conducted to evaluate the effects of photocrosslinkable hydrogel formulation, including hydrogel stiffness and laminin ligand concentration, on immature NP cell phenotype in vitro (Chapter 3). Additionally, studies were performed to examine the role of an injectable laminin functionalized hydrogel carrier in promoting cell survival and cell retention in the IVD space (Chapter 4).

1.1 Intervertebral Disc Structure and Function

The IVD is a fibrocartilaginous tissue that provides load support, flexibility and energy dissipation in the spine. The IVDs are situated between each of the cervical, thoracic and lumbar vertebral bodies of the spinal column. Each disc is comprised of three primary anatomical regions: the outer AF, the centrally located inner NP (Figure 1), and the cartilaginous endplates that are situated on top and bottom of each disc, adjacent to the vertebral bodies [35]. The hyaline cartilage endplates separate the disc from the vertebral bodies, and provide a pathway for nutrient transfer from the vascularized vertebral bodies to the avascular disc [36].

The AF is composed of highly organized collagen fibers (approximately 70% dry weight) arranged in concentric rings, or lamellae, that enclose the NP (Figure 1) [37]. Within the AF lamellae, the collagen fibers lie parallel to each other at approximately a 60°-70° angle to the axis of the spine, with each successive layer altering in fiber direction (approximately 120° to each other) [38]. The periphery of the AF attaches to the posterior longitudinal ligament and inserts into the vertebral body. Mechanically, the AF acts to resist compressive and torsional stresses, and aids in stabilizing the spine by restricting motion between adjacent vertebrae. The ECM of the AF has a low proteoglycan content compared to the NP, and is mainly composed of type I collagen, with smaller amounts of types III, V, VI, IX, and XI [39]. The outer AF consists primarily of type I collagen fibers, with increasing percentage of type II collagen towards the innermost region [40], which merges horizontally with the NP. The cells of the AF also vary from the outer to inner regions. The outer AF contains elongated fibroblast-like cells that align parallel to the collagen fibers within each concentric ring, and the inner AF, which integrates with the NP, contains more chondrocyte like cells [41]. Overall, the cell density of the AF is very low compared to other tissues, containing approximately 9×10^6 cells/cm^3 [42].

The NP is a gelatinous, highly hydrated tissue that resists compressive spinal loads and distributes them radially to the AF. With aging and degeneration, a number of biological and anatomical changes occur in the human NP (see Section 1.2). The young, healthy human NP is comprised primarily of water (70 – 90% of wet weight),

proteoglycans (65% of dry weight) and a random network of collagen fibrils dispersed throughout a proteoglycan rich ECM [40, 43]. Proteoglycans in the NP ECM contain mainly chondroitin sulphate and keratan sulphate side chains [44, 45], which play an important role in imbibing water. The high proteoglycan content of the NP ECM results in a negative fixed-charged density and a high interstitial swelling pressure. Smaller proteoglycans such as biglycan, decorin, lumican and fibromodulin are also present [46, 47]. The collagen content of the NP is mainly composed of type II collagen (15 – 20% of dry weight), and small quantities of types III, VI, IX, and XI [39]. NP cell density is very low (4×10^6 cells/cm^3) as compared to other avascular tissues such as cartilage [42]. Additionally, the NP cell population varies considerably with age. In humans, the NP is initially populated by large, vacuolated cells derived from the embryonic notochord.

These morphologically distinct NP cells disappear within the first decade of life, and are replaced by a lesser number of smaller, chondrocyte-like cells [9].

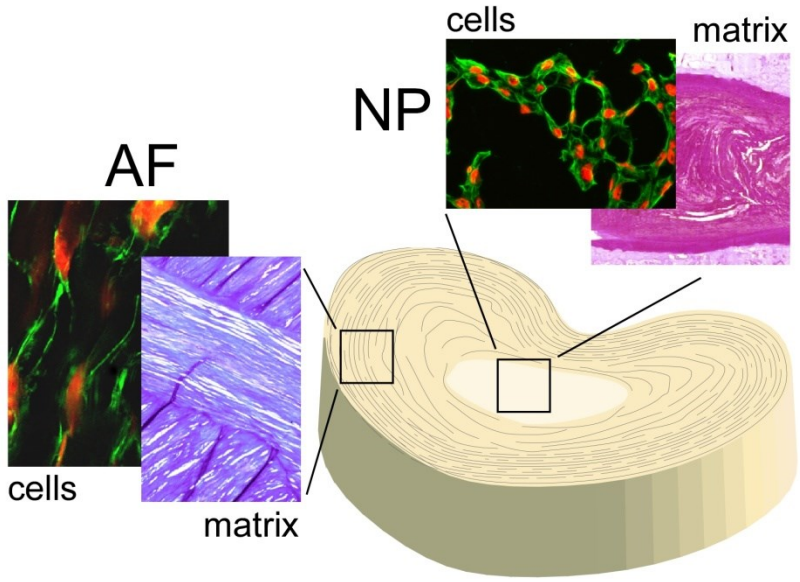

Figure 1. Matrix structure and cellular organization in the immature IVD. Cytoskeletal staining for AF (actin) and NP (vimentin) cells in immature porcine IVD tissues. Adapted from [48].

1.2 Intervertebral Disc Degeneration and Aging

Disc degeneration is complex and is still not clearly defined; however, it is thought to be a process of premature aging, since changes associated with degeneration mimic those of aging, but occur at a faster rate [49]. IVD degeneration is linked to numerous mechanical, biochemical, nutritional, and genetic factors, which can lead to an imbalance between catabolism and anabolism [50]. Non-physiological mechanical loads may initiate

or contribute to degeneration [51, 52]. Additionally, mutations in ECM proteins such as collagen types I, IX and XI, and aggrecan have been shown to correlate with IVD degeneration [53-57]. Calcification of the cartilaginous endplates limits diffusion of nutrients such as glucose and oxygen into the disc [3, 24, 58], creating an acidic and hypoxic environment that may not be well suited for maintaining high cell viability and matrix synthesis [2, 4, 59]. In addition to endplate changes, other anatomical features of disc degeneration include loss of disc height and hydration, extrusion and tears, and disc herniation [3, 4, 60]. These changes may lead to altered mechanical loading, nerve compression, spinal canal impingement and inflammation, which contribute to symptomatic back pain [61].

Disc disorders and related pain may be secondary to changes that first occur in the NP region of the IVD (Figure 2), including significant alterations in tissue cellularity, matrix composition, and structure [2-4]. Cell density decreases shortly after birth, with increasing levels of cell death in the NP with aging-related degeneration [4, 62, 63]. The biochemical composition of the NP ECM changes significantly with degeneration, and is characterized by decreased concentration of proteoglycans [2], an increase in the amount of denatured type II collagen [2, 64], and increased fibronectin content [65]. Formation of fibronectin fragments may contribute to further degeneration by downregulating aggrecan synthesis and upregulating production of matrix metalloproteinases (MMPs) [6]. Loss of proteoglycans, particularly the degradation of large aggrecan molecules [66,

67], and decreased water content leads to a decrease in the osmotic pressure, which impairs the mechanical functionality of the NP. This may result in higher compression loads being transferred to the AF, contributing to tears, cleft formation or rupture.

Figure 2. Representative images of changes in tissue hydration and composition that occur with aging and degeneration. Images courtesy of L.A. Setton.

1.3 Nucleus Pulposus Cells and Disc Degeneration

1.3.1 Notochordal Nucleus Pulposus Cell Fate

The IVD contains cells of both notochordal and mesenchymal origins that populate the NP and AF regions of the disc, respectively. During embryonic development, the notochord, a rod-like line of cells that guides development of the neural tube and the vertebral column, is surrounded and condensed by mesenchymal cells, which form the vertebrae and AF [68, 69]. The entrapped notochordal cells then take part in formation of the NP [7, 38, 69, 70]. These 'notochordal-like' NP cells synthesize a proteoglycan-rich matrix [12], and have been shown to secrete soluble mediators that

regulate proteoglycan synthesis by other cell types [13-16, 71]. These are large, highly vacuolated cells containing large glycogen deposits, and poorly developed mitochondria surrounded by rough endoplasmic reticulum [9, 63, 72, 73]. Notochordal-like cells organize in cell clusters with strong cell-cell interactions [9, 11, 73], and express cadherins (Figure 3) [73, 74]. Additionally, notochordal-like NP cells highly express cytoskeletal proteins including cytokeratins (isoforms 8, 18, 19) (Figure 3) and vimentin intermediate filaments [74-76].

In humans, notochordal-like cells disappear within the first decade of life, and are replaced by smaller, more 'chondrocyte-like' cells [38, 77]. The disappearance of this cell population coincides with changes in NP matrix biochemistry and mechanical properties that are characteristic of disc degeneration, including decreased cellularity, proteoglycan levels, and water content, as well as reduced swelling pressure, and increased matrix stiffness [3, 5, 6, 60, 78, 79]. Additionally, studies have shown that susceptibility to disc degeneration in certain breeds of dogs is linked to a decline in NP notochordal-like NP cell content [11, 13, 69, 80]. Therefore, notochordal-like cell disappearance may be an initiating or contributing factor to degenerative disc disease [17, 81]. In certain animals, such as pigs, rats, and non-chondrodystrophoid dogs, notochordal-like NP cells are retained well past the age of skeletal maturity [82], which allows for controlled *ex vivo* study of their cell biology and function.

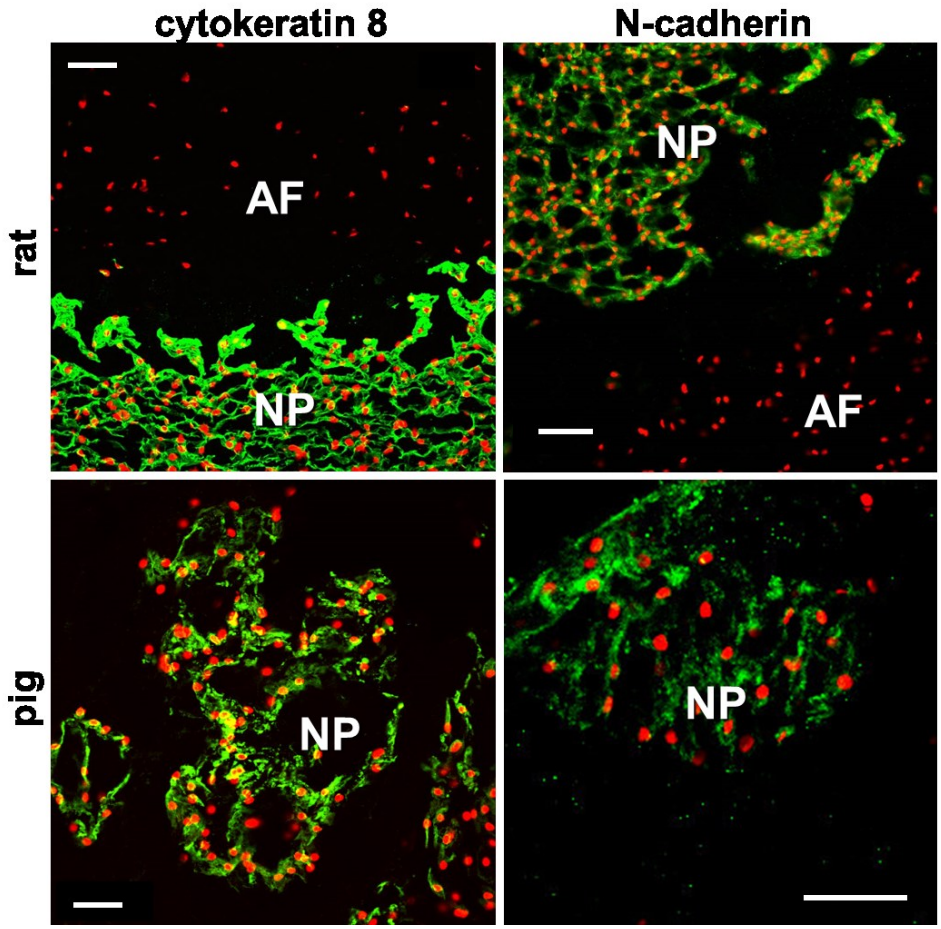

Figure 3. Expression of cytokeratin 8 (left) and N-cadherin (right) in immature rat and porcine NP tissues. Scale bar = 50 μm. Images of rat tissue immunostaining from [83].

1.3.2 Defining the Nucleus Pulposus Cell Phenotype

As discussed above, altered NP cellularity is a noteworthy feature of disc degeneration. Therefore, significant interest exists in defining the NP cell phenotype, particularly that of notochordal-like NP cells, to better inform the development of cell-based strategies for NP regeneration. Recently, numerous studies have sought to define

the NP cell phenotype by evaluating biomarker expression in immature or non-degenerate NP cells as compared to that in AF cells (Table 1) or articular chondrocytes. Notochordal-like NP cells and mature, or 'chondrocyte-like', NP cells have been shown to exhibit some similarities in gene expression profiles. Both cell types express similar levels of aggrecan, collagen II and *Sox*9, which are typical markers of a chondrogenic phenotype [84]. Notochordal-like NP cells more highly express cell-associated laminin ECM proteins and laminin receptors as compared to AF cells (Section 1.5). Other distinct expression patterns in NP cells, including higher expression of cytokeratins 8, 18 and 19, and N-cadherin (cadherin-2), have been shown to be expressed at higher levels in notochordal-like NP cells as compared to mature NP cells [85]. Overall, these studies provide useful biomarkers for understanding the transition between notochordal-like and chondrocyte-like NP cells, and for optimizing NP cell phenotype for cellular and tissue engineering therapies for treating IVD degeneration.

Table 1. Expression of proposed NP cell phenotypic markers. FC = flow cytometry; IHC = immunohistochemistry.

Marker	Species	Elevated in NP (vs. AF)	Reference
Cell surface receptor			
Integrin α6 (CD49e)	Rat, Porcine, Human	Protein (FC, IHC)	[30, 84]
Integrin α3 (CD49c)	Rat, Porcine, Human	Protein (IHC, FC)	[30]
Integrin β4 (CD104)	Rat, Porcine, Human	Protein (IHC)	[30]
Lu (BCAM, CD239))	Rat, Porcine, Human	mRNA, Protein (FC,IHC)	[30]
CD24	Rat, Human Bovine	mRNA, Protein (FC, IHC) mRNA	[86-88] [85]
CD151	Rat, Porcine, human	mRNA, Protein (FC,IHC)	[30]
CDH1 (CD324)	Human, Rat	Protein (IHC)	[73, 74]
CDH2 (CD325)	Human, Bovine, Rat	mRNA, Protein (IHC)	[73, 85]
Galectin-1	Rat, Porcine, Human	mRNA, Protein (IHC)	[88]
Syndecan 4	Rat	mRNA, Protein (Western)	[88, 89]
Cytoskeleton			
KRT8	Bovine Porcine Human	mRNA,Protein (IHC) higher for cells in clusters Protein (IHC) Protein (IHC)	[85, 90] [90] [74, 75, 91]
KRT18	Bovine Human Canine	mRNA, Protein (IHC) higher for cells in clusters mRNA, Protein (IHC) mRNA, Protein (IHC)	[85, 90] [74, 75, 91] [92]
KRT19	Rat, Bovine Human	mRNA mRNA, Protein (IHC)	[85, 87] [74, 75, 91, 93]
Vimentin	Human, Rat, Bovine Rat, Porcine	Protein (IHC, Western) mRNA	[74, 75, 91, 94]
Matrix-related protein			
Laminin α5	Rat, Porcine, Human	Protein (IHC)	[30]
Laminin γ2	Porcine	Protein (IHC)	[95]
Type II collagen	Porcine Porcine	mRNA Protein (BC, IHC)	[84] [40, 96]
Aggrecan	Porcine, Bovine	mRNA	[84, 85]

1.4 Cell Based Therapies for Treatment of Disc Degeneration

Significant interest exists in cell based therapies for treating IVD disorders, with the majority of strategies focused on regenerating or repairing the NP region of the disc as a means to impede or reverse disc degeneration. These include cells cultured with biomaterial scaffolds in vitro, delivery of cells alone, and cells delivered to the NP region of the disc within an injectable biomaterial carrier.

1.4.1 NP Cell-Biomaterial Constructs

Due to the avascular nature of the IVD, and the limited nutrient supply to the NP region of the disc, a suitable scaffold will likely be necessary for NP tissue regeneration in vivo. Both natural and composite biomaterials have been investigated for NP regeneration (Table 2), mainly in the form of hydrogels due to the fact that they approximate the gel-like properties of the native NP tissue. Few studies have examined synthetic hydrogels as potential tissue engineered scaffolds for NP regeneration; however, synthetic-natural hybrid materials are being actively investigated. A wide variety of scaffolds have shown some ability to maintain or promote a rounded NP-like cell phenotype, and to promote collagen and proteoglycan matrix generation by the entrapped cells; however, there is little agreement on the ECM composition required to achieve a functional tissue engineered NP construct.

Table 2. Representative biomaterials evaluated for NP ECM regeneration.

Scaffold Material	Cell Source(s)	Reference
Alginate	Ovine NP HNPSV-1 Bovine NP Human AF, NP Porcine AF, NP Rabbit AF, NP	[97-100] [101] [102] [103] [104] [105]
Agarose	Human AF, NP	[103]
Collagen	Human AF, NP Ovine NP	[103] [106]
Fibrin Gel	Human AF, NP	[103, 107]
Atelocollagen	Bovine NP HNPSV-1 Rabbit MSCs	[108] [101] [109]
Carboxymethylcellulose	Bovine NP	[110]
Hyaluronan	Rat MSCs Human MSCs	[111] [112]
Hyaluronan/elastin-like polypeptide	Human IVD	[113]
Hyaluronan-poly(N-isopropylacrylamide)	Human MSCs	[114, 115]
Chitosan	Bovine NP, AF Human MSCs	[116] [117, 118]
Collagen type II/Polyethylene glycol/Hyaluronan	Human ADSCs	[119]
Collagen/hyaluronan	Bovine AF, NP	[120]
Fibrin/hyaluronan	Porcine NP	[121]
Calcium Polyphosphate	Bovine NP	[122]
Polyethylene glycol	Human MSCs	[123]
Gelatin/Chondroitin-6 Sulfate/Hyaluronan	Human NP	[124]
Small Intestinal Submucosa	Human AF, NP	[125]
Decellularized Porcine NP Tissue	Human ADSCs	[126, 127]

Naturally derived materials such as hyaluronan, collagen, alginate, chitosan, carboxymethylcellulose and agarose have all been studied as potential scaffolds for NP

tissue engineering since they are components of or have macromolecular properties similar to the natural ECM [128]. The use of chitosan was investigated in a study by Roughley and coworkers, in which chitosan was crosslinked by glycerophosphate in the presence of hydroxyethyl cellulose [116]. Results showed that bovine NP cells were able to proliferate and retain almost 75% of sGAG produced by the cells over 20 days in culture; however sGAG levels achieved were only approximately 10% of that found in the native bovine NP, and proteoglycan production eventually diminished. One limitation of using naturally derived materials is that their physical properties can not be easily controlled. Therefore, researchers have modified natural polymers to contain functional groups that allow for photopolymerization. Since alginate has been shown to maintain a rounded NP-like cell morphology in culture, Chou and coworkers attempted to overcome its lack of mechanical integrity by modifying alginate to contain methacrylate groups for photocrosslinking [102]. Although increasing the degree of methacrylation did lead to increased gel modulus, cell viability decreased. Reza and coworkers utilized similar chemical methods to develop hydrogels with tunable mechanical properties by methacrylating carboxymethylcellulose, and showed that specific formulations promoted a rounded cell phenotype and pericellular proteoglycan deposition [110], suggesting maintenance of NP cell phenotype.

As an alternative to naturally derived biopolymers, tissue-based scaffolds have also been generated for a variety of tissue engineering applications by decellularizing

xenogenic or allogenic tissues. Le Visage and coworkers utilized porcine small intestine submucosa, which is primarily made up of collagen type I, GAGs and growth factors, as a bioactive scaffold for culturing human disc cells obtained from degenerated discs [125]. Results showed that over 3 months in standard cell culture conditions, the cells were able to migrate into the scaffold, where they remained and synthesized sGAG. Tissue-based scaffolds formed from the host-tissues themselves may be advantageous in directing cells to generate appropriate matrix molecules, since the scaffolds already contain the appropriate ECM composition, architecture and biological signals. Recently, a biomimetic acellular porcine NP hydrogel was developed [127] and reported to promote proteoglycan and collagen deposition, and ECM remodeling [126].

1.4.2 Injectable Biomaterials for Cell Delivery

Although NP tissue engineered scaffolds grown in vitro before being implanted into the disc space are advantageous in that cells would be able to generate appropriate ECM in a controlled, favorable environment, implanting the scaffold would cause significant damage to the AF. Cell delivery to the disc space via injection would limit damage to the adjacent AF tissue; however, calcification of the cartilaginous end plates severely limits diffusion of glucose and oxygen into the disc, creating a hostile extracellular environment not well suited to maintain cell viability or promote matrix synthesis. Additionally, a recent study of mesenchymal stem cells (MSCs) delivered to rabbit IVDs raised concern that delivered cells can migrate out of the nucleus and induce

undesirable osteophyte formation [129]. Therefore, it is likely that functional regeneration of NP tissue via cells delivered to the disc space will require an appropriate biomaterial carrier to retain cells in the IVD space and to promote NP cell survival and phenotype.

Cell delivery to the IVD has been performed in animal models for IVD regeneration both with and without the use of a biomaterial carrier, and shown that reinsertion of autologous disc cells or stem cells delays degeneration in experimental models of degeneration [111, 130-134]. Ganey and colleagues studied a canine model, in which autologous disc cells were delivered without any carrier matrix to injured discs, and showed significantly better maintenance of disc height and structure in dogs receiving transplants as compared to controls [130]. Meisel and colleagues have brought autologous disc cell transplantation to clinical study, comparing safety and efficacy of cell transplantation plus discectomy with discectomy alone [135]. Although these studies have shown some maintenance of disc height and reduction in patient pain compared to discectomy alone, it is thought that a biomaterial carrier will improve cell retention and survival in the disc space, and may lead to the generation of new matrix. A study by Bertram and colleagues provided strong evidence for this, in which luciferase expressing cells were injected into a nucleotomized rabbit disc space either in media or within a two component fibrin matrix that polymerizes upon injection in to the disc space [136]. Results showed that approximately 30-50% of the cells injected within the fibrin biomaterial remained 30 minutes after injection, whereas media injected cells were rapidly lost from

the disc space. While the fibrin carrier improved efficiency of cell delivery to the disc space, it may not be the ideal biomaterial for generating an NP-like matrix. Crevensten and colleagues isolated bone marrow derived MSCs, stained the cells with a CM-DiI membrane stain and delivered them into rat coccygeal discs with a hyaluronan carrier [111]. Results showed the injected cells survived and proliferated, and could be detected within the disc space over the 28-day period; however, there was a marked decrease in cell number over the first 7 days in culture. In a more recent study by Sakai and colleagues [109], autologous MSCs were transplanted from bone marrow into a rabbit model of disc degeneration within an atelocollagen carrier. Results showed that 24 weeks post MSC-transplantation, degenerated discs that received MSCs regained a disc height of approximately 91%, as compared to about 67% for the sham operated group. Additionally, X-gal staining for LacZ expressing transplanted MSCs showed increased staining at 24 weeks as compared to 2 weeks, suggesting that injected cells survived and proliferation within the disc space. Since this study did not include a control group of cells without biomaterial, it is not clear exactly what therapeutic role was played by the atelocollagen carrier; however, these results combined with previous findings [101] suggests that an atelocollagen carrier may help promote an NP-like phenotype.

For detecting cells within the region of interest at various time points, much of the work using animal models of disc degeneration has relied on histological techniques subsequent to animal sacrifice at specific time-points, which precludes in vivo assessment

and longitudinal tracking of cell therapy. To address this, Saldanha and colleagues labeled MSCs with iron oxide particles, delivered the cells within a fibrin gel to the rat IVD, and demonstrated initial detection of the transplanted cell population via magnetic resonance imaging (MRI) [123]. Although in vivo longitudinal cell tracking was not performed, this study introduced a new technique that may be useful for evaluating biomaterial carriers' ability to promote cell survival and retention at the injection site. More recently, luciferase expressing porcine MSCs were delivered within a fibrin matrix to the disc space of minipigs following partial nucleotomy to assess the persistence and activity of delivered cells [137]. Results demonstrated that only 7% of the injected cells could be detected 3 days post injection, suggesting a need for improved biomaterial carriers and increasing focus on anulus reconstruction to reduce cell loss following delivery.

Towards developing improved injectable carriers, a number of groups have modified natural materials and created hybrid natural-synthetic materials to obtain greater control over material properties. Halloran and coworkers compared uncrosslinked atelocollagen to enzymatically crosslinked, atelocollagen type II based scaffolds containing varying concentrations of aggrecan and hyaluronan [108]. Bovine NP cells were cultured within the scaffolds in vitro for 7 days, with results showing that crosslinking did not reduce cell viability and improved proteoglycan retention within the scaffolds when compared to uncrosslinked atelocollagen. The authors did not assess the effects of crosslinking on gelation time, which is an important parameter to control in

order to prevent cells from leaking back out through the injection site following delivery. An injectable biomaterial for NP regeneration was recently developed in which type II collagen was crosslinked with a 4-arm PEG derivative, enriched with hyaluronan and used to entrap adipose derived stem cells (ADSCs) [119]. Gelation occurred in less than 10 minutes under physiological conditions, and NP cell viability remained high (>80%) over 14 days in culture. In another recent study, Peroglio and colleagues developed injectable, thermoreversible hyaluronan-based hydrogels for NP cell encapsulation and showed that the materials gelled upon heating to approximately 30°C [114]. Short term in vitro studies demonstrated that scaffolds could induce human MSC differentiation towards the disc phenotype [115]. Although these studies represent steps towards the development of novel injectable biomaterials for cell delivery, additional in vitro studies are needed to further investigate cell phenotype and matrix production within these biomaterials, as well as in vivo studies to assess their ability to promote NP cell retention and survival in the disc space.

1.5 Laminins and the Intervertebral Disc

It is well-known that ECM proteins play an important role in regulating cellular functions. Laminins are cross-shaped heterotrimeric ECM proteins consisting of α, β, and γ polypeptide chains (Figure 4) that form at least 15 different known laminin isoforms, with expression profiles varying significantly between tissue types and developmental

stages [138]. Laminins mediate matrix assembly and a number of cellular functions including adhesion, survival, migration and differentiation [138, 139]. Cellular interactions with laminins are mediated via integrin receptors including α3β1, α6β1, α7β1, α6β4 and α1β1, and non-integrin-type receptors, such as Lutheran (CD239), syndecans, α-dystroglycan and tetraspanin (CD151) [138, 140-142].

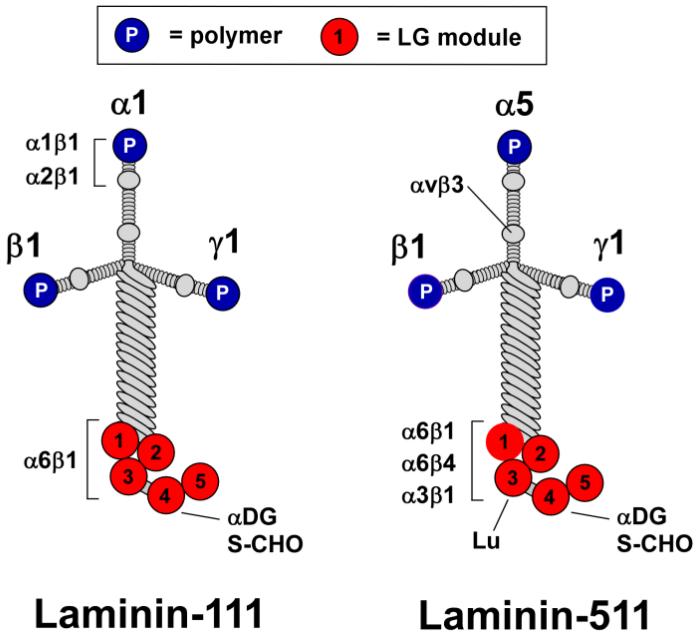

Figure 4. Structure and ligand binding regions of laminin-111 and -511 isoforms. Image adapted from [138]. Laminin receptor binding and cleavage information from [138, 140, 143].

Cell attachment to laminins directs many cellular processes. Numerous groups have demonstrated that laminins and their receptors, particularly integrins α6β1 and α6β4, contribute to the invasive phenotype and survival of carcinoma cells [144-148]. Laminin-511 (LM511) has been shown to promote endothelial cell adhesion and migration

[149], and reported effects of laminin-111 (LM111) include cell proliferation, and induction or maintenance of the differentiated state [139]. Laminins also induce stem cell differentiation into different cell lineages. LM111 induces neurite outgrowth in human MSCs [150], and has been shown to regulate neural differentiation of human embryonic stem cells [151]. Finally, Battista and coworkers demonstrated that LM111 increased the ability of embryonic stem cells to differentiate into cardiomyocytes [152]. These findings suggest that laminins play an important role in regulating and directing cell phenotype, and may be able to direct stem cell differentiation.

Previous studies have demonstrated NP cell – laminin interactions unique to the immature NP region of the disc, suggesting that laminins may be important contributors to region-specific IVD biology [30-32, 46]. Immunohistochemistry results demonstrated higher expression levels of the laminin α5 and γ1 chains in immature porcine and rat NP tissues (Figure 5), as well as in juvenile human NP tissues, as compared to AF tissues [30, 95]. Furthermore, a number of laminin receptors (integrin α3, α6, β4 subunits, as well as non-integrin receptors Lutheran (CD239) and tetraspanin (CD151)) have been shown to be uniquely expressed in immature NP tissues [30-32]. Strong expression of integrins α6 and β4, and CD239 was observed for immature porcine and rat NP tissues. Expression patterns varied slightly for immature (12-year-old) human IVD tissues, which more highly expressed integrins α3 and β1 [30]. Together these findings indicate that both

laminins and receptors which mediate cellular interactions with laminins are distinctly expressed in the NP region of the immature IVD.

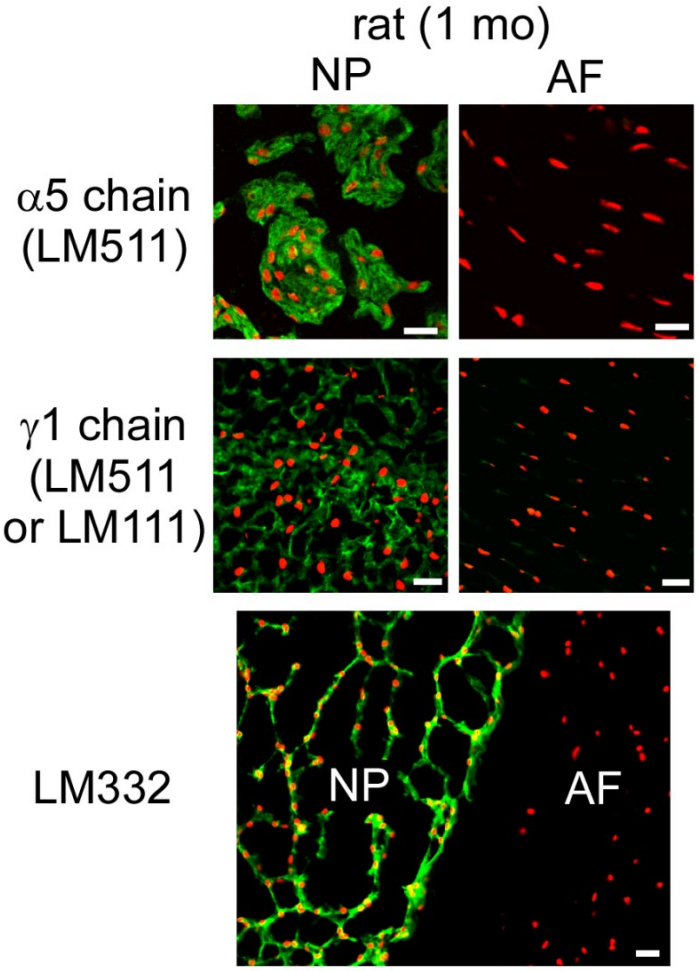

Figure 5. Expression of laminin α5 (LM511) and γ1 chains (LM511 or LM111) and LM332 in immature rat IVD tissue (1 month old). Green = laminin; Red = cell nuclei. Scale bars = 50 μm. Image adapted from [83].

Immature NP cell adhesion to LM111 was found to be mediated by the α6 integrin subunit, particularly for larger, notochordal-like cells [31]. This finding differs from a

study of human IVD cell interactions with ECM proteins, which identified integrin subunits $\alpha 3$, $\alpha 5$ and $\alpha 1$ as key mediators of human NP cell adhesion to LM111 [29]. Additional studies have shown that porcine NP cells adhere in higher numbers to laminins (LM111, LM511, and LM332) as compared to cells from the adjacent AF (Figure 6). Furthermore, NP cells spread more on and attached with greater strength of adhesion to laminins, particularly LM332 and LM511 isoforms, as compared to collagen II or fibronectin [95]. Overall, these findings demonstrate that laminin and laminin receptor expression identified in immature NP tissues translates to functional NP cell adhesion behaviors.

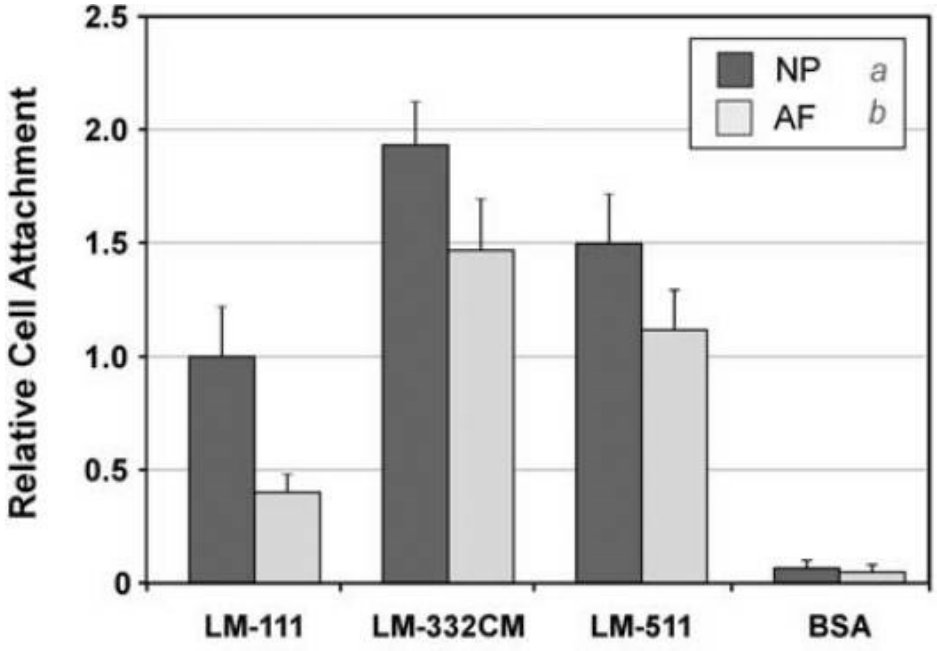

Figure 6. Primary porcine NP and AF cell adhesion to LM111, LM332 and LM511 isoforms. NP cells were found to attach to laminin substrates at significantly higher numbers as compared to AF cells ($p<0.01$. Image from [95].

In addition to evaluating notochordal-like NP cell adhesion to ECM ligands, previous studies in our laboratory have investigated the role of substrate stiffness in regulating NP cell behaviors. It is well known that substrate elasticity plays an important role in modulating cell adhesion, spreading, motility, and phenotype [153-155]. For primary notochordal-like NP cells cultured on substrates of varying stiffnesses and ligand presentation in vitro, soft, laminin-rich basement membrane extract (BME) substrates were found to promote cell-cell interactions and formation of multi-cell clusters similar to those observed in situ (Figure 7) [33]. Furthermore, NP cells cultured on soft BME substrates produced significantly more sGAG as compared to cells cultured on rigid BME

or collagen II presenting substrates. Together these findings demonstrate that NP cell organization and phenotype is dependent upon both substrate stiffness and ECM ligand.

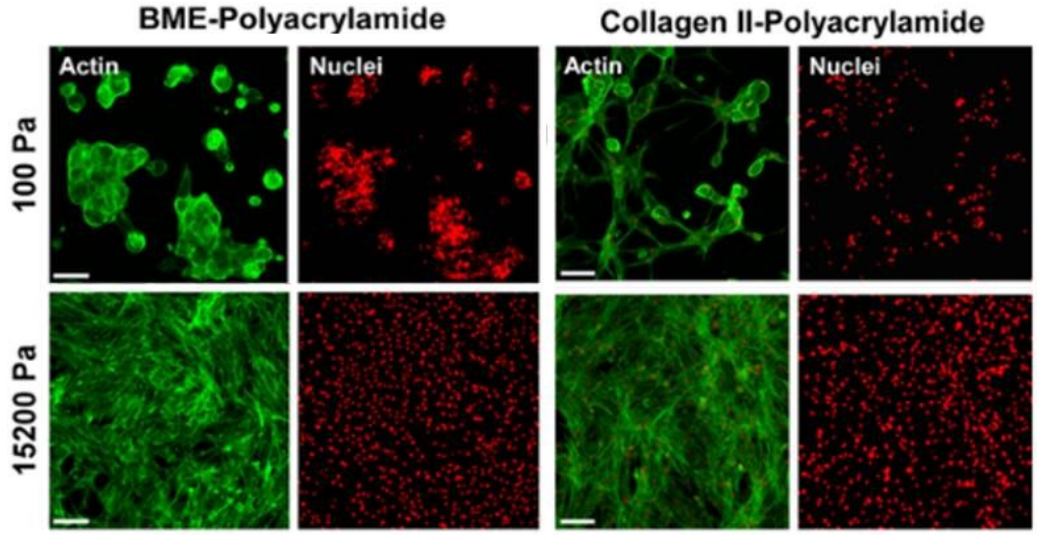

Figure 7. NP cell organization and morphology on soft (100 Pa, top row) or stiff (15200 Pa, bottom row) polyacrylamide gels functionalized with either laminin-rich BME or Collagen II. Green = actin. Red = cell nuclei. Image adapted from [33].

1.6 Protein Functionalized Poly(ethylene glycol) Scaffolds

PEG has been widely used in drug delivery [156, 157] and tissue engineering applications [26, 128, 158] since it is biologically inert and can be coupled directly to bioactive peptides and proteins. Due to its non-fouling and tunable mechanical properties, PEG provides a suitable environment for studying ECM ligand and matrix stiffness effects on cell behavior. Therefore, full length ECM proteins such as collagen

[159, 160], fibrinogen [159, 161], and laminin [162], and numerous growth factors [163-166] have been incorporated into PEG hydrogels for controlled study of the effect of biochemical and mechanical cues on cell behavior.

Seliktar and coworkers developed photocrosslinkable PEG-fibrinogen hydrogels via a two-step synthesis process in which fibrinogen was denatured to expose free thiols for conjugating the protein to PEG-diacrylate (PEG-DA) [161]. PEGylated fibrinogen was then crosslinked upon the addition of PEG-DA and exposure to UV light to form proteolytically degradable hydrogels with elastic moduli dependent on the molecular weight of the PEG constituent and the total weight percent polymer. PEG-fibrinogen scaffold composition was shown to affect smooth muscle cell morphology and migration. Additionally, PEG-fibrinogen scaffold physical properties were found to influence contraction of cardiomyocytes [167] and smooth muscle cell spreading and remodeling [168]. PEG-collagen I and PEG-albumin hydrogels were synthesized in a similar manner, and were shown to sustain both cell adhesion and proteolytic degradation [159]. Overall, these findings demonstrate the use of Michael-type addition reactions between various proteins and PEG to form biosynthetic materials that emulate the biochemical characteristics of the native ECM with added control over scaffold physical properties.

Since free thiol groups are rarely present in native non-denatured proteins, bioactive hydrogels are most commonly synthesized by PEG-N-hydroxysuccinimide ester coupling to free amino groups of lysine residues within ECM proteins or peptides [34]. In

this manner, Willits and coworkers synthesized PEG-collagen I and PEG-laminin conjugates, and crosslinked conjugates upon addition of PEG-DA and exposure to UV light [160, 162]. Laminin conjugation to PEG hydrogels resulted in improved dorsal root ganglia neurite extension in hydrogels of varying stiffnesses [162]. Together, these findings illustrate the use of protein functionalized PEG hydrogels for controlled in vitro study of ECM ligand presentation and matrix stiffness on cell behaviors.

2. Photocrosslinked PEG-LM111 Hydrogel Synthesis and Characterization

2.1 Introduction

It is widely known that ECM protein composition and matrix elasticity play important roles in regulating cellular function. Previous studies in our laboratory have demonstrated NP cell – laminin interactions that are unique to the immature disc, suggesting that laminins may be important contributors to NP-specific cell biology. Immunohistochemistry and flow cytometry results demonstrated higher expression levels of the laminin α5 and γ1 chains, laminin receptors (integrin α3, α6, β4 subunits, CD239), and related binding proteins in NP cells as compared to cells from the adjacent AF [30-32]. Additional studies have shown that soft, laminin–rich BME substrates promote immature NP cell morphology, cell-cell interactions, and proteoglycan synthesis for cells of the NP [33]. Finally, immature porcine NP cells adhere to laminins in higher numbers as compared to cells from the adjacent AF [95]. These findings provide support for known interactions between immature NP cells and multiple laminin isoforms that regulate NP cell biology, and motivate our interested in developing a LM111 functionalized hydrogel with tunable mechanical properties.

PEG hydrogels have been widely used in tissue engineering applications since they are biocompatible, hydrophilic polymers that readily allow for incorporation of biological signals derived from the native ECM [128]. The non-fouling nature of PEG, combined with its tunable mechanical properties, allows for control over biological signal

presentation and hydrogel stiffness. Therefore, full length ECM-derived proteins, including collagen, fibrinogen and laminin, have been covalently coupled to PEG hydrogels for a variety of tissue engineering applications and shown to influence cell behavior in both 2D and 3D [34, 162, 168, 169].

The objective of this work was to develop a LM111-functionalized PEG hydrogel suitable for evaluating the effects of hydrogel stiffness and LM111 concentration on NP cell phenotype in vitro. We describe here the synthesis and characterization of multiple PEGylated LM111 (PEG-LM111) conjugates with functional acrylates for crosslinking, and subsequent hydrogel formation upon the addition of PEG-DA and exposure to UV light. The effect of degree of LM111 modification on PEG-LM111 conjugate bioactivity and protein incorporation into PEG-LM111 hydrogels was evaluated. Based on these findings, a single PEG-LM111 conjugate was chosen and evaluated for its ability to promote NP cell survival within 3D photocrosslinked PEG-based hydrogels.

2.2. Materials and Methods

2.2.1 PEG-Laminin (PEG-LM111) Conjugate Synthesis

Laminin-111 (LM111, Trevigen®, Gaithersburg, MD) was PEGylated with acrylate-PEG-N-hydroxysuccinimide (Ac-PEG-NHS, MW = 10kDa, Creative PEGworks, Winston Salem, NC) to introduce functional acrylate groups for crosslinking. LM111 was dialyzed into a 0.1M sodium bicarbonate buffer, pH 8.5, and diluted to a concentration of

2 mg/ml. Ac-PEG-NHS was solubilized in ice cold 0.1M sodium bicarbonate buffer and added to LM111 solution at 10:1, 25:1, 100:1 or 500:1 molar ratio of Ac-PEG-NHS to LM111. Reactions were carried out for two hours at room temperature. Precursor PEG-LM111 conjugate solutions were dialyzed against 1x PBS to remove any unreacted Ac-PEG-NHS. LM111 concentration in each PEG-LM111 conjugate precursor solution was determined by measuring the absorbance at 280 nm, and conjugates were stored at -80°C until further use.

2.2.2 Degree of LM111 Modification

A TNBS (2,4,6-trinitrobenzene sulfonic acid) assay [170] was modified to measure the free amino groups in each PEG-LM111 conjugate compared to unmodified protein, and to estimate the degree of modification due to Ac-PEG-NHS substitution. Each PEG-LM111 conjugate and unmodified LM111 were diluted to 500 μg/ml in PBS, which was determined to be within the linear range for LM111 using this assay. TNBS was diluted to 0.01% in 0.1M sodium bicarbonate buffer, pH 8.5. Samples (PEG-LM111 conjugates or LM111) were mixed with 0.01% TNBS at a 1:1 ratio by volume, and incubated for 30 minutes at 60°C. Absorbance was measured at 340 nm using a microplate reader (Enspire, PerkinElmer, Waltham, MA) and used to calculate degree of modification (%): 100 x {1 – ((A340 PEG-LM111)/(A340 LM111))}. An ANOVA was performed to analyze degree of

modification, using Tukey's post hoc test ($p<0.01$, $n=3$) to detect differences between PEG-LM111 conjugates synthesized with different Ac-PEG-NHS to LM111 ratios.

2.2.3 Cell Isolation and Culture

Cells isolated from the porcine NP have a unique notochordal-like phenotype, and were therefore used to evaluate both PEG-LM111 conjugate bioactivity and for in vitro and in vivo cell delivery experiments. Lumbar spines were obtained from pigs shortly after sacrifice (L1–L5, 4-7 months, Nahunta Pork Outlet, Raleigh NC). Cells were isolated from the NP regions of IVDs by enzymatic digestion [171] and cultured in monolayer for 3 – 7 days in culture media (Ham's F-12 media supplemented with 10% fetal bovine serum (FBS), 10 mM HEPES, 100 U/ml penicillin, and 100 U/ml streptomycin) prior to experiments. For control studies, cells from a lung epithelial cell line (WI26VA4, ATCC No. CCL-95-1) were cultured in monolayer (37°C, 5% CO2, 20% O2) with media changes every 3-4 days (Dulbecco's Modified Eagle's Medium supplemented with 10% FBS, 10 mM HEPES) prior to experiments.

2.2.4 PEG-LM111 Conjugate Bioactivity in 2D

To evaluate cell attachment to PEG-LM111 conjugates, wells of 96-well plates were coated with PEG-LM111 conjugates synthesized with various ratios of Ac-PEG-NHS to LM111 at 5, 10, and 25 μg/ml LM111 by overnight incubation at 4°C. Coated wells were blocked with 3.75% bovine serum albumin (BSA) for 3 hours at 37°C to prevent non-specific adhesion. LM111 coated wells and BSA only coated wells were used as positive

and negative controls, respectively. Porcine NP cells in monolayer were detached using trypsin/EDTA, washed with trypsin neutralizing solution and resuspended in serum free media. Cells (4000 cells/well) were allowed to adhere to the LM111 and PEG-LM111 conjugate coated surfaces for 2 hours at 37°C. Wells were rinsed with serum free media to remove non-adherent cells, and the number of adherent cells per well was determined using CellTiterGlo® (Promega Corporation, Madison, WI) luminescent cell viability reagent. Differences in attachment numbers to PEG-LM111 conjugates at 25 μg/ml LM111 were detected via ANOVA with Tukey's post hoc test ($p < 0.05$, $n=3$ separate cell isolations).

To determine if PEG-LM111 conjugate maintains the ability to induce ERK activation upon cell adhesion, wells of 6-well tissue culture plates were coated by overnight incubation at 4°C with 20 μg/ml LM111 or PEG-LM111 that had been PEGylated at the highest ratio of Ac-PEG-NHS shown to promote cell attachment at levels similar to native protein. All wells were blocked with 3.75% BSA to prevent non-specific adhesion. Cells from a lung epithelial cell line WI26VA4 (ATCC No. CCL-95-1) that had been cultured to confluence, then serum deprived for 24 hours, were seeded onto LM111 or PEG-LM111 conjugate coated surfaces (500,000 cells/well). WI26VA4 cells cultured in suspension served as negative controls. After 30 and 60 minutes, cells were lysed with ice cold cell lysis buffer containing protease and phosphatase inhibitors (RIPA, Cell Signaling Technologies, Danvers, MA), spun down at 4°C, and cell lysates were stored at -80°C.

Total protein concentration in each of the cell lysates was determined using the BCA Protein Assay (Thermo Scientific, Waltham, MA). All lysates were diluted in cell lysis buffer to equal concentrations of total protein and a phospho-ERK ELISA (Cell Signaling Technologies) was used to detect relative levels of phosphorylated ERK.

2.2.5 Photocrosslinked PEG-LM111 Hydrogel Preparation

PEG-LM111 hydrogels were formed by mixing PEG-LM111 conjugate with additional PEG-diacrylate (PEG-DA), and crosslinking via exposure to UV light (Figure 8). Briefly, PEG-DA (10kDa, Creative PEGworks) was weighed, sterilized by exposure to UV light (265nm) for 30 minutes, and transferred to sterile eppendorf tubes. To form PEG-LM111 hydrogels, varying amounts of PEG-LM111 conjugate (0 – 1000 μg/ml) and 10 kDa PEG-DA (2 – 10% (w/v)) were mixed, injected into custom molds [172] using a 22 gauge needle and 1 ml syringe and polymerized upon 5minute exposure to UV light (3-4 mW/cm2) in the presence of 0.1% (w/v) photoinitiator (Irgacure 2959®, Ciba Speciality Chemicals, Tarrytown, NY).

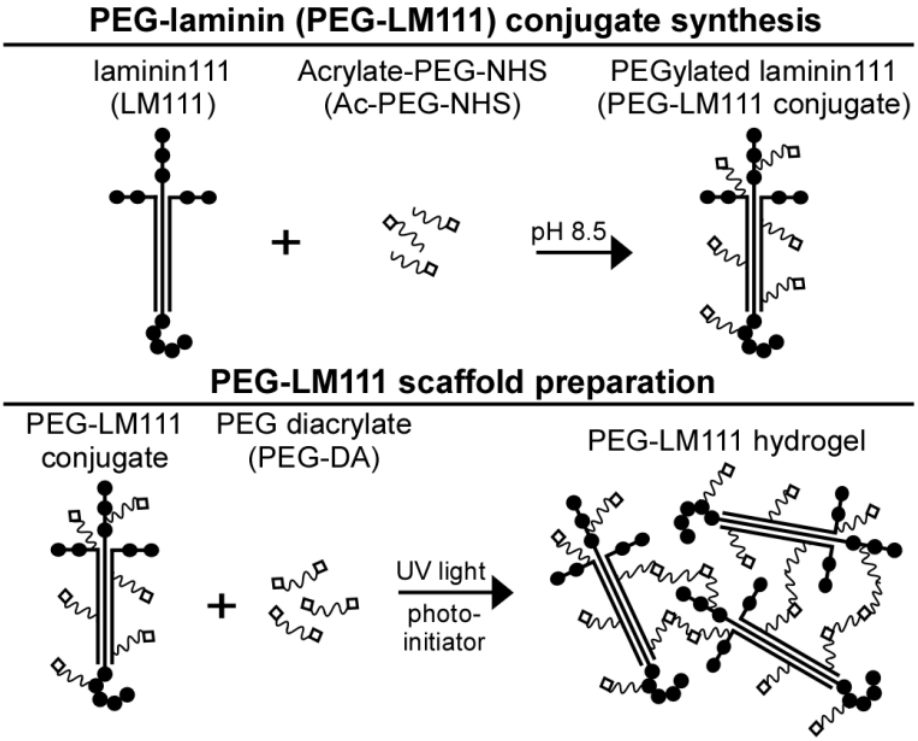

Figure 8. Schematic of photocrosslinkable PEG-laminin (PEG-LM111) hydrogel preparation. PEG-LM111 conjugates were synthesized by the addition of ac-PEG-NHS to introduce functional acrylate groups for crosslinking. Conjugates were mixed with additional PEG-DA and crosslinked via exposure to UV light to form PEG-LM111 hydrogels of varying stiffness and LM111 concentration.

2.2.6 LM111 Distribution in PEG-LM111 Hydrogels

Immunostaining of PEG-LM111 hydrogels was performed to evaluate effects of Ac-PEG-NHS to LM111 ratio used in conjugate synthesis on the amount of protein incorporated into PEG-LM111 hydrogels. PEG-LM111 hydrogels were crosslinked as described above to obtain 4 different hydrogel formulations containing 5% (w/v) PEG-DA and 200 μg/ml PEG-LM111 conjugate synthesized at either 10:1, 25:1, 100:1 or 500:1 molar ratio of Ac-PEG-NHS to LM111. Blank 5% (w/v) PEG-DA hydrogels and 5% (w/v) PEG-

DA gels mixed with 200 μg/ml LM111 prior to crosslinking were photocrosslinked in the same manner as compared to other groups. Samples were frozen in Tissue-Tek® O.C.T. compound (Sakura Finetek USA, Torrance, CA) and cryosectioned to obtain 20 μm thick sections. For each gel formulation, 6-8 sections were stained with a primary antibody specific to the γ chain of LM111 (L9393, Sigma-Aldrich, St. Louis, MO), followed by a goat anti-rabbit secondary antibody (Alexa Fluor 488®, Invitrogen, Carlsbad, CA). Samples were imaged by confocal microscopy to obtain 3 image fields per section (Zeiss LSM 510, 10x objective; Zeiss, Jena, Germany). Quantitative image analysis was performed using a custom written MATLAB script. Briefly, images were converted to grayscale, thresholded by subtracting out a blank PEG-DA image, and mean fluorescence intensity per image field was obtained as a measure of the amount of LM111 incorporated into each hydrogel. Mean intensity values were normalized to that of hydrogels containing entrapped LM111. A one-way ANOVA was performed to analyze mean fluorescence intensity per image field, using Tukey's post hoc test to detect differences between PEG-LM111 conjugates synthesized with different ac-PEG-NHS to LM111 ratios ($p<0.05$, n = 6 or 8 separate sections per hydrogel formulation, 3 images per section).

2.2.7 PEG-LM111 Conjugate Bioactivity in 3D

Preliminary cell encapsulation experiments were performed to evaluate PEG-LM111 conjugate bioactivity and to assess the ability of LM111 to promote NP cell survival

in 3D culture under low cell density, serum free conditions. Primary porcine NP cells were encapsulated in blank PEG-DA hydrogels (6% PEG-DA), PEG-DA hydrogels with unmodified LM111 that had been mixed in prior to crosslinking (6% PEG-DA, 200 μg/ml entrapped LM111), or PEG-LM111 hydrogels (6% PEG-DA, 200 μg/ml PEGylated LM111). Briefly, porcine NP cells were pelleted and resuspended in hydrogel precursor solutions (2 million cells/ml), injected into custom injection molds, and polymerized upon exposure to UV light in the presence of 0.1% (w/v) photoinitiator (Irgacure 2959®) as described above. After polymerization, cylindrical constructs were cored using a 6mm biopsy punch and cultured in 24 well plates in serum free media (F-12 supplemented with 10 mM HEPES, 100 U/ml penicillin, and 100 U/ml streptomycin) with gentle agitation. At each time point, cell-gel constructs (n=5 per formulation) were submerged in live/dead staining solution (Invitrogen) and incubated at 37°C for 30 minutes. Cell viability and distribution were visualized by confocal microscopy on days 0 and 7. Images (4 per cell-gel construct) were analyzed using ImageJ (NIH) to determine the percent of live cells present at each time point. Differences in cell viability amongst hydrogel formulations were analyzed via two-way ANOVA (time point, hydrogel formulation) with Tukey's post hoc test ($p<0.05$, n=5 per hydrogel formulation).

2.3 Results

2.3.1 Degree of LM111 Modification

PEG-LM111 conjugates with functional acrylate groups for crosslinking were synthesized via amine reactive NHS groups (Figure 9). Degree of LM111 modification, as measured by the reduction in number of reactive amines in each PEG-LM111 conjugate, significantly increased with increasing ratios of Ac-PEG-NHS to LM111 in the reaction solution (Figure 9). A minimum 25-fold molar excess of Ac-PEG-NHS over LM111 in the PEGylation reaction was necessary to detect protein modification (6%) using the TNBS assay. A 500-fold molar excess of Ac-PEG-NHS resulted in 39% LM111 modification, which was significantly higher (ANOVA, $p<0.001$) than that of PEG-LM111 conjugates synthesized at 10-fold, 25-fold or 100-fold molar excess Ac-PEG-NHS over LM111.

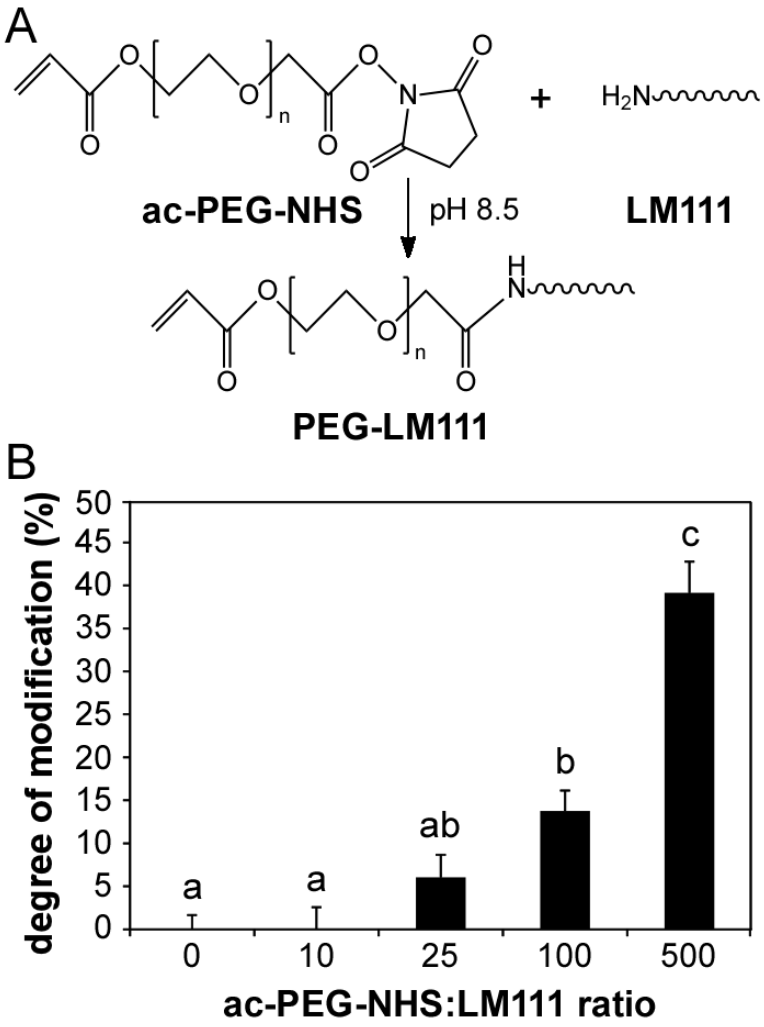

Figure 9. PEG-LM111 conjugate synthesis and degree of modification (%). (A) Conjugation of PEG molecules to laminin via amine reactive NHS groups. (B) Degree of modification of LM111 calculated from LM111 and PEG-LM111 conjugate absorbance at 340nm using TNBS assay. Degree of modification increased with increasing molar excess of Ac-PEG-NHS in the PEGylation reaction (mean ± SEM, n=3, conditions labeled with different letters significantly different, $p<0.01$).

2.3.2 PEG-LM111 Conjugate Bioactivity in 2D

To determine the relationship between the degree of LM111 modification and level of cell attachment, porcine NP cell attachment to PEG-LM111 conjugates with varying degrees of modification was assessed. Results for NP cell adhesion to PEG-LM111 conjugates demonstrated decreased cell attachment with increasing molar excess of Ac-PEG-NHS over LM111 used in conjugate synthesis, as compared to NP cell attachment to unmodified LM111 (Figure 10A). Cell attachment was significantly reduced (ANOVA, $p<0.001$) for conjugates synthesized with large molar excesses of PEG (100:1 or 500:1); however, cell attachment numbers for PEG-LM111 conjugate synthesized with a 25:1 ratio of Ac-PEG-NHS to LM111 were greater than 89% of values for NP cell attachment to native LM111. Therefore, PEG-LM111 conjugate synthesized at a 25-fold molar excess of Ac-PEG-NHS over LM111, which corresponds to 6% degree of modification by TNBS, was used for all subsequent experiments.

To further verify bioactivity of PEG-LM111 conjugate with a low degree of modification, we investigated activation of the MAPK/ERK signaling pathway subsequent to cell attachment to LM111 and PEG-LM111 conjugate. Since it has been shown that cell attachment to LM111 leads to ERK activation in a lung epithelial cell line (WI26VA4) [173], we hypothesized that a PEG-LM111 conjugate capable of maintaining levels of cell adhesion similar to that of native LM111 would also support ERK phosphorylation. As shown in Figure 10B, LM111 induced a 3-fold increase in

phosphorylated-ERK over cells cultured in suspension after 30 minutes and a 1.6-fold increase after 60 minutes. PEG-LM111 conjugate induced similar levels of phosphorylated ERK as compared to LM111 with 2.8-fold and 1.7-fold higher levels of ERK phosphorylation over negative controls after 30 and 60 minutes, respectively.

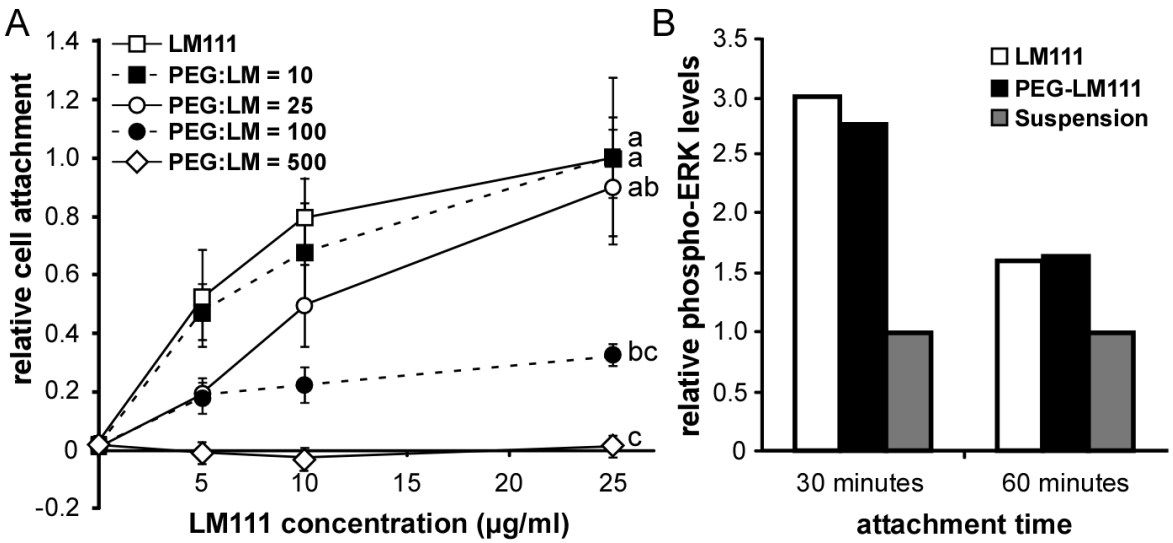

Figure 10. Bioactivity of PEG-LM111 conjugates. (A) Porcine NP cells were allowed to attach to LM111 and PEG-LM111 conjugates for 2 hours. NP cell attachment to PEG-LM111 conjugates decreased with increasing molar excess Ac-PEG-NHS in the PEGylation reaction (cell attachment levels normalized to NP cells on 25 µg/ml LM111, mean ± SEM, n=3, conditions labeled with different letters significantly different, $p<0.04$). (B) LM111 induced ERK activation in a lung epithelial cell line. Cells from a lung epithelial cell line (WI26VA4) were seeded onto LM111 and PEG-LM111 conjugate coated surfaces, or cultured in suspension. After 30 and 60 minutes, cells were lysed and levels of phosphorylated ERK in cell lysates were compared using ELISA.

2.3.3 LM111 Distribution in PEG-LM111 Hydrogels

Immunostaining of PEG hydrogels was performed to determine the effect of Ac-PEG-NHS to LM111 ratio used in the PEGylation reaction on the amount of LM111 incorporated into each hydrogel formulation. Immunostaining results demonstrate that the ratio of PEG to LM111 used in PEG-LM111 conjugate synthesis affects the amount of LM111 incorporated into the hydrogel (Figure 11). Fluorescence images show more intense staining for LM111 in hydrogels containing PEG-LM111 conjugate synthesized with a high ac-PEG-NHS PEG to LM111 ratio (500:1) as compared to those containing PEG-LM111 conjugates synthesized with a low ratio of ac-PEG-NHS to LM111 (25:1) or physically entrapped LM111 (Figure 11). Mean fluorescence intensity per image field significantly increased with increasing molar excess ac-PEG-NHS in PEG-LM111 conjugate synthesis (ANOVA, $p<0.03$). Very high levels of PEGylation (500:1) resulted in ~3.5 times more intense staining for LM111 in PEG-based hydrogels, as compared to PEG-DA hydrogels containing entrapped unmodified LM111; however, this degree of LM111 modification has been shown to inhibit NP cell adhesion to the PEGylated protein. Therefore, PEG-LM111 conjugate synthesized with a low molar excess ac-PEG-NHS (25:1) was utilized in all subsequent cell entrapment studies.

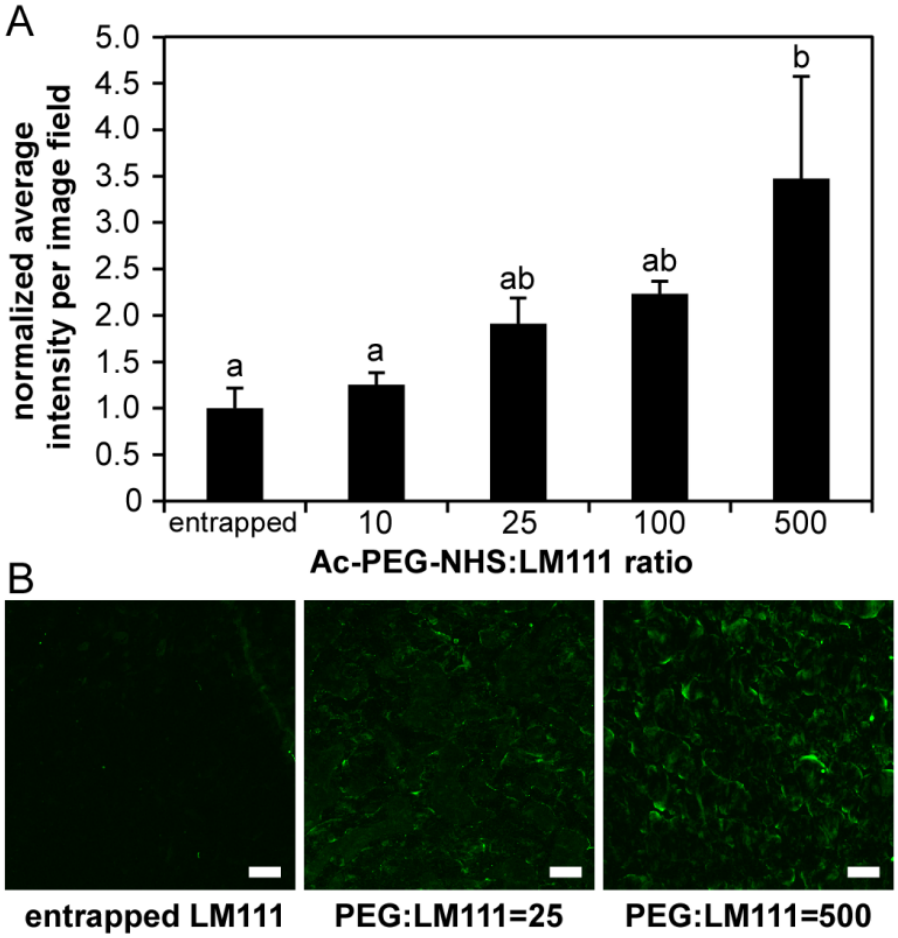

Figure 11. Immunostaining of PEG-LM111 hydrogels. (A) Mean fluorescence intensity per image field in PEG hydrogels containing entrapped LM111, or PEG-LM111 hydrogels containing PEG-LM111 conjugates synthesized with various Ac-PEG-NHS to LM111 ratios. Fluorescence intensity increased with increasing molar excess of Ac-PEG-NHS:LM111 ratio in the PEG-LM111 conjugate synthesis reaction (mean ± SEM, n > 6 sections, 3 images per section, conditions labeled with different letters significantly different, $p<0.03$). (B) Representative images of LM111 immunostaining in PEG hydrogels. Scale bars = 100 μm.

2.3.4 PEG-LM111 Conjugate Bioactivity in 3D

To verify the bioactivity of crosslinked PEG-LM111 conjugate, and to assess the ability of LM111 to promote NP cell survival in 3D PEG hydrogels under low cell density, serum free conditions, primary porcine NP cells were entrapped in PEG-DA hydrogels containing the same concentration of PEG-LM111 conjugate or entrapped unmodified LM111 and cultured for 7 days. Cells remained viable through photocrosslinking, with >82% cell viability for all hydrogel formulations on day 0. Cell viability was significantly lower after 7 days in culture for all hydrogel formulations ($p<0.001$); however NP cell survival on day 7 was significantly higher in PEG hydrogels containing entrapped LM111 or PEG-LM111 conjugate as compared to blank PEG-DA gels (Tukey's, $p<0.02$) (Figure 12).

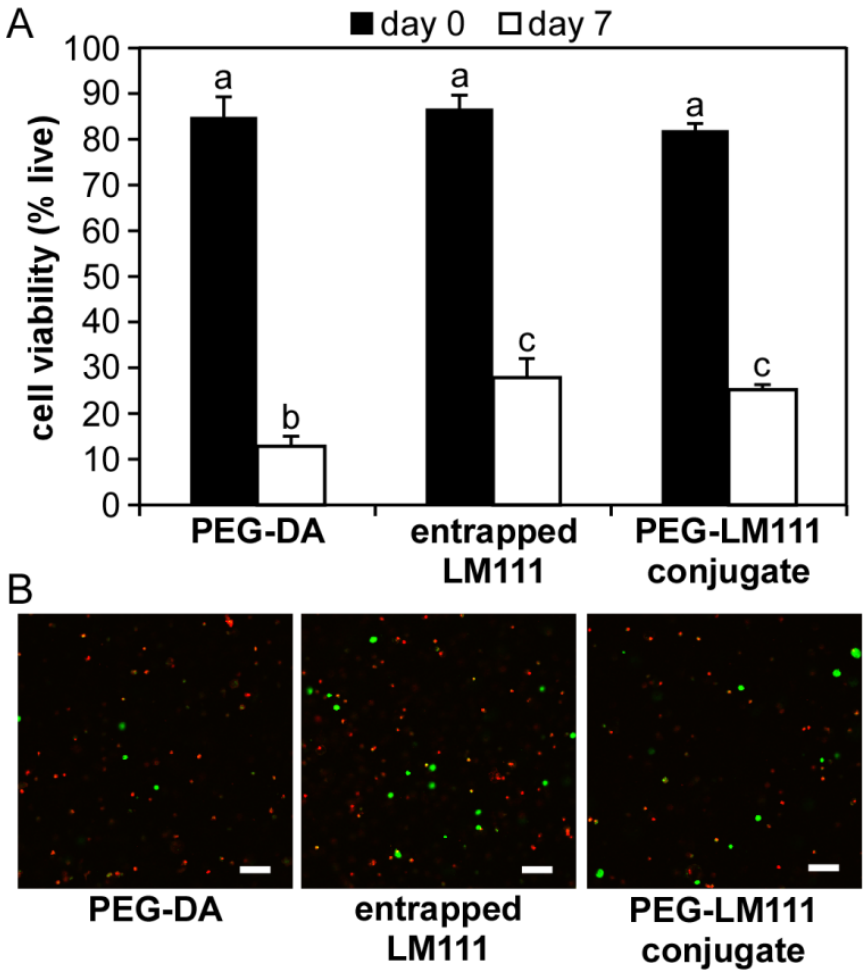

Figure 12. Cell viability in PEG hydrogels. (A) NP cell viability in PEG-based hydrogels after 0 and 7 days of culture in serum free media. Percent viability determined by counting the number of live cells as a percentage of total cells in images of hydrogels stained with Live/Dead viability assay (mean ± SEM, n=5, conditions labeled with different letters significantly different, $p<0.02$). (B) Representative images of Live/Dead stained cell-laden hydrogels, where live cells fluoresce green and dead cells fluoresce red. Scale bars = 100 μm.

2.4 Discussion

Laminin presenting substrates have previously been shown to promote the morphology and phenotype of immature NP cells in vitro, and to promote increased cell attachment and elevated glycosaminoglycan synthesis for primary NP cells in culture [33, 95]. For these reasons, LM111 was PEGylated to introduce functional acrylate groups onto the native protein for crosslinking. Conjugation of the laminin protein, LM111 to synthetic PEGs was performed with varying levels of protein modification in order to identify a formulation that could maintain LM111 functionality, and appropriate cell-laminin interactions. As expected, the degree of laminin modification increased with increasing molar excess of Ac-PEG-NHS in the conjugate synthesis reaction, up to a maximum value of 40% primary amine modification with a 500-fold molar excess of Ac-PEG-NHS, as measured by the TNBS colorimetric methods. While TNBS allows for determination of the average degree of protein modification by PEG, it does not provide information on the heterogeneity of the PEGylated protein or the sites of PEGylation [174]. Therefore, it was necessary to evaluate PEG-LM111 conjugate bioactivity to assess whether bound PEG chains hinder cell – LM111 interaction.

Primary NP cell adhesion to PEG-LM111 conjugates significantly decreased with increasing degree of PEGylation, with no cells adhering to PEG-LM111 conjugate with the highest degree of modification. This finding was expected as PEGylation of therapeutic compounds has been shown to modify their structure and bioactivity [175]. Nevertheless,

low levels of PEGylation (up to 25:1 Ac-PEG-NHS to LM111) did not significantly reduce NP cell adhesion to PEG-LM111 conjugates, nor inhibit MAPK/ERK activation upon binding to the modified protein. This low level of LM111 modification still enabled the PEG-LM111 conjugate to participate in a photocrosslinking reaction that was shown to be effective in promoting LM111 distribution in PEG-LM111 hydrogels. Together, these findings demonstrate that LM111 PEGylation via a heterobifunctional Ac-PEG-NHS allows for the additional of functional acrylates groups onto native LM111 without significantly altering the protein's ability to mediate cellular function.

Increasing the degree of LM111 PEGylation (ratio of Ac-PEG-NHS to LM111 in the PEGylation reaction) was shown to significantly increase the amount of LM111 incorporated into PEG-LM111 hydrogels. This is likely due to an increased number of acrylate groups on LM1111 that can participate in the photocrosslinking reaction. Low levels of PEGylation, however, were not found to significantly increase the amount of protein incorporated into PEG-LM111 hydrogels as compared to physically entrapped LM111. This finding suggests that a threshold level of protein modification that must be achieved in order for PEG-LM111 to become part of the hydrogel backbone. While increased ligand density within PEG-LM111 hydrogels is desirable, cell attachment results demonstrate that a high degree of LM111 modification by Ac-PEG-NHS significantly reduces its bioactivity and inhibits immature NP cell adhesion to the modified protein. Therefore, PEG-LM111 conjugate synthesized with a low level of

PEGylation (25:1 Ac-PEG-NHS to LM111) was chosen and evaluated for its ability to promote NP cell survival in 3D.

While 2D studies afford very good control of the substrate stiffness and ECM chemistry, culturing cells within a 3D matrix is much more representative of the native environment. In preliminary studies, the majority of NP cells cultured in PEG-only hydrogels at very low cell densities under serum free conditions died over 7 days (Appendix A). Studies were performed to determine if LM111 could act as a survival ligand under these culture conditions. As expected, the majority of primary NP cells encapsulated in PEG-based hydrogels at a very low cell density and cultured under serum-free conditions died over 7 days in culture; however, significantly more cells survived when encapsulated in hydrogels containing LM111 as compared to PEG-only gels. It is well known that LM111 promotes cell survival for a number of cell types in vitro [139]; therefore, this finding suggests that LM111 may be a survival ligand for primary NP cells. Viability was similar for cells cultured in PEG-LM111 hydrogels and PEG hydrogels containing an equal concentration of entrapped, unmodified LM111. This finding suggests that PEGylated LM111 retains the bioactivity of the native protein in 3D, and that survival is mediated by cell-LM111 interactions irrespective of ligand presentation. Overall, cell viability was likely affected by the small mesh size of PEG hydrogels formed by photopolymerizing PEG-DA, which limits nutrient and waste

diffusion in cultured hydrogels [176], and may inhibit cell-cell interactions when cells are encapsulated at very low densities.

2.5 Conclusion

Overall, these findings demonstrate that PEG-LM111 conjugates synthesized using a PEG to LM111 ratio of 25:1 maintain their ability to support NP cell attachment and cell survival in 3D hydrogels in a manner similar to unmodified LM111. At this ratio, immunostaining results suggest that LM111 incorporation into photocrosslinked PEG-DA hydrogels is increased compared to PEG-DA gels containing physically entrapped LM111. Together, these findings demonstrate that the addition of functional acrylate groups onto native LM111 through the use of a heterobifunctional Ac-PEG-NHS allows for increased protein incorporation into PEG-DA hydrogels without significantly altering the proteins ability to mediate cellular function. Therefore, LM111 functionalized PEG hydrogels may be useful for promoting IVD cell-matrix interactions while promoting the rounded cell morphology and unique phenotype of IVD cells.

3. Effects of Photocrosslinkable PEG-LM111 Hydrogel Properties on NP Cell Phenotype In Vitro

3.1 Introduction

A variety of synthetic, natural and hybrid materials have been investigated as scaffolds for NP regeneration [177], mainly in the form of hydrogels, which mimic the highly hydrated nature of the native NP. Natural components of the ECM such as hyaluronan [111, 112, 178], collagen [101, 103], and fibrin [103], and naturally derived polysaccharides such as alginate [97, 100, 103], chitosan [116-118], and agarose [103], have all been studied as potential scaffolds for NP tissue engineering. Although these naturally derived materials mimic many features of the native ECM, few peptide and protein functionalized scaffolds have been developed that can direct biological responses of cells for NP regeneration [28]. One limitation of using natural polymers for tissue engineering is that their mechanical properties can not easily be controlled. To overcome this, hybrid biomaterials of both natural and synthetic materials [113, 118, 119, 178], and natural polymers modified to contain functional groups that allow for photocrosslinking [102, 110] have been explored as potential scaffolds for NP tissue engineering.

Few studies have attempted to evaluate a scaffold for its ability to maintain or promote the immature NP cell phenotype. This is likely due to the lack of specific markers that distinguish immature NP cells from smaller more chondrocyte-like NP cells, anulus fibrosus cells, and articular chondrocytes. A number of recent studies have focused on defining the NP cell phenotype by evaluating biomarker expression in immature or non-

degenerate NP cells as compared to that in degenerate NP cells, anulus fibrosus cells or articular chondrocytes [84, 85, 87, 90, 179]. Laminin binding integrin subunits α3, α6 and β4 have been shown to be uniquely expressed in cells of the immature NP [30, 84]. N-cadherin has been shown to be more highly expressed in NP cells as compared to articular chondrocytes [85] and AF cells [88]. Finally, cytokeratin 8, an intermediate filament protein, is known to be expressed in notochordal-like disc cells [74] and more recently has been shown to be differentially expressed in NP cells [85, 90]. These findings provide useful biomarkers for choosing those scaffold biochemical and physical properties that can promote or maintain an immature NP cell phenotype.

In this chapter, photocrosslinkable PEG-LM111 hydrogels developed in Chapter 2 were used to investigate the effect of laminin ligand presentation and matrix stiffness on immature NP cell phenotype. We evaluated immature NP cell organization and proteoglycan synthesis when cells were cultured on top of PEG-LM111 hydrogels. Additionally, we describe here the effects of hydrogel stiffness and LM111 concentration on NP cell metabolism and NP phenotypic marker expression, including integrin subunits α3, α6, and β1, as well as cytokeratin 8, when cells were cultured within 3D PEG-LM111 hydrogels.

3.2 Methods

3.2.1 Photocrosslinked PEG-LM111 Hydrogel Mechanical Properties

PEG-DA was dissolved in PEG-LM111 conjugate solution (synthesized at 25-fold molar excess ac-PEG-NHS) and 0.1% Irgacure 2959® solution to obtain 6 different hydrogel formulations (5 or 10% PEG-DA and 0, 100 or 500 μg/ml PEG-LM111 conjugate). Hydrogel precursor solutions were injected into a custom injection mold as described above. After crosslinking, 6 mm diameter samples were cored and allowed to equilibrate in PBS before testing. All samples were tested in oscillatory shear in a 37°C, temperature-controlled phosphate buffered saline bath using a stress controlled rheometer (AR-G2, TA Instruments, New Castle, DE). Immediately prior to testing, each gel was digitally photographed to obtain the sample diameter. Samples were places in the center of a preheated sintered steel lower platen (8 mm diameter) and subjected to a compressive tare load (1-2g) with a sintered steel upper platen (8 mm diameter). After equilibrating, samples were subjected to a 10% compressive strain followed by 20 minute relaxation. Samples were subjected to an oscillatory torsional strain (1 – 20 rad/s) with a maximum amplitude of shear strain (γ, 0.01). The complex shear moduli ($|G^*|$) were reported at a frequency of 10 rad/sec. Differences in shear moduli amongst hydrogels with varying concentrations of PEG-DA and PEG-LM111 conjugate were analyzed via two-way ANOVA with Tukey's post hoc test ($p<0.05$, n=5 per hydrogel formulation).

3.2.2 Cell Isolation and Culture

Porcine NP cells were used for study as the majority of cells isolated from the immature porcine NP are known to resemble notochordally-derived NP cells [84]. Lumbar spines were obtained from pigs shortly after sacrifice (L1–L5, 4-7 months, Nahunta Pork Outlet, Raleigh NC). Cells were isolated from the NP regions of IVDs by enzymatic digestion [171] and cultured in monolayer for 1 – 7 days in culture media (F-12 media supplemented with 10% Fetal Bovine Serum (FBS), 10 mM HEPES, 100 U/ml penicillin, and 100 U/ml streptomycin) prior to experiments.

3.2.3 Primary NP Cell Behavior in PEG-LM111 Hydrogels in 3D

Primary porcine NP cells (20 million/ml) were mixed with PEG-DA (5 or 10%), PEG-LM111 conjugate (0, 100, or 500 μg/ml) and 0.1% Irgacure 2959® for a total of 6 material formulations. Precursor solutions were injected into custom molds and crosslinked by UV exposure (5 min, 3-4 mW/cm2). Samples were cored using a 3mm biopsy punch (n=9 per formulation) and cultured in vitro (F-12 media supplemented with 10% FBS, 10 mM HEPES, 100 U/ml penicillin, and 100 U/ml streptomycin) with gentle agitation. Fifty percent volume media changes were performed every 3-4 days for 28 days.

3.2.3.1 Measurement of Media Metabolites

Media aliquots from NP cell-PEG samples, and media from wells containing no PEG or cells were obtained on day 4 and stored at -80°C until further use. On the day of analysis, media aliquots were thawed and filtered through a 10 kDa MW cut-off centrifugal filter device (Nanosep, Pall Life Sciences, East Hills, NY). Fifteen microliter samples were then transferred to plastic vials, briefly spun, and analyzed for glucose, lactate, and pyruvate concentrations on a CMA 600 microdialysis analyzer (CMA Microdialysis, North Chelmsford, MA). The difference between each metabolite concentration in media collected from wells containing cell-laden PEG hydrogel samples and day 0 media that had been cultured for the same period was calculated for each sample. For each metabolite, differences amongst hydrogel formulations were analyzed via two-factor ANOVA (% PEG-DA, PEG-LM111 conjugate concentration) with Tukey's post hoc test ($p<0.05$, n=9 per hydrogel formulation).

3.2.3.2 Phenotypic Marker Immunostaining

Cell-laden hydrogel samples were immunostained for N-cadherin, cytokeratin 8, integrin $\alpha 3$, and integrin $\alpha 6$ to evaluate the effects of PEG-LM111 hydrogel stiffness and LM111 concentration on NP cell phenotype. On day 28, samples (n=3 per formulation) were embedded in Tissue Tek® OCT embedding compound and flash frozen in liquid nitrogen. Samples were stored at -80°C until further use. Frozen cell-laden PEG-LM111

hydrogel sections (8 μm thick) were fixed in 4% paraformaldehyde (10 minutes at room temperature) for labeling with antibodies detecting N-cadherin and cytokeratin 8. For labeling integrin subunits α3 and α6, sections were fixed in acetone (10 minutes at -20°C). Following fixation, all sections were incubated with blocking solution (3.75% BSA/5% goat serum) for 45 minutes at room temperature, and then incubated for 2 hours at room temperature with one of the following primary antibodies: N-cadherin (ab12221, Abcam, Cambridge, MA), cytokeratin 8 (SM3079P, Acris Antibodies, San Diego, CA), integrin α3 (AB1920, EMD Millipore, Billerica, MA), and integrin α6 (555734, BD Biosciences, San Jose, CA). Sections were washed twice with PBS and incubated with secondary antibody (AlexaFluor 488, Molecular Probes, Eugene, OR) for 30 minutes in blocking solution. Control sections were incubated with appropriate IgG controls or secondary antibody alone as a negative control for polyclonal antibodies. All sections were counterstained with propidium iodide (Sigma) at room temperature for 30 minutes to label cell nuclei. Sections were imaged via confocal microscopy (Zeiss, 20X NA 0.5 objective). Digital images acquired for each cell-laden hydrogel (n=9 images per hydrogel formulation) were evaluated by two blinded graders coming to consensus for fluorescence staining uniformity with the following ordinal scale: 0 (no stain), 1 (<10% cells positively stained), 2 (10 – 50% cells positively stained), 3 (>50% of cells positively stained) for each image. Grades of immunohistochemical staining were analyzed for differences amongst hydrogel formulations using Kruskal-Wallis one-way ANOVA ($p<0.05$). When

significance was observed, post-hoc Wilcoxon tests with Bonferroni correction for multiple comparisons were performed to detect differences amongst hydrogel formulations.

3.2.4 Primary NP Cell Behavior on PEG-LM111 Hydrogels in 2D

3.2.4.1 sGAG Production

Primary porcine NP cells (88,000 cells/cm2) were seeded onto PEG-LM111 hydrogels of varying concentrations of PEG (2 or 10% PEG-DA) and LM111 (0 or 1 mg/ml LM111) for a total of four hydrogel substrate formulations (n=6 per substrate). Primary NP cells (88,000 cells/cm2) were also seeded onto a laminin-rich ECM-derived basement membrane extract (BME) product (Trevigen, Inc; growth factor-reduced, 13.8 mg/mL) as a positive control. BME is a solubilized basement membrane preparation extracted from the Engelbreth-Holm-Swarm (EHS) mouse sarcoma tumor, which contains high concentrations of several ECM proteins: LM111 (~60%), type IV collagen (~30%), entactin (~8%), and heparin sulfate [180]. When polymerized into a "thick" gel, BME provides a laminin-rich environment of stiffness close to that of the native NP tissue (0.2 kPa) [33, 178, 181]. Cells were cultured on top of each hydrogel formulation for 4 days in culture media, after which sGAG production by NP cells was analyzed with dimethylmethylene blue (DMMB) spectrophotometric method as previously described [33]. All media overlay from culture samples was collected, while cells and gel proteins remaining in

corresponding wells after removal of media were digested in papain solution (125 μg/ml in PBS with 5 mM EDTA and 5mM cysteine, 2 hours, 65°C). Samples from control wells (n=2 per substrate) which only contained gels, were collected and processed similarly. sGAG content was measured by mixing samples with DMMB dye and absorbance (535 nm) was measured on a plate reader (Perkin-Elmer Enspire Multimode Reader, Waltham, MA). sGAG concentrations were calculated from a standard curve prepared from chondroitin-4-sulfate (Sigma). Total concentration of sGAG (media overlay plus cell digest) was normalized to total DNA content (Quant-iT PicoGreen dsDNA Kit, Invitrogen) for each sample. Differences in sGAG production (sGAG/DNA) across hydrogel substrate formulations were analyzed via one-way ANOVA with Tukey's post hoc analysis ($p<0.05$, n=6 per substrate formulation).

3.2.4.2 Cell Morphology

Immature porcine NP cells (88,000 cells/cm2) were seeded onto PEG only hydrogels (2 or 10% PEG-DA), and PEG-LM111 hydrogels (2 or 10% PEG-DA, 1 mg/ml LM111) as described above (n=6 per substrate formulation). The same number of NP cells were seeded onto BME gels for comparison. After 4 days of culture upon gels, NP cells were fixed with 4% paraformaldehyde (Electron Microscopy Sciences, Hatfield, PA; diluted in DPBS) for 20 minutes at room temperature. NP cells were then washed with DPBS and labeled for actin (Alexafluor-488 phalloidin, Invitrogen, 200x dilution in DPBS

for 30 minutes at room temperature) followed by a cell nuclei stain (propidium iodide, Sigma, 0.33 mg/ml for 20 minutes at room temperature). Immediately after staining, NP cells were imaged via confocal microscopy (Zeiss LSM510, 10x magnification).

3.3 Results

3.3.1 Photocrosslinked PEG-LM111 Hydrogel Mechanical Properties

PEG-LM111 hydrogels were tested in oscillatory torsional shear to investigate the effects of PEG-LM111 conjugate concentration and PEG-DA concentration on hydrogel mechanical properties. Photocrosslinked PEG-LM111 hydrogel stiffness (|G*|) significantly increased with increasing PEG-LM111 conjugate concentration for gels formed with either 5% or 10% PEG-DA (two-way ANOVA, $p<0.03$) (Figure 13). PEG-LM111 hydrogel stiffnesses (|G*|) were significantly higher in gels containing 10% PEG-DA as compared to 5% PEG-DA (two-way ANOVA, $p<0.001$).

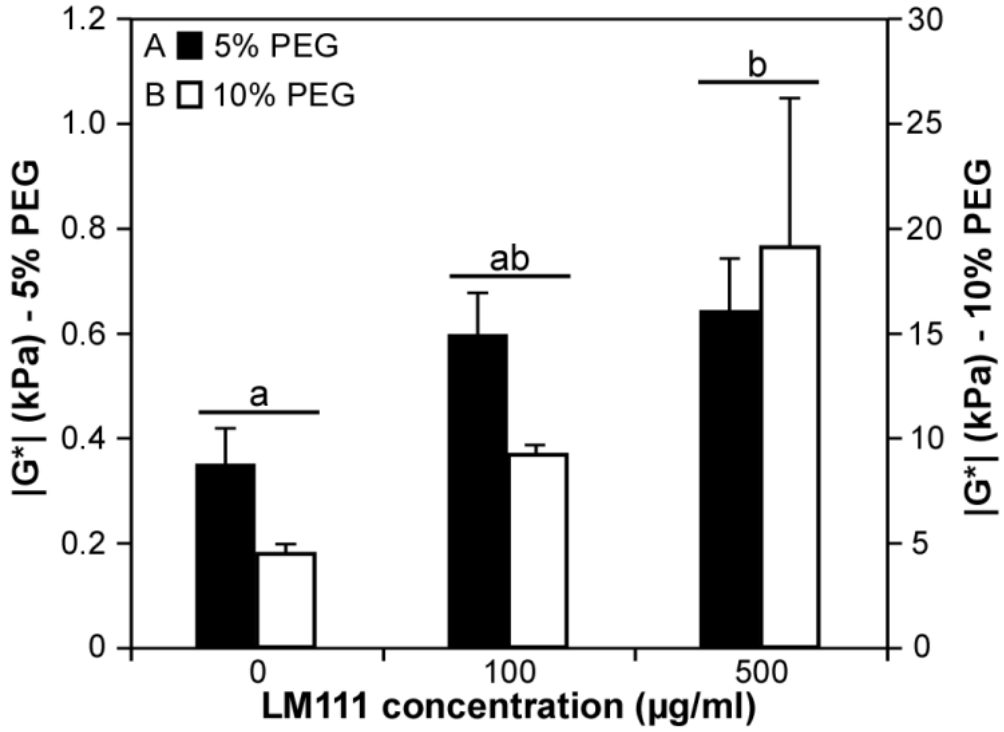

Figure 13. Physical characterization of photocrosslinked PEG-LM111 hydrogels. Torsional shear stiffness (|G*|, 5 rad/s) of 5% (w/v) and 10% PEG (w/v) hydrogels (mean ± SEM, n=5, conditions labeled with different letters significantly different, p<0.03).

3.3.2 Primary NP Cell Behavior in PEG-LM111 Hydrogels 3D

3.3.2.1 Measurement of Media Metabolites

Media aliquots from NP cell-laden PEG-LM111 hydrogels were analyzed for glucose, lactate and pyruvate to evaluate the effects of hydrogel stiffness and LM111 concentration on NP cell metabolism. Lactate and pyruvate levels were significantly affected by PEG-LM111 conjugate concentration (two-way ANOVA, $p<0.001$); however, glucose consumption was similar for all material formulations. Cells cultured in gels

containing 100 μg/ml PEG-LM111 conjugate consumed more pyruvate and produced more lactate over the 4 day culture period than cells cultured in gels containing 0 or 500 μg/ml PEG-LM111 conjugate (Figure 14).

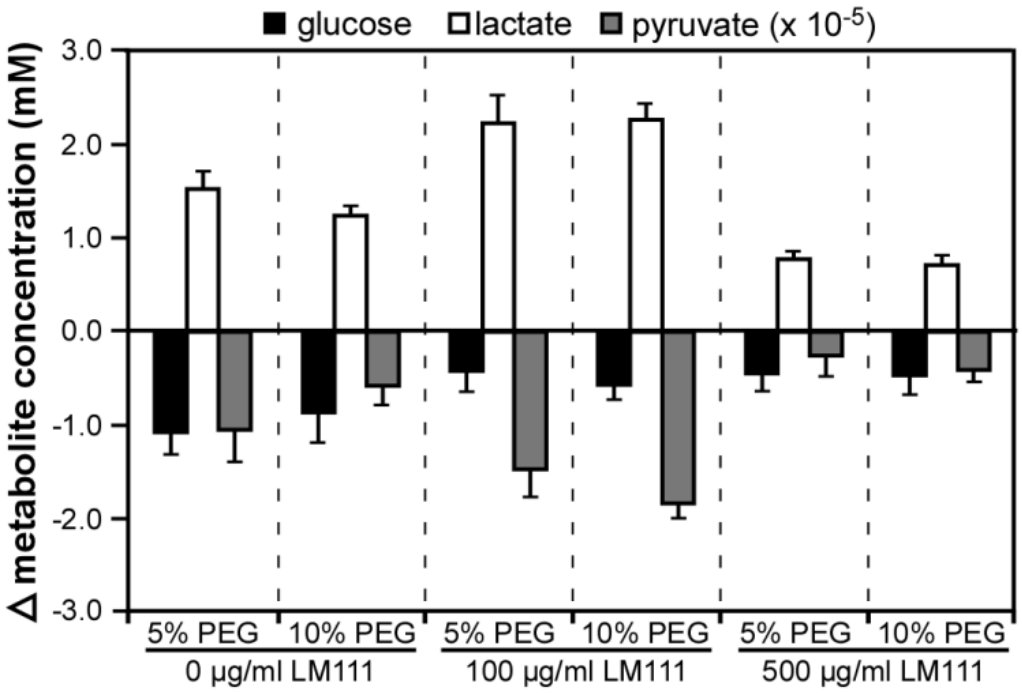

Figure 14. Media metabolite concentrations (change from day 0 media) in media aliquots obtained from NP cell-PEG constructs. Cells in gels containing 100 μg/ml LM111 consumed significantly more pyruvate and produced significantly more lactate than cells in all other hydrogel formulations (mean ± SEM, n=9, p<0.01).

3.3.2.2 Phenotypic Marker Immunostaining

Cytokeratin 8, N-cadherin, integrin α3 and integrin α6 expression by NP cells cultured in PEG-LM111 hydrogels was evaluated by immunohistochemical analysis (Table 3, Figure 15). The percentage of cells staining positively for cytokeratin 8 was

significantly higher in softer PEG-LM111 gels containing 5% PEG and 100 or 500 μg/ml LM111 (one-way ANOVA, Bonferroni correction, $p<0.003$) as compared to stiffer gels containing 10% PEG and equivalent amounts of LM111, and PEG-only (no LM111) gels. N-cadherin expression was significantly higher for NP cells cultured in PEG-LM111 hydrogels containing 5% PEG and high concentrations of LM111 (500 μg/ml) (one-way ANOVA, Bonferroni correction, $p<0.003$) as compared to cells cultured in all other hydrogel formulations. Integrin $\alpha 3$ expression varied significantly with hydrogel formulation ($p<0.0001$) with the highest percentage of cells staining positively for cells cultured in PEG-LM111 gels containing 5% or 10% PEG and 100 μg/ml LM111, or 5% PEG and 500 μg/ml LM111. Very low or no staining of integrin $\alpha 6$ was observed for all hydrogel formulations.

Table 3. Frequency of phenotypic marker immunohistochemical scores for NP cell-laden hydrogels of varying formulations.

N-cadherin						
Score	5% PEG 0 µg/ml LM111	10% PEG 0 µg/ml LM111	5% PEG 100 µg/ml LM111	10% PEG 100 µg/ml LM111	5% PEG[a] 500 µg/ml LM111	10% PEG 500 µg/ml LM111
0	4	0	6	4	0	6
1	5	8	1	4	1	3
2	0	1	2	0	4	0
3	0	0	0	0	4	0
cytokeratin 8						
score	5% PEG 0 µg/ml LM111	10% PEG 0 µg/ml LM111	5% PEG[b] 100 µg/ml LM111	10% PEG 100 µg/ml LM111	5% PEG[b] 500 µg/ml LM111	10% PEG 500 µg/ml LM111
0	0	0	0	0	0	0
1	7	6	1	6	0	8
2	2	3	2	3	4	1
3	0	0	6	0	5	0
integrin α3						
score	5% PEG 0 µg/ml LM111	10% PEG 0 µg/ml LM111	5% PEG[b] 100 µg/ml LM111	10% PEG 100 µg/ml LM111	5% PEG[c] 500 µg/ml LM111	10% PEG 500 µg/ml LM111
0	1	0	0	0	0	0
1	5	7	0	4	1	4
2	0	2	1	3	4	5
3	0	0	8	2	4	0
integrin α6[d]						
score	5% PEG 0 µg/ml LM111	10% PEG 0 µg/ml LM111	5% PEG 100 µg/ml LM111	10% PEG 100 µg/ml LM111	5% PEG 500 µg/ml LM111	10% PEG 500 µg/ml LM111
0	5	6	4	8	9	8
1	1	3	2	1	0	1
2	0	0	0	0	0	0
3	0	0	0	0	0	0

[a] Significantly different from hydrogels containing 5% PEG (0 or 100 µg/ml LM111) and formulations containing 10% PEG (0, 100 or 500 µg/ml) ($p<0.003$)

[b] Significantly different from formulations containing 10% PEG (0, 100 or 500 µ/ml LM111) and hydrogels containing 5% PEG (0 µg/ml LM111) ($p<0.003$)

[c] Significantly different from formulations containing 5% (0 µg/ml LM111) or 10% PEG (0 µg/ml LM111) ($p<0.003$)

[d] No significant difference amongst hydrogel formulations (chi-squared, $p> 0.05$)

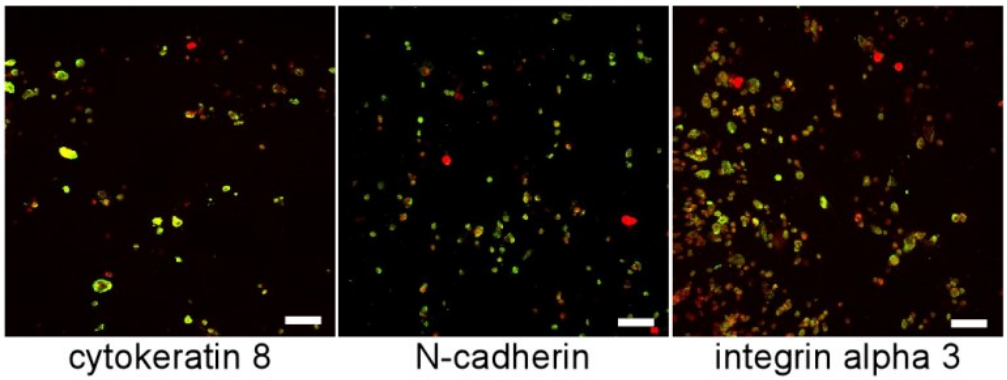

Figure 15. Representative images of day 28 NP cell-laden PEG-LM111 hydrogels containing 5% PEG and 100 μg/ml LM111 (left) or 500 μg/ml LM111 (right) stained for cytokeratin 8, N-cadherin and integrin α3. Scale bar = 50 μm.

3.3.3 Primary NP Cell Behavior on PEG-LM111 Hydrogels in 2D

3.3.3.1 sGAG Production

To determine if immature NP cells form multi-cell clusters and synthesize ECM on PEG-LM111 hydrogel substrates, primary NP cells were seeded on PEG-LM111 hydrogels containing 1 mg/ml LM111 and varying concentrations of PEG (2 or 10%). NP cells seeded on soft, PEG-LM111 hydrogels containing low amounts of PEG synthesized similar levels of sGAG as compared to cells plated on laminin containing, polymerized BME substrates (one-way ANOVA, Tukey's post hoc test, $p>0.05$) (Figure 16). Primary NP cells seeded onto PEG-LM111 hydrogel substrates containing high amounts of PEG synthesized significantly less sGAG (Tukey's, $p<0.0001$), with total sGAG production similar to that of cells seeded onto PEG hydrogels containing no protein.

3.3.3.2 Cell Morphology

Over 4 days in culture, primary NP cells were found to form large, multi-cell clusters when seeded on PEG-LM111 hydrogels containing low concentrations of PEG (2%) or polymerized BME substrates (Figure 16). In contrast, NP cells seeded on PEG-LM111 substrates containing high concentrations of PEG (10%) or PEG-only substrates (no LM111) remained attached as single cells with uniform distribution.

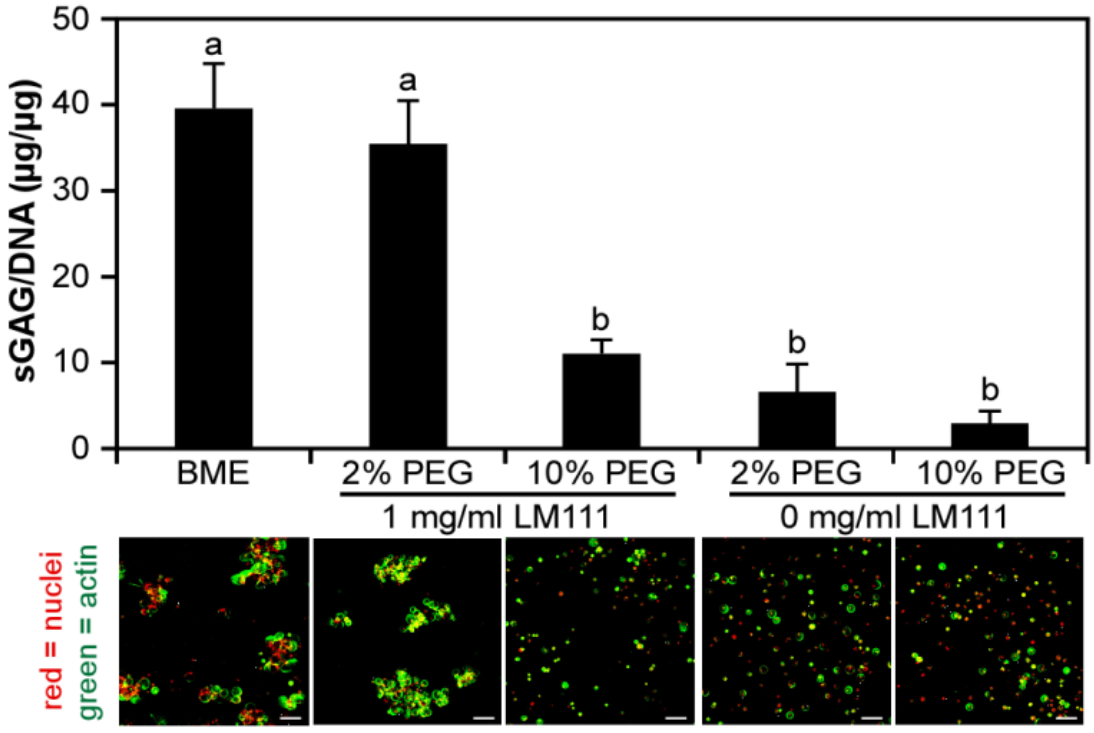

Figure 16. NP cell clustering and sGAG synthesis on PEG-LM111 hydrogels. Immature porcine NP cells were cultured on top of laminin-rich basement membrane extract (BME), PEG-LM111 hydrogels and PEG-only hydrogels for 4 days. NP cells clustered and synthesized higher amount of sGAG on BME and PEG-LM111 substrates containing 2% PEG and 1 mg/ml LM111 (mean ± SEM, n=5, conditions labeled with different letters significantly different, $p<0.0001$). Scale bars = 100 µm.

3.4 Discussion

The goal of this work was to develop a laminin functionalized hydrogel with tunable mechanical properties and to evaluate the effects of matrix stiffness and LM111 ligand concentration on immature NP cell phenotype in vitro. Previous work has shown that BME polymerized gels or soft BME upon polyacrylamide promote formation of multi-cell clusters for cultured primary disc cells [33, 182]. Rather than work with a model polyacrylamide substrate system, we engineered a biomaterial by attaching LM111 to PEG-based hydrogels, as PEG is non-cytotoxic, non-fouling, and has a long history of clinical use as a drug delivery agent for therapeutic proteins [156]. In addition, mechanical properties of PEG hydrogels formed by UV photopolymerization of PEG-DA can be easily manipulated [34]. Results reveal that specific formulations of the PEG-LM111 hydrogel appear to preserve features of the immature NP cell phenotype.

Characterization of the bulk mechanical properties of PEG-LM111 hydrogels showed that PEG concentration (% w/v) was a dominant variable in determining the stiffness of PEG-LM111 hydrogels, with dynamic stiffness values for gels containing 10% PEG an order of magnitude higher than that of gels formed with 5% PEG. PEG-LM111 hydrogel stiffness, however, could not be completely decoupled from ligand concentration, as increasing the amount of PEG-LM111 conjugate also increased PEG-LM111 hydrogel stiffness for gels containing both 5% and 10% PEG. This finding differs

from that of a recent study, in which increasing the amount of LM111 conjugate in PEG-DA hydrogels was reported to significantly decrease hydrogel stiffness [162]. Our finding may be related to the PEG-LM111 conjugate having an increased degree of modification by the addition of PEG onto LM111, thereby increasing the number of acrylate groups on LM1111 that can participate in the photocrosslinking reaction. This feature may reduce the likelihood that a single PEGylated LM111 molecule can result in chain termination. Overall, these findings demonstrate that PEG-LM111 hydrogel mechanical properties can be tuned within the range of dynamic shear moduli values previously reported for human NP [183] by altering both the total PEG concentration and PEG-LM111 conjugate concentration, with hydrogel stiffness being dominated by the former.

For primary NP cells cultured within 3D PEG-LM111 hydrogels of varying stiffnesses and LM111 ligand concentration, media metabolite concentrations suggest that LM111 ligand density, but not stiffness of the material, has a significant effect on NP cell metabolism, particularly lactate production. NP cells rely on diffusion of nutrients such as oxygen and glucose from the cartilaginous end plates; most of their energy is formed by the conversion of glucose to lactic acid; however, NP cells do require oxygen to function [184-186]. Interestingly, despite increased lactate production and pyruvate consumption by cells cultured in PEG-LM111 gels containing low concentrations of LM111, glucose consumption by NP cells remained low across all hydrogel formulation.

It is important to note that hydrogels were cultured under normoxic conditions, which may have led to increased oxygen consumption and reduced glycolysis by entrapped cells. Increased lactate concentrations in scaffold-chondrocyte cultures at early time points has been shown to be a strong predictor of glycosaminoglycan and hydroxyproline accumulation in chondrocytes [187], suggesting that low levels of LM111 may improve matrix production in PEG scaffolds.

Although it has been hypothesized that promoting or maintaining a notochordal-like immature NP cell phenotype may be important for tissue engineering strategies aimed at NP regeneration, there has been limited assessment of the effects of scaffold design on cell phenotype. This is in part due to the lack of specific markers that distinguish immature, notochordal-like NP cells from small, more chondrocyte-like NP cells, as well as from articular chondrocytes and AF cells. Recently, numerous studies have focused on markers uniquely expressed in the immature or non-degenerate NP, and suggest integrin α3 [30], integrin α6 [30, 84], N-cadherin [85, 88], and cytokeratin 8 [85, 90] as potential NP phenotypic markers. Here, N-cadherin was found to be highly expressed when immature NP cells were cultured in soft, PEG-LM111 hydrogels containing 5% PEG and high concentrations of LM111 (500 μg/ml), characteristic of a soft hydrogel with high LM111 ligand density. Cytokeratin 8 is known to be highly expressed in the human notochord [74] and immature porcine NP [90], and was higher for NP cells cultured in PEG-LM111 gels containing 5% PEG and either low (100 μg/ml) or high (500 μg/ml)

amounts of LM111. This is in contrast to the findings for PEG-LM111 hydrogels formed from 10% PEG or PEG-only (no LM111). The findings for higher N-cadherin and cytokeratin 8 expression in LM111 containing PEG gels of 5% PEG suggests that soft, LM111 functionalized gels may lead to maintenance of these key features of immature NP cell phenotype. NP cells were found to express varying levels of integrin α3 across hydrogel formulations; however, very little immunostaining for integrin α6 was observed for all cell-laden constructs. This was unexpected since porcine NP cells have previously been shown to attach to LM111 via integrin α6 [31], while adult human NP cells make use of α3, α5, and β1 subunits to attach to LM111 [29]. Integrin α3 has been shown to be expressed in the immature human and porcine NP, but not in the adjacent AF [30], and to play a function role in human NP cell adhesion to laminins [29]. In this study, integrin α3 expression was highest for primary NP cells cultured in PEG-LM111 hydrogels that contained 5% PEG and either 100 or 500 μg/ml LM111; however, moderate expression was observed for cells cultured in the stiffer gels containing similar amounts of LM111. This finding may reflect that NP cell-LM111 interactions are mediated at least in part by the integrin α3 subunit when attaching to the modified PEG-LM111 conjugate. Taken together, immunostaining of NP cell-laden PEG-LM111 hydrogels suggest that soft, LM111 functionalized hydrogels may promote both cell-cell and cell-matrix interactions characteristic of an immature NP cell phenotype.

In addition to expression of specific phenotypic markers, immature NP are differentiated from other cells in the disc by their distinct morphology, appearing as large, highly vacuolated cells arranged in multi-cell clusters. In a prior study, immature NP cells seeded onto polymerized BME substrates formed large, multi-cell clusters and synthesized high levels of sGAG as compared to other ECM protein coated 2D rigid substrates [33]. In the present study, immature primary NP behavior on softer, PEG-LM111 substrates was found to correlate closely to that of NP cells seeded onto BME gels. Cells seeded onto softer, PEG-LM111 hydrogels with low levels of PEG and high concentrations of LM111 were found to cluster and to synthesize higher levels of sGAG, as compared to cells seeded onto blank PEG-only or stiffer, PEG-LM111 hydrogels. Overall, this finding suggests that specific formulations of the PEG-LM111 hydrogel are able to mimic physical and biochemical properties of polymerized BME previously shown to promote an immature NP cell phenotype.

3.5 Conclusion

We report here on the development and characterization of a photocrosslinkable LM111 functionalized hydrogel with tunable mechanical properties for evaluating the effects of matrix stiffness and LM111 concentration on NP cell behaviors in both 2D and 3D. In 2D, the softer, LM111 presenting hydrogels were found to promote primary NP cell clustering and increased levels of sGAG production as compared to stiffer LM111

presenting and PEG-only gels. In 3D, hydrogel formulation was found to influence NP cell metabolism and expression of proposed phenotypic markers, with higher expression of N-cadherin and cytokeratin 8 observed for cells cultured in softer (<1 kPa), LM111 functionalized PEG hydrogels. Overall, these findings suggest that softer, LM111 functionalized scaffolds may promote or maintain an immature NP cell phenotype, and that incorporation of the LM111 ligand into scaffolds might be useful for studies aimed at NP regeneration.

4. Injectable PEG-LM111 Hydrogel for Nucleus Pulposus Regeneration

Reproduced in part from: Francisco AT, Mancino RJ, Bowles RD, Brunger JM, Tainter DM, Chen Y, Richardson WM, Guilak F, Setton LA. (2013) Injectable laminin-functionalized hydrogel for nucleus pulposus regeneration. *Biomaterials*, 34:7381-7388.

4.1 Introduction

Cell transplantation to the IVD has been performed clinically, and aims to repopulate the disc with cells capable of synthesizing new ECM to restore function to the diseased IVD. In animal models of IVD regeneration, implantation of autologous disc cells or stem cells has been shown to delay degeneration, as measured by histological and radiographic changes [22, 111, 130-132, 179, 188]. Although the need for a biomaterial carrier to improve cell retention immediately after delivery has been demonstrated [136], few studies have evaluated the role of the carrier in long-term cell survival and retention [188]. Injectable materials for cell delivery to the IVD have received considerable attention since they provide a minimally invasive tissue engineering approach for enhancing IVD regeneration. Numerous hydrogels derived from natural components of the ECM, including fibrin [123, 136, 137], hyaluronan [111, 114, 189], and collagen [109, 119, 132], and natural biopolymers such as chitosan [116, 118, 190] have been investigated as carriers for cell delivery to the disc. The development of injectable biomaterials that support cell retention, cell survival and maintain or promote an NP cell phenotype in vivo remains a significant challenge.

PEG hydrogels have been widely used in tissue engineering applications since they are biocompatible, hydrophilic polymers that readily allow for incorporation of biological signals derived from the native ECM [128]. Therefore, full length ECM-derived proteins, including collagen, fibrinogen and laminin, have been covalently coupled to PEG hydrogels for a variety of tissue engineering applications and shown to influence cell behavior in three dimensions [34, 162, 168, 169]. The majority of these studies rely on photocrosslinking of acrylate functional groups on PEGylated proteins and PEG-multiacrylates to form three-dimensional hydrogels; however, conjugate addition between free thiols and PEG-acrylate or PEG-vinylsulfone allows gelation to occur in situ under physiological conditions [191, 192] without the need for UV light. This chemistry enables a utility of the PEG-crosslinking hydrogel that is more suitable for the delivery of cells in vivo.

The objective of this work was to develop an injectable laminin functionalized PEG hydrogel with tunable mechanical properties, and to assess its potential use as a carrier for cell-based IVD regeneration. We describe here the synthesis and characterization of an injectable PEG-LM111 hydrogel via the addition of PEG-dithiol and PEG-octoacrylate to the PEG-LM111 conjugate developed in Chapter 2. Additionally, we describe the generation of luciferase expressing primary NP cells, and the delivery of these cells to the disc space within our injectable biomaterial carrier.

4.2 Materials & Methods

4.2.1 Injectable PEG-LM111 Hydrogel Synthesis and Mechanical Properties

Preliminary studies were performed to determine if a fiber optic cable could be utilized to promote gelation of photocrosslinkable PEG-LM111 hydrogel precursor solutions in the IVD space (Appendix B). Although gelation in situ could be achieved in a model disc, significant technical challenges arose during pilot in vivo studies. Therefore, a modified PEG-LM111 hydrogel crosslinked via a Michael-type addition reaction was developed to allow for gelation in situ without the need for UV light. PEG-octoacrylate (20kDa, Creative PEGworks) and PEG-dithiol (3.4kDa, Creative PEGworks) were dissolved separately in PEG-LM111 conjugate (25:1 Ac-PEG-NHS to LM111) solutions and PBS to final concentrations of 10% (w/v) PEG and 0, 100, or 500 μg/mL PEG-LM111 conjugate (25:1 Ac-PEG-NHS to LM111). All samples were tested in oscillatory shear under physiological conditions (37°C, pH 7.4) in a humidified atmosphere. Briefly, appropriate volumes of PEG-octoacrylate and PEG-dithiol solutions that had been dissolved in PEG-LM111 conjugate solution were mixed to obtain a PEG-LM111 precursor solution containing a 1:1 ratio of acrylate to thiol groups. Solutions were mixed and immediately pipetted onto the center of a test platen (25mm diameter) within the test chamber of a controlled stress rheometer (AR-G2, TA Instruments, New Castle, DE). The upper platen was lowered to a gap thickness of 1mm and oscillatory shear was applied (ω=0.5Hz, γ0=0.05). The evolution of storage (G′) and loss (G′′) moduli were recorded over

time, and used to calculate the complex shear modulus (|G*|). Gelation time was determined by the crossover of G′ and G′′ for each hydrogel formulation. Differences in gelation time and steady-state complex shear modulus amongst gel formulations were detected by ANOVA with Tukey's post hoc test ($p<0.05$, $n=5$ per formulation).

4.2.2 Cell Isolation and Culture

Cells isolated from the porcine NP have a unique notochordal phenotype, and were therefore used to evaluate both PEG-LM111 conjugate bioactivity and for in vitro and in vivo cell delivery experiments. Lumbar spines were obtained from pigs shortly after sacrifice (L1–L5, 4-7 months, Nahunta Pork Outlet, Raleigh NC). Cells were isolated from the NP regions of IVDs by enzymatic digestion [171] and cultured in monolayer for 3 – 7 days in culture media (Ham's F-12 media supplemented with 10% fetal bovine serum (FBS), 10 mM HEPES, 100 U/ml penicillin, and 100 U/ml streptomycin) prior to experiments.

4.2.3 Generation of Luciferase Expressing Primary NP Cells

To generate transduction media, VSV-G pseudotyped lentivirus driving constitutive expression of the luciferase2 transgene (obtained from pGL4.50; Promega, Madison, WI) under control of the EF1α promoter (LVE-LUC2) was prepared in 293T cells using the standard calcium phosphate precipitation technique [193] and stored at -80°C

until further use. LVE-LUC2 was thawed and supernatant was centrifuged through a 100 kDa MWCO filter (EMD Millipore, Billerica, MA). Preliminary studies were performed to determine optimal LVE-LUC2 vector concentration in the transduction media that would promote long-term, stable luciferase expression in primary NP cells (see Appendix C). A concentrated LVE-LUC2 vector (80x concentration) was mixed with NP culture media (5 μl concentrated virus per ml media) supplemented with 4 μg/ml polybrene® (Sigma-Aldrich, St. Louis, MO). Primary porcine NP cells were isolated as described above, plated at a density of 40,000 cells/cm2 in culture media, and cells were allowed to adhere for 24 hours. Culture media was then aspirated from NP cells and replaced with transduction media. After 24 hours, LVE-LUC2 containing media was aspirated and fresh culture media was added. Luciferase expressing porcine NP (NP-luc) cells were cultured in monolayer with media changes every 2-3 days. To evaluate luciferase expression in cultured cells, bioluminescent imaging was performed using an IVIS© Kinetic, and signal intensities were quantified with Living Imaging software (PerkinElmer, Waltham, MA). NP-luc and control naïve NP cells were lifted at multiple time points post transduction (day 4 to 35), counted and suspended in culture media. These cells were added to separate wells of a 96 well black bottom tissue culture plate (5000 cells/well). Wells were supplemented with 150 μg/ml D-luciferin (PerkinElmer) and imaged 10 minutes after addition of D-luciferin (5 sec exposure time). Total photons per second per cell was calculated from the total photons in a defined circular region of interest (ROI) drawn over

each well. An ANOVA was performed to analyze light emission (photons/sec/cell), using Tukey's post hoc test ($p<0.05$, $n=3$) to detect differences between time points.

4.2.4 Cell Retention in IVD Motion Segments

The effect of PEG-LM111 biomaterial on cell retention and survival in the IVD was evaluated in an organ culture model. Rat tails (n=8 Sprague Dawley, 200 – 250g, Charles River, Wilmington, MA) were harvested within 3 hours of sacrifice, skin and tendons were removed, and 7-8 IVD motion segments were obtained from each animal (C1-C8). Disc motion segments were washed three times, and placed in sterile petri dishes. A nucleotomy was performed by injecting air into the disc space via a 27G needle. PEG-LM111 precursor solution (10% PEG containing 1:1 acrylate to thiol ratio, 500 μg/ml PEG-LM111 conjugate synthesized with 25:1 Ac-PEG-NHS to LM111) was prepared as described above. NP-luc cells that had been cultured in monolayer for at least 10 days were lifted and resuspended at a concentration of 10^6 cells/ml in PEG-LM111 precursor solution or PBS, and 10 μl was delivered to the NP of individual caudal motion segments through a 27G needle. The needle was held in place for 1 minute following cell delivery to reduce leakage. Individual motion segments were separated, placed in separate wells of a 12-well plate, and overlaid with media. Motion segments receiving no additional injection [194] and PEG-LM111 precursor solution only were used as negative controls. All motion segments were cultured out to 14 days at 37°C, 5% CO2 and 20% O2 in culture

media (F12 supplemented with 20% FBS, 100 U/ml penicillin, and 100 U/ml streptomycin) with media changes every day. Cell retention in rat motion segments was evaluated at multiple time points after injection of NP-luc cells using bioluminescence imaging. To evaluate cell retention in IVD motion segments, wells containing rat IVD motion segments were supplemented with 300 μg/ml D-luciferin and light emission was measured 2 minutes later (30 sec exposure time). An oval ROI was drawn around the entire motion segment based on a photographic image. Total photons within each ROI was obtained from the overlay luminescent image. Differences amongst cell delivery vehicles and time post injection were analyzed via two-factor ANOVA with Tukey's post hoc test ($p<0.05$, $n=6$).

4.2.5 Cell Transfer to IVD Motion Segments

4.2.5.1 Bioluminescent Imaging

To assess the effect of the PEG-LM111 biomaterial on initial cell transfer IVD motion segments, the experiment described in Section 4.2.4 was repeated, and cell retention was evaluated by bioluminescence imaging in the 30 minutes immediately following cell delivery. Rat tail IVD motion segments and PEG-LM111 hydrogel precursor solutions were prepared as described in Section 4.2.4. A nucleotomy was performed by air injection into the disc space (C2 – C4), and 1×10^6 cells were delivered to each IVD motion segment as described here: NP-luc cells were lifted and resuspended at

a concentration of 10^6 cells/ml in PEG-LM111 precursor solution or PBS, and 10 μl was delivered to the NP of individual caudal motion segments through a 27G needle. The needle was held in place for approximately 1 minute following injection. IVD motion segments (n=3 per group) were immediately transferred to 12-well plates and 1 ml of media was added to each well. Wells were supplemented with Luciferin-D (300 μg/ml) and light emission was measured immediately, and then at 2 minute intervals for 28 minutes (30 second exposure). An oval ROI was drawn around the entire motion segment based on a photographic image. Total photons within each ROI was obtained from the overlay luminescent image and normalized to the total number of photons in IVD motion segments receiving cells in PEG-LM111 hydrogel precursor solution at time 0. Differences amongst cell delivery vehicles and time post injection were analyzed via two-factor ANOVA with Tukey's post hoc test ($p<0.05$, n=3).

4.2.5.2 IVD Motion Segment Immunostaining

To evaluate PEG-LM111 biomaterial transfer to the disc space in an organ culture model, IVD motion segments were immunostained for LM111. At 30 minutes post cell delivery in either PBS or PEG-LM111 hydrogel precursor solution (n=3 per group), IVD motion segments were fixed in 10% neutral buffered formalin for 48 hours at 4°C, decalcified in Cal-Ex (Fisher Scientific) for 14 days at 4°C, processed in a series of increasing ethanol concentrations, and embedded in paraffin. Eight-micrometer thick

sagittal sections were obtained for immunostaining. Sections (3 sections per motion segment spaced approximately 800 μm apart) were deparaffinized and rehydrated in PBS, followed by antigen retrieval with proteinase K (Sigma). Sections were incubated with blocking solution (PBS/0.05% Tween-20 and 3.75% BSA for 10 minutes followed by PBS/0.05% Tween-20 and 5% Donkey Serum for 30 minutes at room temperature), followed by a primary antibody for LM111 (L9393, Sigma) for 2 hours at room temperature. Sections were washed twice with PBS and incubated with secondary antibody (AlexaFluor 488, Molecular Probes, Eugene, OR) for 30 minutes in blocking solution. Sections were incubated with secondary antibody only as negative controls. Samples were imaged via confocal microscopy (Zeiss LSM510, 10x magnification).

4.2.6 Cell Delivery to Rat Tail IVD

In vivo studies of cell persistence within the rat IVD were performed to test proof-of-concept for use of the PEG-LM111 hydrogel as a carrier for NP-luc cells. NP-luc cells were delivered to the rat tail IVD either in PEG-LM111 hydrogel, PEG-only hydrogel (no PEG-LM111 conjugate) or PBS. Rats (Sprague Dawley, 200 – 250g, Charles River) were anesthetized with isoflurane, and a 3 cm incision was made on the dorsal side of the tail to obtain access to the C3-C4, C4-C5 and C5-C6 disc space. A nucleotomy was performed at the C3-C4 and C5-C6 levels of each tail using a 25G needle, and the anulus fibrosus was closed with one 5-0 Vicryl® suture (Ethicon Inc., Somerville, NJ). Cells in PBS, cells in

PEG-LM111 (PEG-octoacrylate and PEG-dithiol, 500 μg/ml PEG-LM111 conjugate), and cells in PEG-only (PEG-octoacrylate and PEG-dithiol, no PEG-LM111 conjugate) were prepared as described above. Using a Hamilton syringe with a 27G needle, 10 μl of cells in PEG-LM111, cells in PBS, or cells in PEG-only was injected into the middle of the C3-C4 or C5-C6 denucleated disc space (n=3 per group). Disc spaces (C3-C4 or C5-C6) receiving either PEG-LM111 biomaterial only (10 μl) or nucleotomy only served as negative controls. Skin was closed in an interrupted manner using 4.0 nylon sutures. For in vivo bioluminescent imaging, D-luciferin (150 mg/kg) was injected intraperitoneally 15 min before imaging, after which rats were anesthetized with 1-3% isoflurane and imaged (5 min exposure time). For ex vivo bioluminescent imaging, rat tails were harvested immediately after sacrifice, skin and tendons were removed, and IVD motion segments (C2-C6) were obtained from each animal. Disc motion segments were placed in sterile petri dishes, overlaid with culture media, and supplemented with 300 μg/ml D-luciferin. Light emission was measured 2 minutes later (300 sec exposure time). All procedures were approved by the IACUC and were performed in accordance with Duke University guidelines.

4.3 Results

4.3.1 Injectable PEG-LM111 Hydrogel Mechanical Properties

When PEG-LM111 conjugate solution or PBS was mixed with PEG-octoacrylate and PEG-dithiol under physiological conditions (37°C, pH 7.4), hydrogels formed in less than 25 minutes by the reaction of thiols and acrylates, as measured by the point of crossover of G′ and G′′ (Figure 17A). For hydrogels containing 500 μg/ml PEG-LM111 conjugate, the gel point occurred in less than 14 minutes. PEG-only (no PEG-LM111 conjugate) and PEG-LM111 hydrogel mechanical properties continued to evolve for approximately 1 hour. The final gel stiffness (|G*|) increased with increasing concentrations of PEG-LM111 conjugate in the precursor solution (Figure 17B).

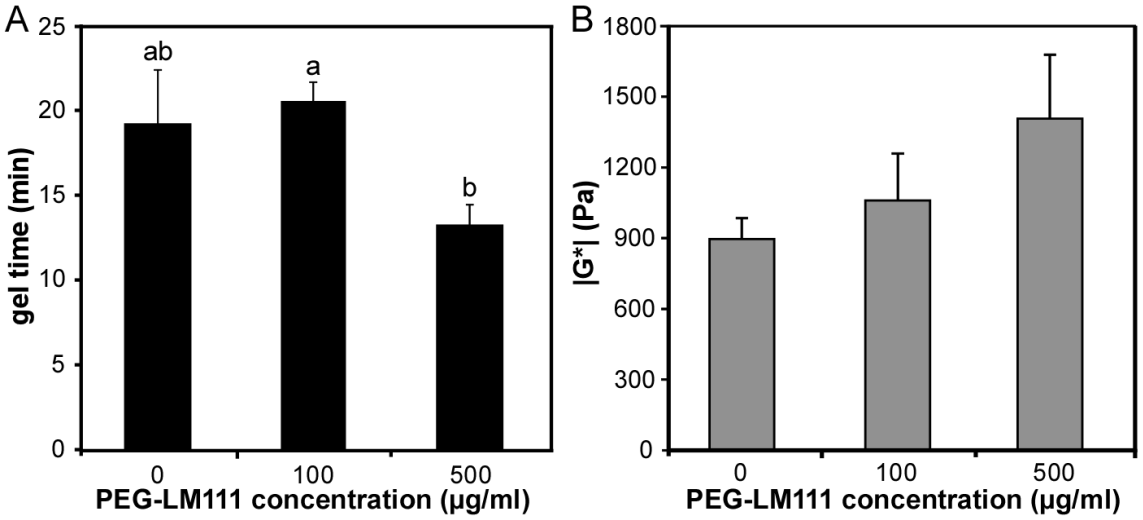

Figure 17. Rheometric characterization of injectable PEG-LM111 hydrogels. (A) Gel point occurred in less than 25 minutes for hydrogels containing different concentrations of PEG-LM111 conjugate (mean ± SEM, n=5, conditions labeled with different letters significantly different, p<0.04). (B) Final gel stiffness (|G*|) of PEG-LM111 hydrogels increased with increasing concentration of PEG-LM111 conjugate in the precursor solution.

4.3.2 Generation of Luciferase Expressing Porcine NP Cells

To track cells following delivery to the IVD using in vivo bioluminescent imaging, it was necessary to verify that NP-luc cells maintain luciferase expression for at least 4 weeks post transduction. Luciferase expression in NP-luc cells cultured in monolayer increased approximately 3.5-fold from day 4 to day 35 post transduction; however, there was no significant difference in expression between day 24 and day 35 (ANOVA, $p>0.05$) (Figure 18).

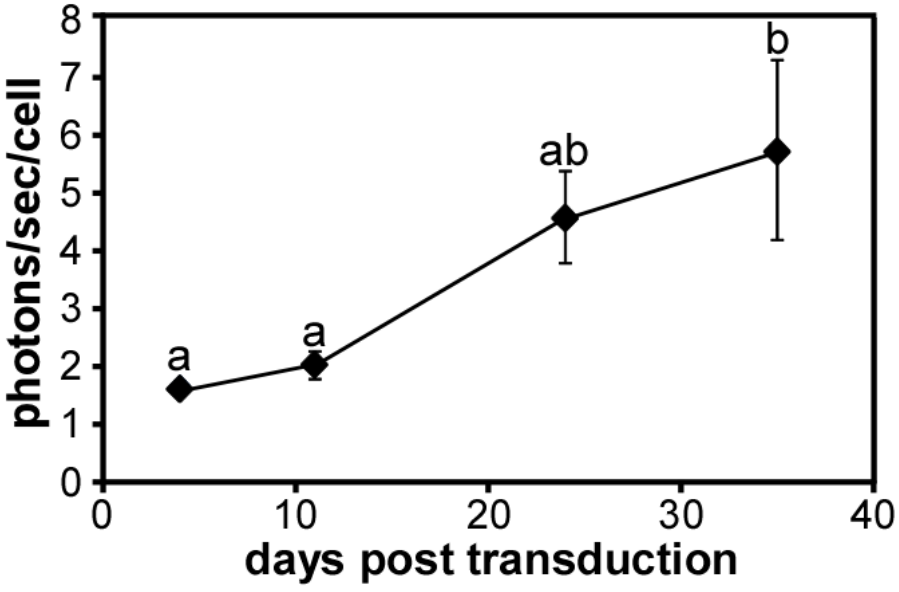

Figure 18. Luciferase activity in cultured porcine NP cells. NP cells transduced with lentivirus encoding for firefly luciferase were cultured for 35 days post transduction. At each time point, photons per second per cell was calculated from measured bioluminescent intensity 10 minutes after addition of luciferin to the media (mean ± SEM, n=3, conditions labeled with different letters significantly different, $p<0.03$).

4.3.3 Cell Retention in IVD Motion Segments

Bioluminescence imaging was utilized to examine the effect of PEG-LM111 hydrogel carrier on NP-luc cell retention and survival in IVD motion segments. The total number of photons in a defined region of interest (ROI) was quantified at multiple time points following cell injection (Figure 19B). Cell retention in IVD explants was significantly higher (ANOVA, $p<0.001$) over 14 days in culture when cells were delivered within a PEG-LM111 hydrogel carrier, as compared to cells in PBS (Figure 19A). At 30 minutes post injection, bioluminescent signal was 13-fold higher when cells were

delivered to IVDs in PEG-LM111 biomaterial; however, signal rapidly decayed over the first 24 hours of culture for both groups. NP-luc cells in IVD explants could be detected via bioluminescent imaging for at least 14 days post injection.

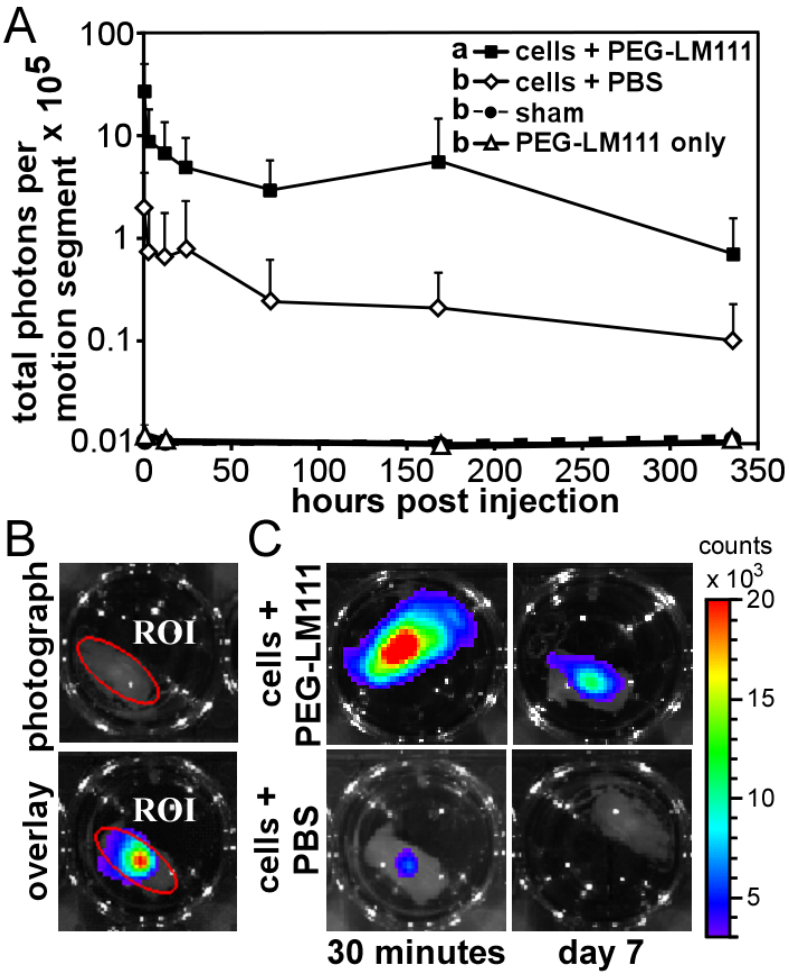

Figure 19. Cell retention in IVD motion segments. (A) NP-luc cells were delivered to rat IVD motion segments and explants were cultured for 14 days. Cell retention, as measured by total photons per motion segment, was higher for cells delivered in PEG-LM111 hydrogel precursor solution as compared to cells delivered in PBS (mean ± SEM, n=6, conditions labeled with different letters significantly different, $p<0.001$). (B) Region of interest (ROI) defined on photographic image of motion segment used quantify total photons per motion segment in overlay image. (C) Representative images of IVD motion segments 30 minutes and 7 days post cell injection within PEG-LM111 biomaterial hydrogel precursor solution or PBS.

4.3.4 Cell Transfer to IVD Motion Segments

To determine whether an optimized PEG-LM111 hydrogel improved cell transfer to the disc space, cell retention immediately following delivery, or both, IVD motion segments that received NP-luc cells delivered in either PBS or PEG-LM111 hydrogel precursor solution were imaged immediately following cell delivery, and every 2 minutes for 28 minutes after delivery (Figure 20). At time 0, bioluminescent signal was the same for cells delivered in PBS and cells delivered in PEG-LM111 hydrogel precursor solution. For both groups, signal decayed over the first 28 minutes following delivery; however, total photons per motion segments decreased more rapidly when cells were delivered in PBS as compared to cells delivered in PEG-LM111 hydrogel precursor solution.

To evaluate PEG-LM111 hydrogel solution transfer to the IVD space, cells were delivered to IVD motion segments within either PBS or the PEG-LM111 hydrogel precursor solution and, 30 minutes after delivery, explants were fixed and processed for immunohistochemical analysis. Immunostaining for LM111 revealed that the PEG-LM111 hydrogel could be detected in the disc space, with positive staining observed when cells were delivered in PEG-LM111 hydrogel precursor solution, but not when cells were delivered in PBS (Figure 21).

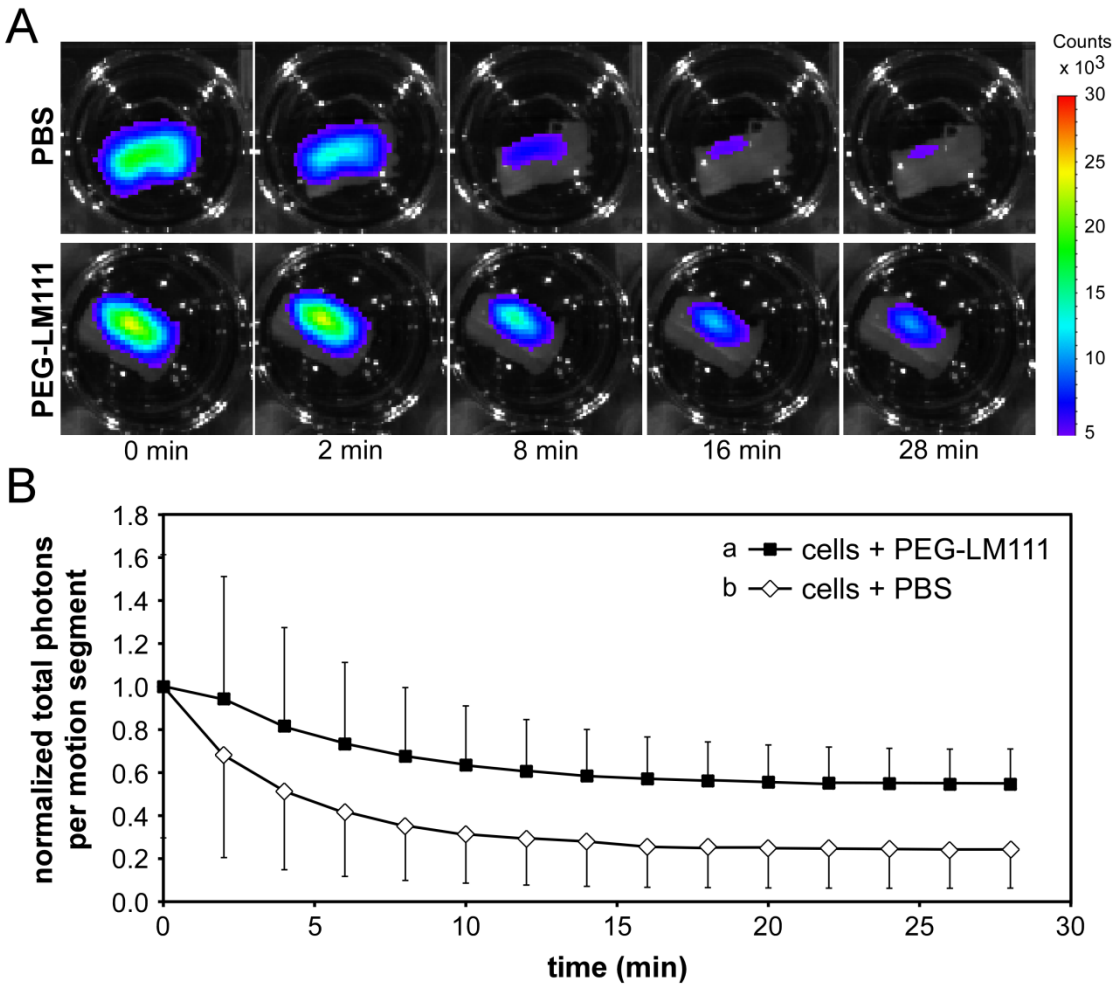

Figure 20. Cell transfer to IVD motion segments. (A) NP-luc cells were delivered to rat IVD motion segments and cell transfer and retention were evaluated via bioluminescent imaging in the 30 minutes immediately following cell delivery. (A) Representative images of IVD motion segments 0, 2, 8, 16, and 28 minutes after NP-luc cells were injected within PBS or PEG-LM111 hydrogel precursor solution. (B) The number of cells delivered to IVD motion segments, as measured by total photons per motion segment, was the same for cells delivered in PEG-LM111 hydrogel precursor solution and PBS at time 0. Cell retention over 30 minutes post injection was higher for cells delivered in PEG-LM111 hydrogel precursor solution as compared to cells delivered in PBS (mean ± SEM, n=3, conditions labeled with different letters significantly different, $p<0.001$).

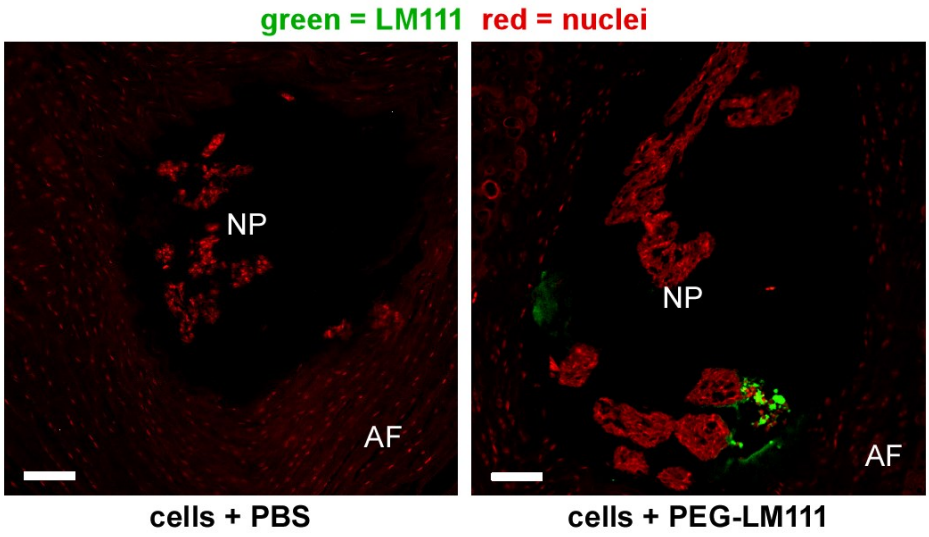

Figure 21. Representative images of IVD motion segments 30 minutes after cells were delivered either in PBS (left) or PEG-LM111 hydrogel precursor solution (right) that were stained for LM111 (green: LM111; red: nuclei). Scale bar = 100 μm.

4.3.5 In Vivo Cell Delivery to Rat IVD

Preliminary studies were performed to determine if NP-luc cells, delivered to the rat tail IVD in PBS, PEG-LM111 hydrogel precursor solution, or PEG-only hydrogel precursor solution, could be detected via in vivo bioluminescent imaging. Cells could be detected in vivo up to 7 days following injection into the IVD space (Figure 22); however, bioluminescent signal was low, variable, and no signal was observed at multiple time points whether cells were delivered in PEG-LM111 hydrogel precursor solution, PEG-only hydrogel precursor solution or PBS. Due to these limitations, and the small sample size of this study, differences between luminescent signal intensities amongst cell carrier (PBS or PEG hydrogel precursor solutions) were not analyzed. In certain animals, cells

could not be detected in vivo, but could be detected in the IVD space ex vivo immediately following sacrifice (Figure 23). For all animals at all in vivo imaging time points, maximum luminescent signal did not exceed 3500 counts over a 5 minute exposure time, possibly due to a low number of delivered cells, low luciferase expression levels, poor luciferin distribution to the tail, and signal attenuation by the collagenous tail skin.

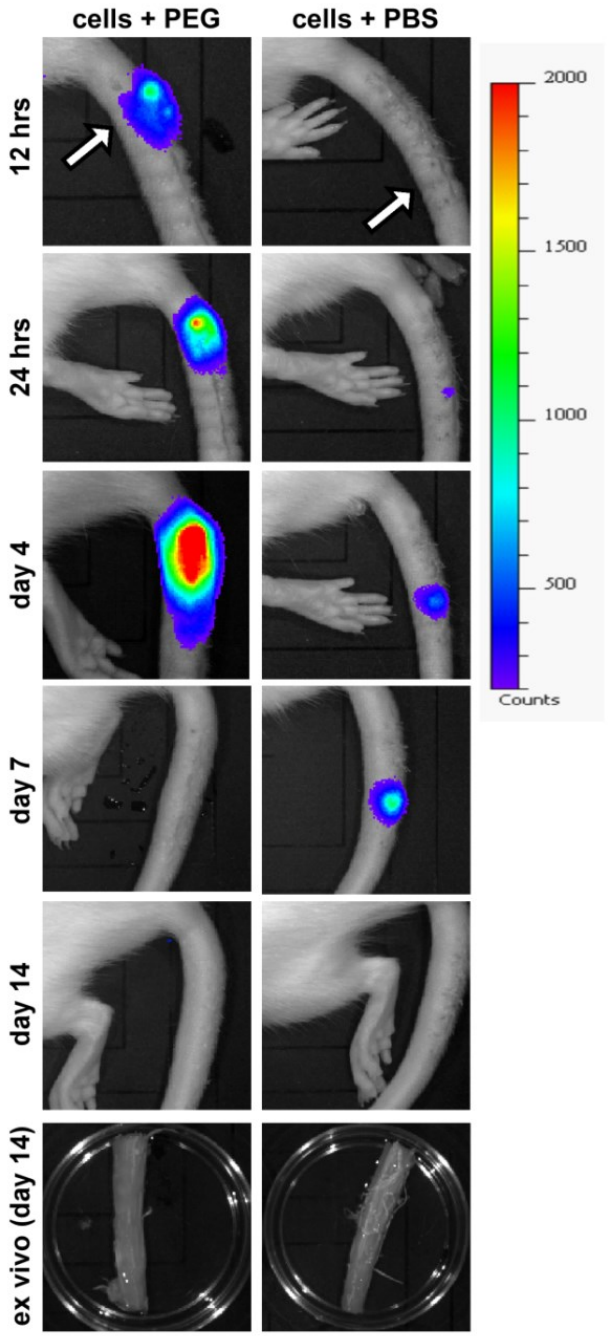

Figure 22. In vivo bioluminescent imaging at several time points after NP-luc cells were injected into the rat tail disc space, and ex vivo imaging of IVD motion segments immediately after animal sacrifice on day 14. Arrows indicate IVDs to which cells were delivered either in a PEG hydrogel precursor solution or PBS.

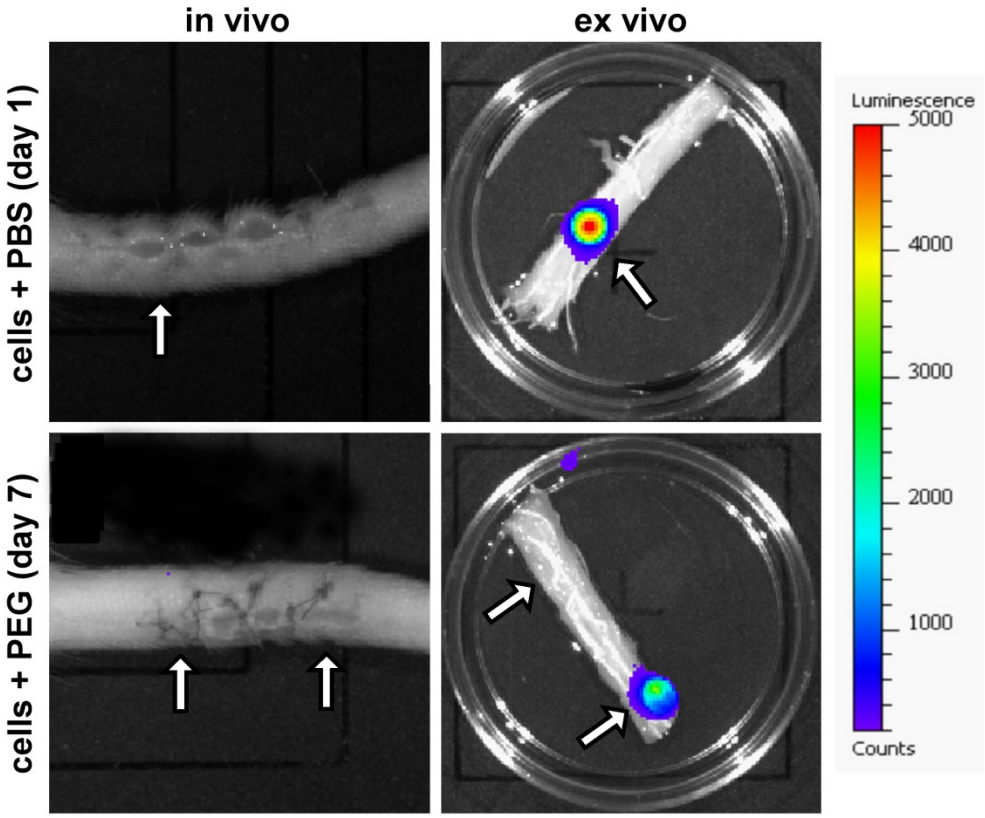

Figure 23. In vivo and ex vivo bioluminescent imaging of rat tail IVDs at specific time points after cells were delivered to the disc in either PBS (top row) or in a PEG hydrogel precursor solution (bottom row). Arrows indicate disc spaces receiving injection of cells either in PBS (top) or in a PEG hydrogel precursor solution (bottom).

4.4 Discussion

The goal of this work was to develop an injectable, laminin-functionalized hydrogel as a biomaterial carrier for cell delivery to the IVD. Laminin presenting substrates have previously been shown to promote the morphology and phenotype of immature NP cells in vitro, and to promote increased cell attachment and elevated

glycosaminoglycan synthesis for primary NP cells in culture [33, 95]. For these reasons, a 3D biomaterial carrier presenting laminin was developed as a carrier for primary NP cells.

PEG-LM111 conjugates were crosslinked to form hydrogels upon the addition of PEG-octoacrylate and PEG-dithiol via a Michael type addition reaction without the need for an initiator, as has been shown for PEG hydrogels designed for protein delivery [191]. Gelation occurred within 20 minutes under physiological conditions independent of the concentration of PEG-LM111 conjugate in the precursor solution. The reaction was thus considered to provide for an acceptable working time for cell delivery in vivo since it allows time for cell suspension and accurate needle placement within the disc space [195]. The dynamic stiffness of PEG-LM111 hydrogels in shear increased slightly from ~0.9 kPa to ~1.5 kPa with increasing concentration of PEG-LM111 conjugate in the precursor solutions, all values that are only slightly lower than values reported previously for the dynamic shear moduli of human NP (7.4 – 19.8 kPa) [181, 183]. Stiffness can be readily manipulated to achieve a targeted goal by modifying the amount of PEG within the crosslinked hydrogel. In a prior report of PEG-laminin hydrogels crosslinked by photopolymerization, hydrogel stiffness decreased with increasing concentration of the PEG-laminin conjugate precursor solutions [162], a finding that differs from that observed in the current study. This difference likely reflects intrinsic differences between step-growth and chain-growth polymerization reactions in the two different systems; our finding suggests that high concentrations of PEG-LM111 conjugate in the precursor

solution reduces the number of non-idealities in the crosslinked hydrogel network, which are introduced in hydrogels formed by Michael-type addition reactions at low PEG concentrations [196]. This is a feature that can be modulated to achieve a targeted outcome through biomaterial design if it should become desirable to modulate the porosity or stiffness, for example, to achieve a specific set of biological outcomes [197]. Here our goal was to obtain a material that retained laminin functionality, provided good working characteristics, and physical properties that approximated that of the native NP. Overall, these findings suggest this laminin-functionalized biomaterial can provide an injectable carrier for delivering cells to the IVD.

To evaluate cell retention within the disc space following delivery, much of the work using animal models of disc degeneration has relied on histological techniques subsequent to animal sacrifice at specific time points, which precludes in vivo assessment and longitudinal tracking of cell therapy. Bioluminescence imaging may be a useful tool for evaluating the efficacy of a biomaterial carrier for cell delivery; however, long-term stable expression of luciferase in delivered cells must be achieved in order to evaluate cell retention and survival in the disc space. Towards the goal of in situ and in vivo assessment of the effect of our PEG-LM111 biomaterial carrier on NP cell retention and survival in the disc space, we demonstrate here sustained expression of the luciferase reporter gene in immature primary NP cells over 5 weeks in culture. This is a significant improvement over a transient luciferase expression reported in rabbit NP cells transfected

with a recombinant adenovirus, which allowed for follow-up of cell viability for only about 6 days [136]. Although sustained luciferase expression in NP cells was achieved, expression levels did vary significantly over time, preventing the use of bioluminescent signal intensity to directly quantify number of cells in cell tracking studies.

Many biomaterials have been investigated as carriers for cell delivery to the IVD in numerous animal models of disc degeneration [22]. While solid scaffolds are widely used to support IVD cell growth ex vivo [19, 100, 198], we have focused in this study on injectable, in situ polymerizing three-dimensional hydrogels that could maintain the rounded phenotype for NP cells. Naturally derived biopolymers and self-polymerizing biomaterials such as collagen, chitosan and fibrin are most commonly utilized for NP regeneration, although the physical properties and chemical composition of these biomaterials is not easily manipulated [26]. Chemical crosslinking of alginate is the most commonly used approach to promote a rounded phenotype for NP cells and is the standard for cell culture studies [105]. More recently, photocrosslinking of alginate has been proposed as a means to manipulate a three-dimensional matrix for NP cells [199], and a self-assembling peptide hydrogel has been similarly investigated [200]. Few injectable biomaterials have presented functional ECM ligands that can retain native NP cell-matrix interactions and facilitate cell-mediated matrix remodeling, which may be important for promoting long-term cell survival and biosynthesis.

While prior studies have established the importance of a biomaterial carrier for improved cell transfer to the disc space immediately following delivery [136], little is known of the role of the biomaterial carrier in promoting long-term cell retention and survival [188]. Studies were performed here to test for an ability of the newly synthesized PEG-LM111 biomaterial to promote NP cell retention and survival in the disc space, by following luciferase expression for immature primary NP cells delivered via needle injection to the disc space in an organ culture model. The optimized PEG-LM111 hydrogel significantly improved primary NP cell retention and survival as compared to cells delivered in an uncrosslinked, liquid suspension. Thirty minutes after injection, bioluminescent signal was 13-fold higher when cells were delivered in a PEG-LM111 biomaterial, suggesting that cell delivery in the absence of a solid-setting carrier may result in dramatic cell loss [136]. These findings suggest that an optimized PEG-LM111 hydrogel is able to crosslink in situ and significantly improve upon the retention of delivered cells. The PEG-LM111 hydrogel was unable to inhibit complete cell loss, however, as cells continued to die or migrate from the disc space over the first 24 hours after delivery, likely due to a high intra-discal pressure that induced extrusion through the injection site. This highlights the need for annular repair techniques in addition to biomaterials for cell delivery, or high-strength crosslinked biomaterial carriers, that may need to be employed to slow or eliminate cell loss following delivery [201].

In a prior study, significantly higher bioluminescent signal was shown when cells were delivered to IVD explants within a fibrin gel carrier, as compared to cells in media, at 30 minutes after delivery [136]. Similar findings were reported here for cells delivered within a PEG-LM111 hydrogel precursor solution compared to cells delivered in PBS; however, these studies did not evaluate whether the difference in bioluminescent signal at this early time point is due to improved initial cell transfer, improved cell retention due to gel crosslinking, or both. Here, short-term bioluminescent imaging studies were performed to evaluate cell retention in IVD motion segments immediately following delivery. At time 0, total photons emitted from IVD motions segments were the same whether cells were delivered with or without a PEG-LM111 hydrogel precursor solution, suggesting an equivalent number of viable cells were initially delivered to each disc regardless of carrier. Although bioluminescent signal decreased for both groups over the first 30 minutes following delivery, total photons per motion segments was significantly higher when cells were delivered in the PEG-LM111 hydrogel precursor solution. These findings provide further evidence that this injectable, PEG-LM111 hydrogel improves retention of delivered cells, at least at early time points, by preventing leakage from the disc space.

In addition to evaluating cell retention in IVD motion segments, it is of interest to evaluate material distribution in the disc space. When cells were delivered to motion segments within a PEG-LM111 hydrogel, the material was detected within in the disc

space 30 minutes after delivery by positive staining for LM111. Staining was isolated to a small region of the NP, suggesting that material either is not able to distribute throughout the disc space, possibly due to incomplete nucleotomy, not distributed uniformly before crosslinking, or that the material is quickly extruded from the disc space due to a high intra-discal pressure. Similar findings were reported for cells delivered to minipig lumbar IVDs within a fibrin carrier supplemented with aluminum oxide particles for evaluation of material retention by micro-computed-tomography [137]. Although the fibrin carrier appeared distributed throughout the disc on day 0, over 90% of the material and 93% of the cells were lost by day 3 [137]. Overall, these findings suggest cell loss following delivery may be attributed to biomaterial carrier extrusion from the disc space and point towards an important role for AF repair.

Cell delivery to the disc space has been performed in animal models of disc degeneration and in human subjects for more than a decade [22]. Cell retention within the disc space is difficult to follow in the living subject, particularly for clinical studies that rely upon minimal modification of delivered cells. Much of the work studying cell delivery to the disc space in animal models has relied on histological techniques subsequent to animal sacrifice at specific time points, which precludes in vivo assessment and longitudinal tracking of cell therapy. In a recent study, investigators demonstrated the feasibility of bioluminescence imaging for monitoring the viability of luciferase expressing cells within the lumbar spine in a rodent model up to 14 days after cell

implantation [202]. Here, we performed preliminary studies to determine if similar in vivo bioluminescent imaging could be used to track NP-luc cells delivered to the rat caudal IVD. Although cells could be detected in the disc space for up to 7 days following delivery, bioluminescent signal intensity was extremely low even over long exposure times, and signal varied over time whether cells were delivered in a PEG hydrogel precursor solution (PEG-LM111 or PEG-only) or in PBS. Photon emission at the tissue surface depends on the number of delivered cells, the photon flux per cell (luciferin expression levels and luciferin availability), and the signal attenuation by the tissue [203]. Therefore, the very low bioluminescent signals that we reported from in vivo imaging are likely due to a combination of factors, including our delivery of comparatively low cell numbers to the disc space, low luciferase expression levels in delivered cells, poor luciferin distribution to the tail, and signal attenuation by the collagenous tail skin. In some cases, cells could not be detected in vivo, but could be detected in the IVD space ex vivo immediately following sacrifice. This finding suggests that either luciferin did not reach the caudal IVD space following intraperitoneal injection, or that signal was attenuated by tissue surrounding the disc space. In a subset of animals, no signal was detected in discs receiving cells injected in either a PEG hydrogel precursor solution (PEG-LM111 or PEG-only) even ex vivo at early time points. This could be due to a failure to inject cells into the NP region of the disc, or rapid extrusion of cells from the IVD space. Overall, these findings demonstrate numerous limitations that must be overcome in order

to use in vivo bioluminescent imaging to evaluate the effects of a PEG-LM111 hydrogel on NP-luc cell retention and survival following delivery to the rat caudal IVD.

4.5 Conclusion

We report here the development and characterization of an injectable laminin functionalized PEG hydrogel as a biomaterial carrier for cell delivery to the IVD. The findings from this study demonstrate the ability of PEG-LM111 hydrogels to crosslink under physiological conditions without the need for an initiator. Additionally, delivery within our PEG-LM111 hydrogel significantly improved primary NP cell retention in the disc space as compared to cells delivered without a carrier in an organ culture model. Bioluminescence imaging for evaluating the effect of our carrier on persistence and viability of delivered cells in vivo merits further investigation. In summary, these findings suggest that this laminin functionalized hydrogel may be a useful carrier for cell-based strategies aimed at regenerating the IVD.

5. Conclusion and Future Directions

There is significant interest in cell-based therapies for treating IVD disorders, with the majority of these strategies focused on NP regeneration as a means to impede or reverse disc degeneration. Aging associated loss of immature, notochordal-like NP cells has been hypothesized to be a contributing factor to IVD degeneration, and suggests that promoting or maintaining this distinct cell phenotype may be useful for NP tissue regeneration. Immature, notochordal-like NP cells reside in an environment rich in laminin ECM proteins and laminin receptors, and NP cell-laminin interactions have been shown to promote cell adhesion and biosynthesis. Motivated by these findings, two types of LM111 functionalized PEG hydrogels were synthesized and characterized, using photo-initiated or spontaneous crosslinking strategies for injectable hydrogel delivery. Immature NP cell interactions with photocrosslinked PEG-LM111 hydrogels were evaluated to determine hydrogel formulations that promote cell-cell interactions and phenotypic marker expression characteristic of notochordal-like NP cells. Additionally, studies were performed to assess the potential use of an in situ crosslinking, injectable PEG-LM111 hydrogel as a biomaterial carrier for cell-based IVD regeneration. Results of the investigations reported in this dissertation produced several key findings:

- LM111 PEGylation via a heterobifunctional Ac-PEG-NHS at low ratios of PEG to LM111 (≤ 25:1) allows for the addition of functional acrylates groups onto native LM111 without significantly altering the protein's ability to mediate cellular function.

- Immunostaining of photocrosslinked PEG-LM111 hydrogels containing conjugates synthesized with varying ratios of Ac-PEG-NHS to LM111 revealed that a threshold level of protein modification likely must be achieved in order for PEG-LM111 conjugates to become part of the hydrogel backbone.
- LM111 may act as a survival ligand for primary immature NP cells cultured in PEG hydrogels under low cell density, serum free conditions, and PEGylated LM111 retains this biological function of the native protein in 3D culture.
- Photocrosslinked PEG-LM111 hydrogel mechanical properties can be tuned within the range of dynamic shear moduli values previously reported for human NP by altering both the total PEG concentration and PEG-LM111 conjugate concentration; however, hydrogel stiffness is dominated by the former.
- NP cells cultured within soft, photocrosslinked PEG-LM111 hydrogels more highly expressed proposed immature NP phenotypic markers N-cadherin and cytokeratin 8, suggesting that soft, LM111 functionalized hydrogels may promote both cell-cell and cell-matrix interactions characteristic of an immature NP cell phenotype.
- NP cells cultured on soft, PEG-LM111 hydrogel substrates behaved similarly to cells cultured on polymerized basement membrane extract (BME) substrates, indicating that specific formulations of the photocrosslinked PEG-LM111 hydrogel are able to mimic physical and biochemical properties of polymerized BME previously shown to promote an immature NP cell phenotype.

- Injectable PEG-LM111 hydrogels synthesized via the addition of PEG-octoacrylate and PEG-dithiol to PEG-LM11 conjugates are able to crosslink under physiological conditions in approximately 20 minutes without the need for an initiator.
- An optimized injectable PEG-LM111 hydrogel is able to crosslink *in situ* and significantly improve upon the retention of cells delivered to the disc as compared to cells delivered without a hydrogel carrier.
- Cell extrusion from the disc space following delivery with or without a hydrogel carrier highlights the need for anular repair techniques in addition to biomaterials for cell delivery, or high-strength crosslinked biomaterial carriers in order to improve cell retention.
- Bioluminescence imaging may be a useful tool for evaluating the effect of PEG-LM111 hydrogel carrier on persistence and viability of delivered cells *in vivo*; however further investigation is necessary to overcome discussed limitations.

The findings presented here also suggest a number of areas for future study:

1. Studies in Chapters 2 and 3 described the development and characterization of PEG-LM111 hydrogels, and evaluated the effects of hydrogel stiffness and LM111 ligand on immature NP cell phenotype *in vitro*. While LM111 is known to support NP cell adhesion, LM332 and LM5111 have been shown to be preferred ligands for NP cell attachment and spreading [95]. NP cell behavior,

include phenotypic marker expression and survival, in PEG hydrogels functionalized with these laminin isoforms remains to be investigated. One major limitation that must be overcome in order to develop PEG-laminin hydrogels functionalized with LM332 or LM511 is ligand availability, since these ligands must be purified from cell supernatant or extracted from tissues. One possible approach would be to recombinantly express these isoforms. Additionally, a high throughput culture system could be developed for evaluating cell behaviors within PEG-laminin hydrogels, which would significantly reduce the amount of laminin ligand needed for each study.

2. Studies in Chapter 3 demonstrated that soft, LM111 functionalized substrates promote proteoglycan synthesis by NP cells in 2D; however, proteoglycan production by immature NP cells encapsulated in 3D PEG-LM111 hydrogels remains to be thoroughly investigated. Although the studies described here were aimed at evaluating the effect of hydrogel formulation on NP cell phenotype, assessing matrix production by NP cells cultured within PEG-LM111 hydrogels will be key to understanding which hydrogel formulations (if any) promote regeneration of a proteoglycan-rich NP-like ECM. Since cell-cell interactions may be important for NP viability and biosynthesis, modifications to the current hydrogel system to include degradable linkages would likely result in improved NP tissue regeneration. One possible

approach would be to incorporate MMP degradable linkages, since MMP expression is known to play an important role in degradation of the NP [204]. Alternatively, a degradable linkage such as poly(lactic acid) could be incorporated into PEG-LM111 hydrogels to engineer scaffolds with tailored degradation behavior [205]. Studies of NP cell behavior in PEG-LM111 hydrogels with controllable degradation properties, including cell clustering and matrix production, would lend further insight into the potential of LM111 functionalized hydrogels for promoting NP tissue regeneration.

3. Studies in Chapter 3 demonstrated higher expression of certain immature, NP markers such as N-cadherin and cytokeratin 8 for immature NP cells cultured in soft, PEG-LM111 hydrogels. While these findings show that these specific hydrogel formulations promote certain characteristics of the immature NP cell phenotype, expression of only a subset of proposed NP cell markers was investigated. Future studies evaluating a broader set of NP markers would be useful for further understanding of the effects of LM111 ligand and matrix stiffness on immature NP cell phenotype.
4. Studies in Chapter 4 revealed that NP cell delivery to IVD motion segments within a PEG-LM111 hydrogel resulted in improved cell retention or survival in the disc space as compared to cells delivered in liquid suspension. Whether this is due to physical gelation of the hydrogel preventing cell leakage,

presence of the LM111 ligand contributing to cell survival, or both, remains to be investigated. Future studies of cell persistence in IVD explants following delivery within the PEG-LM111 hydrogel as compared to that of cells delivered in a PEG-only hydrogel would help elucidate the role of the LM111 ligand in cell retention and survival. Additionally, varying PEG-LM111 hydrogel physical properties to reduce gelation time and increase gel stiffness may reduce cell leakage from the IVD space, and merits further investigation.

5. Preliminary in vivo studies described in Chapter 4 showed that delivered NP-luc cells could be detected within the rat tail IVD space via bioluminescent imaging up to 7 days following delivery. Future work is necessary to determine the effects of the developed PEG-LM111 hydrogel carrier on primary NP cell retention, survival and matrix production in vivo. However, there are several challenges that must be overcome to facilitate these studies. Cell delivery to the rat tail IVD creates numerous surgical challenges due its small size; therefore, future studies in a larger animal model would be useful for evaluating the potential of an injectable PEG-LM111 hydrogel as a carrier for cell-based regeneration of the NP. Challenges related to bioluminescent imaging could potentially be overcome by increasing the number of delivered cells, increasing luciferase expression in transduced NP cells, or through alternate luciferin delivery routes to improve luciferin distribution to the disc

space. While this would provide useful information cell persistence in the disc space, additional outcome measures of cell viability, sGAG production, and NP water content will be key to evaluating the potential of PEG-LM111 hydrogels for cell-based NP regeneration.

6. Studies described in this dissertation utilized primary porcine notochordal-like NP cells; however, there is no available human source of notochordal-like NP cells for cell-based IVD regeneration. For this reason, numerous stem cell sources have been investigated for their ability to differentiate towards and NP-like cell phenotype. Future work to evaluate induced pluripotent stem cell and/or mesenchymal stem cell differentiation in PEG-LM111 hydrogels will be important for determining if laminin-functionalized hydrogels can promote an NP cell phenotype in these more available cell types.
7. Finally, while the NP region of the disc is an immunoprivileged site, it is clear from the studies described in Chapter 4 and those previously reported in the literature that biomaterial carriers can be extruded from the disc space following delivery. Therefore, studies must be performed to evaluate the in vivo immune response to injected or implanted PEG-LM111 hydrogels. Future studies examining the extent of any immune reaction to PEG-LM111 hydrogels implanted subcutaneously in a rat model would be critical to understanding the usefulness of the material as a carrier for cell delivery to the disc.

In summary, this dissertation described the development and characterization of two different LM111 functionalized PEG biomaterials. Studies examining primary NP cell interactions with photocrosslinkable PEG-LM111 hydrogels indicated that soft, LM111 functionalized hydrogels may maintain or promote a notochordal-like NP cell phenotype. Since photocrosslinking can not easily be achieved in the IVD space, a Michael-type addition reaction was employed to synthesize and injectable PEG-LM111 hydrogel capable of crosslinking in situ without the need for an initiator or UV light. Studies examining cell retention in IVD explants showed that cell delivery within an optimized PEG-LM111 hydrogel significantly improved primary NP cell retention in the disc space as compared to cells delivered without a carrier. Overall, these findings suggest that this injectable laminin-functionalized biomaterial may be a convenient and biocompatible carrier for delivering cells to the IVD.

Appendix A

Preliminary studies were performed to determine culture conditions under which the majority of primary porcine NP cells encapsulated in photocrosslinked PEG-DA hydrogel (containing no LM111) would die over 14 days in culture. Cells were encapsulated in PEG-DA hydrogels at two different cell densities (2×10^6 or 10×10^6 cells/ml) as described in Section 2.2.7. Cell laden hydrogels were cultured (37 °C, 5% CO_2, 20% O_2) for 14 days in media (Ham's F-12 media, 10 mM HEPES, 100 U/ml penicillin, and 100 U/ml streptomycin) either with or without 1% FBS. Cell viability (% live) was determined at multiple time points (days 0, 7 and 14) as described in Section 2.2.7. Less than 20% of cells cultured in PEG-DA hydrogels at 2×10^6 cells/ml under serum free conditions remained viable after 14 days in culture (Figure 24). Therefore, these culture conditions were utilized for studies designed to assess the ability of LM111 to promote NP cell survival in 3D culture (Chapter 2).

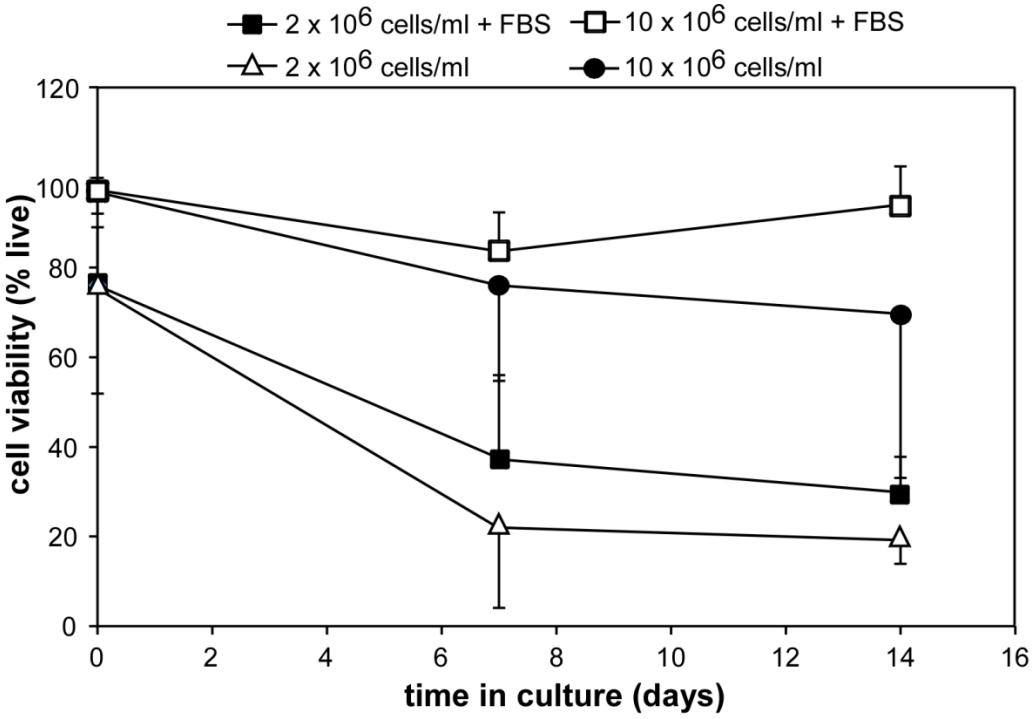

Figure 24. Cell viability in PEG-only hydrogels. NP cell viability in PEG-based hydrogels after 0, 7, and 14 days of culture. Percent viability determined by counting the number of live cells as a percentage of total cells in images of hydrogels stained with Live/Dead viability assay (mean ± SD, n=3).

Appendix B

Cell delivery to the IVD within a PEG-LM1111 hydrogel carrier requires that the hydrogel precursor solution initially be liquid to allow for cell suspension and injection through a needle, and that the solution crosslink in situ following injection into the IVD space. Since photocrosslinkable PEG-LM111 hydrogels require UV light to initiate gelation, a UV fiber coupled LED system was developed in order to promote crosslinking of the PEG-LM111 biomaterial in the disc space via a fiber optic cable threaded through the injection needle.

Studies were performed to determine if a UV fiber coupled LED could be utilized to promote in situ gelation of photocrosslinkable PEG-LM111 hydrogel precursor solutions in a model disc space. A UV fiber optic cable (400 μm core, 0.48 NA fiber) was coupled to a LED light source (High Power Fiber-Coupled LED Light Source, 365nm UV, Mightex Systems, Pleasanton, CA) through a standard SMA fiber adaptor port (Figure 25A). A LED driver (maximum current 1000 mA, Mightex Systems, Pleasanton, CA) was utilized to drive the LED light source. A model disc containing a cylindrical hole in a dacron mold with a side port to allow insertion of the UV fiber optic cable was used to evaluate crosslinking in situ. PEG-LM111 hydrogel precursor solution (10% PEG-DA, 0.1% Irgacure 2959®) was prepared as described in Section 2.2.5 and 20 μl was loaded into the model disc space. The fiber optic tip was then inserted through the side port and 350 mA power was supplied for 5 minutes (Figure 25B). UV light exposure via

the fiber optic cable resulted in a completely crosslinked PEG-LM111 hydrogel that could be removed from the model disc space (Figure 25C).

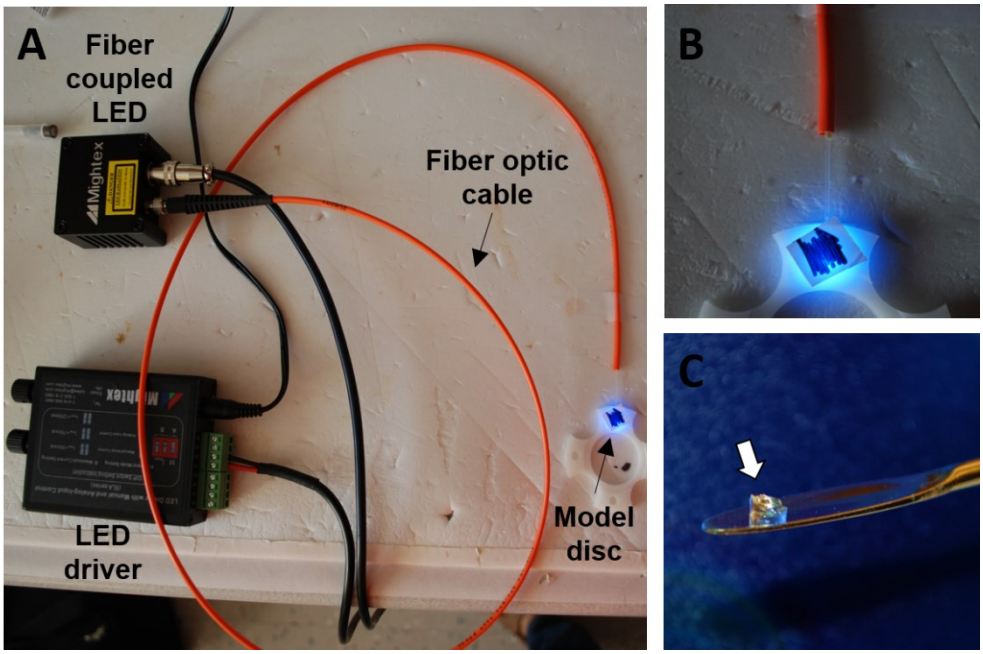

Figure 25. In situ crosslinking of photocrosslinkable PEG-LM111 hydrogel precursor solutions. (A) Setup of fiber coupled LED, driver, and fiber optic cable for UV crosslinking in a model disc. (B) UV irradiation of PEG-LM111 hydrogel precursor solution in a model disc space via a fiber optic cable. (C) Photocrosslinked PEG-LM111 hydrogel following crosslinking in model disc.

Preliminary experiments were performed to determine if the fiber optic cable threaded through a 22 gauge needle could be used to crosslink PEG-LM111 hydrogel precursor solution in a model disc space. Only a very small volume of the PEG-LM111 hydrogel precursor solution crosslinked in situ after 5 minute exposure to UV light (350 mA). This could be due to damage to the fiber optic tip causing light scattering, or due to the needle preventing light from reaching the hydrogel precursor solution.

Appendix C

Preliminary studies were performed to determine optimal LVE-LUC2 vector concentration in the transduction media that would promote long-term, stable luciferase expression in primary NP cells for organ culture and in vivo cell delivery studies (Chapter 4). First, to determine efficiency of lentiviral transduction of primary porcine NP cells, NP cells were transduced with a lentivirus driving constitutive expression of the green fluorescent protein (GFP) transgene under control of the EF1α promoter (LVE-GFP). A concentrated LVE-GFP (~70x concentration) was mixed with NP culture media at varying concentrations (μl concentrated virus per ml media supplemented with 4 μg/ml polybrene®) to prepare transduction media containing varying viral loads. Primary porcine NP cells were isolated as described in Section 4.2.2, plated at a density of 40,000 cells/cm^2 in culture media, and cells were allowed to adhere for 24 hours. Culture media was then aspirated from NP cells and replaced with transduction media containing varying viral loads (6 - 100 μl concentrated virus per ml media). After 24 hours, LVE-GFP containing media was aspirated and fresh culture media was added. GFP expressing porcine NP (NP-GFP) cells were cultured in monolayer (37 °C, 5% CO_2, 20% O_2) with media changes every 2-3 days. NP-GFP cells and untransduced control cells were lifted at multiple time points, washed twice in PBS, and the mean fluorescence intensity and percent of GFP positive cells was measured by flow cytometry (Accuri C6, BD Accuri Cytometers Inc., Ann Arbor, MI). Negative untransduced control cells were

used to establish a gate containing 98.5% of the GFP negative cells; the percent above this gate were considered positively labeled.

At day 3 post transduction, mean fluorescence intensity values increased with increasing viral load (μl concentrated LVE-GFP per ml media); however, similar expression levels were observed for all viral loads at later time points (Figure 26). At day 3 post transduction, greater than 97% of cells were GFP positive for all viral loads (data not shown).

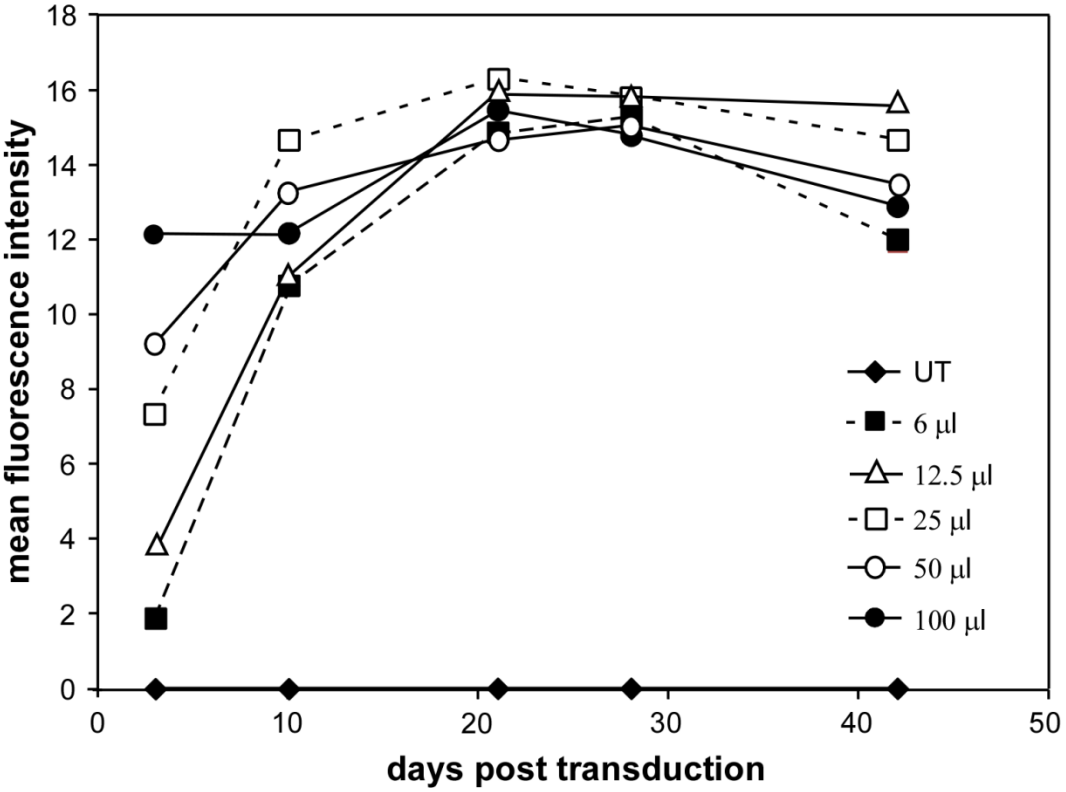

Figure 26. GFP expression in primary NP cells transduced with varying viral loads (μl concentrated LVE-GFP per ml media). UT = untransduced cells. At each time point, cells were lifted and analyzed by flow cytometry.

Since preliminary studies showed high levels of transduction and sustained GFP expression in primary NP cells after a single exposure to LVE-GFP containing supernatant, the luciferase2 transgene was cloned into the same lentiviral expression plasmid. The lentivirus driving constitutive expression of the luciferase2 transgene under control of the EF1α promoter (LVE-LUC2) was prepared as described in Section 4.2.3. Preliminary studies using this vector were performed to determine optimal LVE-LUC2 concentration in the transduction media that would promote long-term, stable luciferase expression in primary NP cells. A concentrated LVE-LUC2 vector (80x concentration) was mixed with NP culture media in varying amounts to prepare transduction media containing varying viral loads. Primary porcine NP cells were isolated as described in Section 4.2.2, plated at a density of 40,000 cells/cm^2 in culture media, and cells were allowed to adhere for 24 hours. Culture media was then aspirated from NP cells and replaced with transduction media containing varying amounts of concentrated LVE-LUC2 vector (5 – 38.3 μl per ml media supplemented with 4 mg/ml polybrene®). After 24 hours, transduction media was aspirated and fresh culture media was added. Luciferase expressing porcine NP (NP-luc) cells were cultured in monolayer (37 °C, 5% CO_2, 20% O_2) with media changes every 2-3 days and luciferase expression was evaluated as described in Section 4.2.3.

As expected, luciferase expression in NP cells increased with increasing concentrations of LVE-LUC2 vector in the transduction media (Figure 27). The most

stable luciferase expression was observed in cells transduced with the lowest amount of LVE-LUC2 vector (5 µl per ml media). Although this group was also shown to have the lowest luciferase expression, long-term stability of reporter gene expression is important for longitudinal cell tracking, and therefore this viral load was utilized for subsequent organ culture experiments described in Chapter 4.

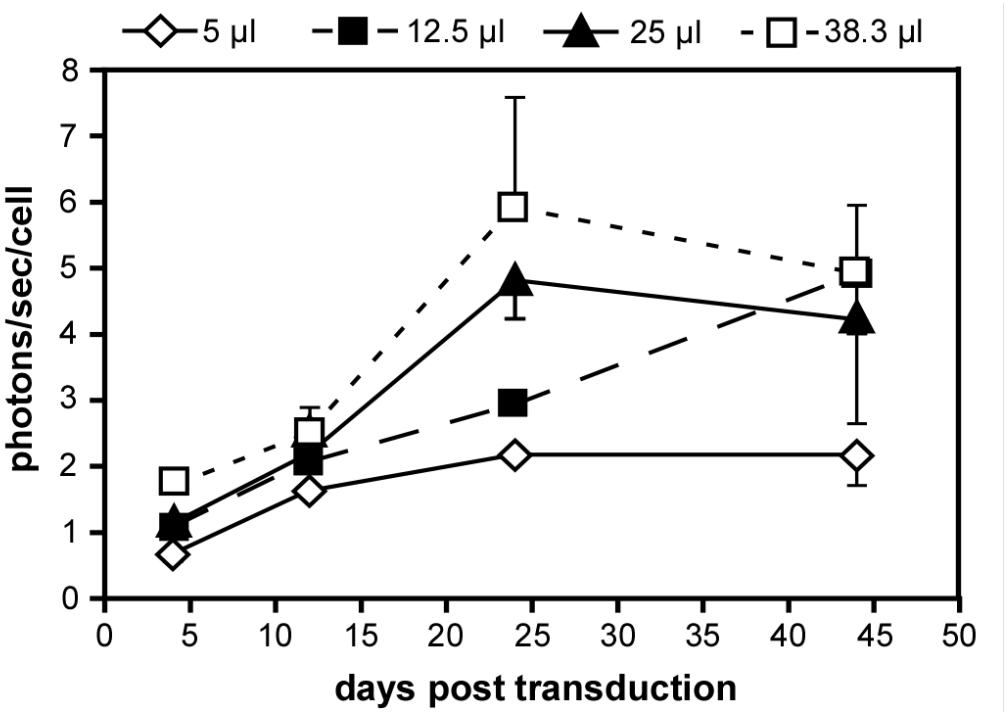

Figure 27. Luciferase activity in cultured porcine NP cells. NP cells transduced with lentivirus encoding for firefly luciferase at varying viral loads (µl concentrated LVE-LUC2 per ml media) to assess stability of luciferase expression over time in culture. At each time point, photons per second per cell was calculated from measured bioluminescent intensity 10 minutes after addition of luciferin to the media (mean ± SEM, n=3).

References

[1] Owens P. Emergency Department Visits and Inpatient Stays Related to Back Problems, 2008. In: Quality AfHRa, editor. Rockville, MD2011.

[2] Antoniou J, Steffen T, Nelson F, Winterbottom N, Hollander AP, Poole RA, et al. The human lumbar intervertebral disc - Evidence for changes in the biosynthesis and denaturation of the extracellular matrix with growth, maturation, ageing, and degeneration. J Clin Invest. 1996;98:996-1003.

[3] Boos N, Weissbach S, Rohrbach H, Weiler C, Spratt KF, Nerlich AG. Classification of age-related changes in lumbar intervertebral discs: 2002 Volvo Award in basic science. Spine (Phila Pa 1976). 2002;27:2631-44.

[4] Buckwalter JA. Aging and degeneration of the human intervertebral disc. Spine (Phila Pa 1976). 1995;20:1307-14.

[5] Lyons G, Eisenstein SM, Sweet MBE. Biochemical-Changes in Intervertebral-Disk Degeneration. Biochim Biophys Acta. 1981;673:443-53.

[6] Urban JP, Roberts S. Degeneration of the intervertebral disc. Arthritis Research & Therapy. 2003;5:120-30.

[7] Choi KS, Cohn MJ, Harfe BD. Identification of nucleus pulposus precursor cells and notochordal remnants in the mouse: implications for disk degeneration and chordoma formation. Dev Dyn. 2008;237:3953-8.

[8] Rufai A, Benjamin M, Ralphs JR. The development of fibrocartilage in the rat intervertebral disc. Anatomy and embryology. 1995;192:53-62.

[9] Trout JJ, Buckwalter JA, Moore KC, Landas SK. Ultrastructure of the Human Intervertebral-Disk .1. Changes in Notochordal Cells with Age. Tissue Cell. 1982;14:359-69.

[10] Guilak F, Ting-Beall HP, Baer AE, Trickey WR, Erickson GR, Setton LA. Viscoelastic properties of intervertebral disc cells. Identification of two biomechanically distinct cell populations. Spine (Phila Pa 1976). 1999;24:2475-83.

[11] Hunter CJ, Matyas JR, Duncan NA. The three-dimensional architecture of the notochordal nucleus pulposus: novel observations on cell structures in the canine intervertebral disc. Journal of Anatomy. 2003;202:279-91.

[12] Cappello R, Bird JLE, Pfeiffer D, Bayliss MT, Dudhia J. Notochordal cell produce and assemble extracellular matrix in a distinct manner, which may be responsible for the maintenance of healthy nucleus pulposus. Spine. 2006;31:873-82.

[13] Aguiar DJ, Johnson SL, Oegema TR. Notochordal cells interact with nucleus pulposus cells: Regulation of proteoglycan synthesis. Exp Cell Res. 1999;246:129-37.

[14] Boyd LM, Chen J, Kraus VB, Setton LA. Conditioned medium differentially regulates matrix protein gene expression in cells of the intervertebral disc. Spine. 2004;29:2217-22.

[15] Erwin WM, Inman RD. Notochord cells regulate intervertebral disc chondrocyte proteoglycan production and cell proliferation. Spine (Phila Pa 1976). 2006;31:1094-9.

[16] Korecki CL, Taboas JM, Tuan RS, Iatridis JC. Notochordal cell conditioned medium stimulates mesenchymal stem cell differentiation toward a young nucleus pulposus phenotype. Stem cell research & therapy. 2010;1:18.

[17] Oegema TR, Jr. The role of disc cell heterogeneity in determining disc biochemistry: a speculation. Biochem Soc Trans. 2002;30:839-44.

[18] Setton LA, Bonassar L.J., Masuda K. Regeneration and Replacement of the Intervertebral Disc. In: Lanza R. LR, Vacanti J.P., editor. Principles of Tissue Engineering. 3rd ed2007. p. 878-96.

[19] O'Halloran DM, Pandit AS. Tissue-engineering approach to regenerating the intervertebral disc. Tissue Eng. 2007;13:1927-54.

[20] Nerurkar NL, Elliott DM, Mauck RL. Mechanical design criteria for intervertebral disc tissue engineering. J Biomech. 2010;43:1017-30.

[21] Hudson KD, Alimi M, Grunert P, Hartl R, Bonassar LJ. Recent advances in biological therapies for disc degeneration: tissue engineering of the annulus fibrosus, nucleus pulposus and whole intervertebral discs. Curr Opin Biotechnol. 2013.

[22] Sakai D. Future perspectives of cell-based therapy for intervertebral disc disease. Eur Spine J. 2008;17 Suppl 4:452-8.

[23] Kandel R, Roberts S, Urban JP. Tissue engineering and the intervertebral disc: the challenges. Eur Spine J. 2008;17 Suppl 4:480-91.

[24] Horner HA, Urban JP. 2001 Volvo Award Winner in Basic Science Studies: Effect of nutrient supply on the viability of cells from the nucleus pulposus of the intervertebral disc. Spine (Phila Pa 1976). 2001;26:2543-9.

[25] Urban JP, Smith S, Fairbank JC. Nutrition of the intervertebral disc. Spine (Phila Pa 1976). 2004;29:2700-9.

[26] Lutolf M, Hubbell J. Synthetic biomaterials as instructive extracellular microenvironments for morphogenesis in tissue engineering. Nature biotechnology. 2005;23:47-55.

[27] Shin H, Jo S, Mikos AG. Biomimetic materials for tissue engineering. Biomaterials. 2003;24:4353-64.

[28] Petit A, Yao G, Rowas SA, Gawri R, Epure L, Antoniou J, et al. Effect of synthetic link N peptide on the expression of type I and type II collagens in human intervertebral disc cells. Tissue Eng Part A. 2011;17:899-904.

[29] Bridgen DT, Gilchrist CL, Richardson WJ, Isaacs RE, Brown CR, Yang KL, et al. Integrin-mediated interactions with extracellular matrix proteins for nucleus pulposus cells of the human intervertebral disc. J Orthop Res. 2013.

[30] Chen J, Jing L, Gilchrist CL, Richardson WJ, Fitch RD, Setton LA. Expression of laminin isoforms, receptors, and binding proteins unique to nucleus pulposus cells of immature intervertebral disc. Connect Tissue Res. 2009;50:294-306.

[31] Gilchrist CL, Chen J, Richardson WJ, Loeser RF, Setton LA. Functional integrin subunits regulating cell-matrix interactions in the intervertebral disc. J Orthop Res. 2007;25:829-40.

[32] Nettles DL, Richardson WJ, Setton LA. Integrin expression in cells of the intervertebral disc. J Anat. 2004;204:515-20.

[33] Gilchrist CL, Darling EM, Chen J, Setton LA. Extracellular matrix ligand and stiffness modulate immature nucleus pulposus cell-cell interactions. PloS one. 2011;6:e27170.

[34] Zhu J. Bioactive modification of poly(ethylene glycol) hydrogels for tissue engineering. Biomaterials. 2010;31:4639-56.

[35] Humzah MD, Soames RW. Human intervertebral disc: structure and function. Anat Rec. 1988;220:337-56.

[36] Urban JP, Holm S, Maroudas A, Nachemson A. Nutrition of the intervertebral disc: effect of fluid flow on solute transport. Clin Orthop Relat Res. 1982:296-302.

[37] Schollmeier G, Lahr-Eigen R, Lewandrowski KU. Observations on fiber-forming collagens in the anulus fibrosus. Spine (Phila Pa 1976). 2000;25:2736-41.

[38] Walmsley R. The development and growth of the intervertebral disc. Edinb Med J. 1953;60:341-64.

[39] Roberts S, Menage J, Duance V, Wotton S, Ayad S. 1991 Volvo Award in basic sciences. Collagen types around the cells of the intervertebral disc and cartilage end plate: an immunolocalization study. Spine (Phila Pa 1976). 1991;16:1030-8.

[40] Eyre DR, Muir H. Quantitative analysis of types I and II collagens in human intervertebral discs at various ages. Biochim Biophys Acta. 1977;492:29-42.

[41] Setton LA, Chen J. Cell mechanics and mechanobiology in the intervertebral disc. Spine (Phila Pa 1976). 2004;29:2710-23.

[42] Maroudas A, Stockwell RA, Nachemson A, Urban J. Factors involved in the nutrition of the human lumbar intervertebral disc: cellularity and diffusion of glucose in vitro. J Anat. 1975;120:113-30.

[43] Gower WE, Pedrini V. Age-related variations in proteinpolysaccharides from human nucleus pulposus, annulus fibrosus, and costal cartilage. J Bone Joint Surg Am. 1969;51:1154-62.

[44] Kitahara H. Histochemical study of the human intervertebral disc. Nihon Seikeigeka Gakkai zasshi. 1979;53:817-30.

[45] Jahnke MR, McDevitt CA. Proteoglycans of the human intervertebral disc. Electrophoretic heterogeneity of the aggregating proteoglycans of the nucleus pulposus. The Biochemical journal. 1988;251:347-56.

[46] Hayes AJ, Benjamin M, Ralphs JR. Extracellular matrix in development of the intervertebral disc. Matrix Biol. 2001;20:107-21.

[47] Sztrolovics R, Alini M, Mort JS, Roughley PJ. Age-related changes in fibromodulin and lumican in human intervertebral discs. Spine (Phila Pa 1976). 1999;24:1765-71.

[48] Gilchrist CL, Cao L., Setton L.A. Intervertebral Disc Cell Mechanics and Mechanobiology. In: B.A. W, editor. Orthopaedic Biomechanics: CRC Press; 2013. p. 75-100.

[49] Adams MA, Roughley PJ. What is intervertebral disc degeneration, and what causes it? Spine (Phila Pa 1976). 2006;31:2151-61.

[50] Hadjipavlou AG, Tzermiadianos MN, Bogduk N, Zindrick MR. The pathophysiology of disc degeneration: a critical review. J Bone Joint Surg Br. 2008;90:1261-70.

[51] Adams MA, Freeman BJ, Morrison HP, Nelson IW, Dolan P. Mechanical initiation of intervertebral disc degeneration. Spine (Phila Pa 1976). 2000;25:1625-36.

[52] Stokes IA, Iatridis JC. Mechanical conditions that accelerate intervertebral disc degeneration: overload versus immobilization. Spine (Phila Pa 1976). 2004;29:2724-32.

[53] Annunen S, Paassilta P, Lohiniva J, Perala M, Pihlajamaa T, Karppinen J, et al. An allele of COL9A2 associated with intervertebral disc disease. Science. 1999;285:409-12.

[54] Battie MC, Videman T. Lumbar disc degeneration: epidemiology and genetics. J Bone Joint Surg Am. 2006;88 Suppl 2:3-9.

[55] Boyd LM, Richardson WJ, Allen KD, Flahiff C, Jing L, Li Y, et al. Early-onset degeneration of the intervertebral disc and vertebral end plate in mice deficient in type IX collagen. Arthritis Rheum. 2008;58:164-71.

[56] Kawaguchi Y, Osada R, Kanamori M, Ishihara H, Ohmori K, Matsui H, et al. Association between an aggrecan gene polymorphism and lumbar disc degeneration. Spine (Phila Pa 1976). 1999;24:2456-60.

[57] Noponen-Hietala N, Kyllonen E, Mannikko M, Ilkko E, Karppinen J, Ott J, et al. Sequence variations in the collagen IX and XI genes are associated with degenerative lumbar spinal stenosis. Annals of the rheumatic diseases. 2003;62:1208-14.

[58] Moore RJ. The vertebral end-plate: what do we know? Eur Spine J. 2000;9:92-6.

[59] Bibby SR, Urban JP. Effect of nutrient deprivation on the viability of intervertebral disc cells. Eur Spine J. 2004;13:695-701.

[60] Roberts S, Evans H, Trivedi J, Menage J. Histology and pathology of the human intervertebral disc. J Bone Joint Surg Am. 2006;88 Suppl 2:10-4.

[61] Hurri H, Karppinen J. Discogenic pain. Pain. 2004;112:225-8.

[62] Liebscher T, Haefeli M, Wuertz K, Nerlich AG, Boos N. Age-related variation in cell density of human lumbar intervertebral disc. Spine (Phila Pa 1976). 2011;36:153-9.

[63] Trout JJ, Buckwalter JA, Moore KC. Ultrastructure of the human intervertebral disc: II. Cells of the nucleus pulposus. Anat Rec. 1982;204:307-14.

[64] Hollander AP, Heathfield TF, Liu JJ, Pidoux I, Roughley PJ, Mort JS, et al. Enhanced denaturation of the alpha (II) chains of type-II collagen in normal adult human intervertebral discs compared with femoral articular cartilage. J Orthop Res. 1996;14:61-6.

[65] Oegema TR, Jr., Johnson SL, Aguiar DJ, Ogilvie JW. Fibronectin and its fragments increase with degeneration in the human intervertebral disc. Spine (Phila Pa 1976). 2000;25:2742-7.

[66] Oegema TR, Jr. Biochemistry of the intervertebral disc. Clinics in sports medicine. 1993;12:419-39.

[67] Sztrolovics R, Alini M, Roughley PJ, Mort JS. Aggrecan degradation in human intervertebral disc and articular cartilage. The Biochemical journal. 1997;326 (Pt 1):235-41.

[68] Cleaver O, Krieg PA. Notochord patterning of the endoderm. Dev Biol. 2001;234:1-12.

[69] Hunter CJ, Matyas JR, Duncan NA. The notochordal cell in the nucleus pulposus: A review in the context of tissue engineering. Tissue Eng. 2003;9:667-77.

[70] Goto S, Uhthoff HK. Notochord action on spinal development. A histologic and morphometric investigation. Acta Orthop Scand. 1986;57:85-90.

[71] Erwin WM, Ashman K, O'Donnel P, Inman RD. Nucleus pulposus notochord cells secrete connective tissue growth factor and up-regulate proteoglycan expression by intervertebral disc chondrocytes. Arthritis and Rheumatism. 2006;54:3859-67.

[72] Gruber HE, Hanley EN, Jr. Recent advances in disc cell biology. Spine (Phila Pa 1976). 2003;28:186-93.

[73] Hayes AJ, Benjamin M, Ralphs JR. Role of actin stress fibres in the development of the intervertebral disc: cytoskeletal control of extracellular matrix assembly. Dev Dyn. 1999;215:179-89.

[74] Gotz W, Kasper M, Fischer G, Herken R. Intermediate filament typing of the human embryonic and fetal notochord. Cell Tissue Res. 1995;280:455-62.

[75] Stosiek P, Kasper M, Karsten U. Expression of cytokeratin and vimentin in nucleus pulposus cells. Differentiation. 1988;39:78-81.

[76] Lehtonen E, Stefanovic V, Saraga-Babic M. Changes in the expression of intermediate filaments and desmoplakins during development of human notochord. Differentiation. 1995;59:43-9.

[77] Wolfe HJ, Putschar WG, Vickery AL. Role of the Notochord in Human Intervetebral Disk. I. Fetus and Infant. Clin Orthop Relat Res. 1965;39:205-12.

[78] Urban JP, McMullin JF. Swelling pressure of the lumbar intervertebral discs: influence of age, spinal level, composition, and degeneration. Spine (Phila Pa 1976). 1988;13:179-87.

[79] Iatridis JC, Setton LA, Weidenbaum M, Mow VC. Alterations in the mechanical behavior of the human lumbar nucleus pulposus with degeneration and aging. J Orthop Res. 1997;15:318-22.

[80] Hunter CJ, Matyas JR, Duncan NA. The functional significance of cell clusters in the notochordal nucleus pulposus: survival and signaling in the canine intervertebral disc. Spine (Phila Pa 1976). 2004;29:1099-104.

[81] Yang F, Leung VY, Luk KD, Chan D, Cheung KM. Injury-induced sequential transformation of notochordal nucleus pulposus to chondrogenic and fibrocartilaginous phenotype in the mouse. J Pathol. 2009;218:113-21.

[82] Hunter CJ, Matyas JR, Duncan NA. Cytomorphology of notochordal and chondrocytic cells from the nucleus pulposus: a species comparison. J Anat. 2004;205:357-62.

[83] Gilchrist CL. The Effects of Extracellular Matrix Mechanics and Composition on the Behaviors of Nucleus Pulposus Cells from the Intervertebral Disc: Duke University; 2009.

[84] Chen J, Yan W, Setton LA. Molecular phenotypes of notochordal cells purified from immature nucleus pulposus. Eur Spine J. 2006;15 Suppl 3:S303-11.

[85] Minogue BM, Richardson SM, Zeef LA, Freemont AJ, Hoyland JA. Transcriptional profiling of bovine intervertebral disc cells: implications for identification of normal and degenerate human intervertebral disc cell phenotypes. Arthritis Research & Therapy. 2010;12:R22.

[86] Fujita N, Miyamoto T, Imai J, Hosogane N, Suzuki T, Yagi M, et al. CD24 is expressed specifically in the nucleus pulposus of intervertebral discs. Biochem Biophys Res Commun. 2005;338:1890-6.

[87] Lee CR, Sakai D, Nakai T, Toyama K, Mochida J, Alini M, et al. A phenotypic comparison of intervertebral disc and articular cartilage cells in the rat. Eur Spine J. 2007;16:2174-85.

[88] Tang X, Jing L, Chen J. Changes in the molecular phenotype of nucleus pulposus cells with intervertebral disc aging. PloS one. 2012;7:e52020.

[89] Wang J, Markova D, Anderson DG, Zheng Z, Shapiro IM, Risbud MV. TNF-alpha and IL-1beta promote a disintegrin-like and metalloprotease with thrombospondin type I motif-5-mediated aggrecan degradation through syndecan-4 in intervertebral disc. J Biol Chem. 2011;286:39738-49.

[90] Gilson A, Dreger M, Urban JP. Differential expression level of cytokeratin 8 in cells of the bovine nucleus pulposus complicates the search for specific intervertebral disc cell markers. Arthritis Research & Therapy. 2010;12:R24.

[91] Weiler C, Nerlich AG, Schaaf R, Bachmeier BE, Wuertz K, Boos N. Immunohistochemical identification of notochordal markers in cells in the aging human lumbar intervertebral disc. Eur Spine J. 2010;19:1761-70.

[92] Sakai D, Nakai T, Mochida J, Alini M, Grad S. Differential phenotype of intervertebral disc cells: microarray and immunohistochemical analysis of canine nucleus pulposus and anulus fibrosus. Spine (Phila Pa 1976). 2009;34:1448-56.

[93] Rutges J, Creemers LB, Dhert W, Milz S, Sakai D, Mochida J, et al. Variations in gene and protein expression in human nucleus pulposus in comparison with annulus fibrosus and cartilage cells: potential associations with aging and degeneration. Osteoarthritis Cartilage. 2010;18:416-23.

[94] Li S, Duance VC, Blain EJ. Zonal variations in cytoskeletal element organization, mRNA and protein expression in the intervertebral disc. J Anat. 2008;213:725-32.

[95] Gilchrist CL, Francisco AT, Plopper GE, Chen J, Setton LA. Nucleus pulposus cell-matrix interactions with laminins. Eur Cell Mater. 2011;21:523-32.

[96] Nerlich AG, Schleicher ED, Boos N. 1997 Volvo Award winner in basic science studies. Immunohistologic markers for age-related changes of human lumbar intervertebral discs. Spine (Phila Pa 1976). 1997;22:2781-95.

[97] Mizuno H, Roy AK, Vacanti CA, Kojima K, Ueda M, Bonassar LJ. Tissue-engineered composites of anulus fibrosus and nucleus pulposus for intervertebral disc replacement. Spine (Phila Pa 1976). 2004;29:1290-7; discussion 7-8.

[98] Mizuno H, Roy AK, Zaporojan V, Vacanti CA, Ueda M, Bonassar LJ. Biomechanical and biochemical characterization of composite tissue-engineered intervertebral discs. Biomaterials. 2006;27:362-70.

[99] Bowles RD, Williams RM, Zipfel WR, Bonassar LJ. Self-assembly of aligned tissue-engineered annulus fibrosus and intervertebral disc composite via collagen gel contraction. Tissue Eng Part A. 2010;16:1339-48.

[100] Bowles RD, Gebhard HH, Hartl R, Bonassar LJ. Tissue-engineered intervertebral discs produce new matrix, maintain disc height, and restore biomechanical function to the rodent spine. Proceedings of the National Academy of Sciences of the United States of America. 2011;108:13106-11.

[101] Sakai D, Mochida J, Iwashina T, Watanabe T, Suyama K, Ando K, et al. Atelocollagen for culture of human nucleus pulposus cells forming nucleus pulposus-like tissue in vitro: influence on the proliferation and proteoglycan production of HNPSV-1 cells. Biomaterials. 2006;27:346-53.

[102] Chou AI, Akintoye SO, Nicoll SB. Photo-crosslinked alginate hydrogels support enhanced matrix accumulation by nucleus pulposus cells in vivo. Osteoarthritis Cartilage. 2009;17:1377-84.

[103] Gruber HE, Leslie K, Ingram J, Norton HJ, Hanley EN. Cell-based tissue engineering for the intervertebral disc: in vitro studies of human disc cell gene expression and matrix production within selected cell carriers. Spine J. 2004;4:44-55.

[104] Baer AE, Wang JY, Kraus VB, Setton LA. Collagen gene expression and mechanical properties of intervertebral disc cell-alginate cultures. J Orthop Res. 2001;19:2-10.

[105] Chiba K, Andersson GB, Masuda K, Thonar EJ. Metabolism of the extracellular matrix formed by intervertebral disc cells cultured in alginate. Spine (Phila Pa 1976). 1997;22:2885-93.

[106] Sun Y, Hurtig M, Pilliar RM, Grynpas M, Kandel RA. Characterization of nucleus pulposus-like tissue formed in vitro. J Orthop Res. 2001;19:1078-84.

[107] Yang SH, Wu CC, Shih TT, Chen PQ, Lin FH. Three-dimensional culture of human nucleus pulposus cells in fibrin clot: comparisons on cellular proliferation and matrix synthesis with cells in alginate. Artif Organs. 2008;32:70-3.

[108] Halloran DO, Grad S, Stoddart M, Dockery P, Alini M, Pandit AS. An injectable cross-linked scaffold for nucleus pulposus regeneration. Biomaterials. 2008;29:438-47.

[109] Sakai D, Mochida J, Iwashina T, Hiyama A, Omi H, Imai M, et al. Regenerative effects of transplanting mesenchymal stem cells embedded in atelocollagen to the degenerated intervertebral disc. Biomaterials. 2006;27:335-45.

[110] Reza AT, Nicoll SB. Characterization of novel photocrosslinked carboxymethylcellulose hydrogels for encapsulation of nucleus pulposus cells. Acta Biomater. 2010;6:179-86.

[111] Crevensten G, Walsh AJ, Ananthakrishnan D, Page P, Wahba GM, Lotz JC, et al. Intervertebral disc cell therapy for regeneration: mesenchymal stem cell implantation in rat intervertebral discs. Ann Biomed Eng. 2004;32:430-4.

[112] Nesti LJ, Li WJ, Shanti RM, Jiang YJ, Jackson W, Freedman BA, et al. Intervertebral disc tissue engineering using a novel hyaluronic acid-nanofibrous scaffold (HANFS) amalgam. Tissue Eng Part A. 2008;14:1527-37.

[113] Moss IL, Gordon L, Woodhouse KA, Whyne CM, Yee AJ. A Novel Thiol-Modified-Hyaluronan and Elastin-Like Polypetide Composite Material for Tissue Engineering of the Nucleus Pulposus of the Intervertebral Disc. Spine (Phila Pa 1976). 2010.

[114] Peroglio M, Grad S, Mortisen D, Sprecher CM, Illien-Junger S, Alini M, et al. Injectable thermoreversible hyaluronan-based hydrogels for nucleus pulposus cell encapsulation. Eur Spine J. 2012;21 Suppl 6:S839-49.

[115] Peroglio M, Eglin D, Benneker LM, Alini M, Grad S. Thermoreversible hyaluronan-based hydrogel supports in vitro and ex vivo disc-like differentiation of human mesenchymal stem cells. Spine J. 2013.

[116] Roughley P, Hoemann C, DesRosiers E, Mwale F, Antoniou J, Alini M. The potential of chitosan-based gels containing intervertebral disc cells for nucleus pulposus supplementation. Biomaterials. 2006;27:388-96.

[117] Richardson SM, Hughes N, Hunt JA, Freemont AJ, Hoyland JA. Human mesenchymal stem cell differentiation to NP-like cells in chitosan-glycerophosphate hydrogels. Biomaterials. 2008;29:85-93.

[118] Dang JM, Sun DD, Shin-Ya Y, Sieber AN, Kostuik JP, Leong KW. Temperature-responsive hydroxybutyl chitosan for the culture of mesenchymal stem cells and intervertebral disk cells. Biomaterials. 2006;27:406-18.

[119] Collin EC, Grad S, Zeugolis DI, Vinatier CS, Clouet JR, Guicheux JJ, et al. An injectable vehicle for nucleus pulposus cell-based therapy. Biomaterials. 2011.

[120] Alini M, Li W, Markovic P, Aebi M, Spiro RC, Roughley PJ. The potential and limitations of a cell-seeded collagen/hyaluronan scaffold to engineer an intervertebral disc-like matrix. Spine (Phila Pa 1976). 2003;28:446-54; discussion 53.

[121] Stern S, Lindenhayn K, Schultz O, Perka C. Cultivation of porcine cells from the nucleus pulposus in a fibrin/hyaluronic acid matrix. Acta Orthop Scand. 2000;71:496-502.

[122] Seguin CA, Grynpas MD, Pilliar RM, Waldman SD, Kandel RA. Tissue engineered nucleus pulposus tissue formed on a porous calcium polyphosphate substrate. Spine (Phila Pa 1976). 2004;29:1299-306; discussion 306-7.

[123] Saldanha KJ, Piper SL, Ainslie KM, Kim HT, Majumdar S. Magnetic resonance imaging of iron oxide labelled stem cells: applications to tissue engineering based regeneration of the intervertebral disc. Eur Cell Mater. 2008;16:17-25.

[124] Yang SH, Chen PQ, Chen YF, Lin FH. An in-vitro study on regeneration of human nucleus pulposus by using gelatin/chondroitin-6-sulfate/hyaluronan tri-copolymer scaffold. Artif Organs. 2005;29:806-14.

[125] Le Visage C, Yang SH, Kadakia L, Sieber AN, Kostuik JP, Leong KW. Small intestinal submucosa as a potential bioscaffold for intervertebral disc regeneration. Spine (Phila Pa 1976). 2006;31:2423-30; discussion 31.

[126] Mercuri JJ, Patnaik S, Dion G, Gill SS, Liao J, Simionescu DT. Regenerative potential of decellularized porcine nucleus pulposus hydrogel scaffolds: stem cell differentiation, matrix remodeling, and biocompatibility studies. Tissue Eng Part A. 2013;19:952-66.

[127] Mercuri JJ, Gill SS, Simionescu DT. Novel tissue-derived biomimetic scaffold for regenerating the human nucleus pulposus. J Biomed Mater Res A. 2011;96:422-35.

[128] Drury JL, Mooney DJ. Hydrogels for tissue engineering: scaffold design variables and applications. Biomaterials. 2003;24:4337-51.

[129] Vadala G, Sowa G, Hubert M, Gilbertson LG, Denaro V, Kang JD. Mesenchymal stem cells injection in degenerated intervertebral disc: cell leakage may induce osteophyte formation. Journal of tissue engineering and regenerative medicine. 2012;6:348-55.

[130] Ganey T, Libera J, Moos V, Alasevic O, Fritsch KG, Meisel HJ, et al. Disc chondrocyte transplantation in a canine model: a treatment for degenerated or damaged intervertebral disc. Spine (Phila Pa 1976). 2003;28:2609-20.

[131] Gruber HE, Johnson TL, Leslie K, Ingram JA, Martin D, Hoelscher G, et al. Autologous intervertebral disc cell implantation: a model using Psammomys obesus, the sand rat. Spine (Phila Pa 1976). 2002;27:1626-33.

[132] Sakai D, Mochida J, Yamamoto Y, Nomura T, Okuma M, Nishimura K, et al. Transplantation of mesenchymal stem cells embedded in Atelocollagen gel to the intervertebral disc: a potential therapeutic model for disc degeneration. Biomaterials. 2003;24:3531-41.

[133] Zhang YG, Guo X, Xu P, Kang LL, Li J. Bone mesenchymal stem cells transplanted into rabbit intervertebral discs can increase proteoglycans. Clin Orthop Relat Res. 2005:219-26.

[134] Miyamoto T, Muneta T, Tabuchi T, Matsumoto K, Saito H, Tsuji K, et al. Intradiscal transplantation of synovial mesenchymal stem cells prevents intervertebral disc degeneration through suppression of matrix metalloproteinase-related genes in nucleus pulposus cells in rabbits. Arthritis Research & Therapy. 2010;12:R206.

[135] Meisel HJ, Ganey T, Hutton WC, Libera J, Minkus Y, Alasevic O. Clinical experience in cell-based therapeutics: intervention and outcome. Eur Spine J. 2006;15 Suppl 3:S397-405.

[136] Bertram H, Kroeber M, Wang H, Unglaub F, Guehring T, Carstens C, et al. Matrix-assisted cell transfer for intervertebral disc cell therapy. Biochemical and biophysical research communications. 2005;331:1185-92.

[137] Omlor GW, Bertram H, Kleinschmidt K, Fischer J, Brohm K, Guehring T, et al. Methods to monitor distribution and metabolic activity of mesenchymal stem cells following in vivo injection into nucleotomized porcine intervertebral discs. Eur Spine J. 2010;19:601-12.

[138] Miner JH, Yurchenco PD. Laminin functions in tissue morphogenesis. Annu Rev Cell Dev Biol. 2004;20:255-84.

[139] Ekblom P, Lonai P, Talts JF. Expression and biological role of laminin-1. Matrix Biol. 2003;22:35-47.

[140] Nishiuchi R, Takagi J, Hayashi M, Ido H, Yagi Y, Sanzen N, et al. Ligand-binding specificities of laminin-binding integrins: a comprehensive survey of laminin-integrin interactions using recombinant alpha3beta1, alpha6beta1, alpha7beta1 and alpha6beta4 integrins. Matrix Biol. 2006;25:189-97.

[141] Lammerding J, Kazarov AR, Huang H, Lee RT, Hemler ME. Tetraspanin CD151 regulates alpha6beta1 integrin adhesion strengthening. Proc Natl Acad Sci U S A. 2003;100:7616-21.

[142] Suzuki N, Yokoyama F, Nomizu M. Functional sites in the laminin alpha chains. Connect Tissue Res. 2005;46:142-52.

[143] Kikkawa Y, Sanzen N, Fujiwara H, Sonnenberg A, Sekiguchi K. Integrin binding specificity of laminin-10/11: laminin-10/11 are recognized by alpha 3 beta 1, alpha 6 beta 1 and alpha 6 beta 4 integrins. Journal of cell science. 2000;113 (Pt 5):869-76.

[144] Cress AE, Rabinovitz I, Zhu W, Nagle RB. The alpha 6 beta 1 and alpha 6 beta 4 integrins in human prostate cancer progression. Cancer Metastasis Rev. 1995;14:219-28.

[145] Mercurio AM, Bachelder RE, Chung J, O'Connor KL, Rabinovitz I, Shaw LM, et al. Integrin laminin receptors and breast carcinoma progression. J Mammary Gland Biol Neoplasia. 2001;6:299-309.

[146] Chung J, Mercurio AM. Contributions of the alpha6 integrins to breast carcinoma survival and progression. Mol Cells. 2004;17:203-9.

[147] Jaeger RG, Scarabotto-Neto N, Azambuja N, Jr., Freitas VM. Secretion of collagen I and tenascin is modulated by laminin-111 in 3D culture of human adenoid cystic carcinoma cells. Int J Exp Pathol. 2008;89:98-105.

[148] Gu J, Fujibayashi A, Yamada KM, Sekiguchi K. Laminin-10/11 and fibronectin differentially prevent apoptosis induced by serum removal via phosphatidylinositol 3-kinase/Akt- and MEK1/ERK-dependent pathways. J Biol Chem. 2002;277:19922-8.

[149] Doi M, Thyboll J, Kortesmaa J, Jansson K, Iivanainen A, Parvardeh M, et al. Recombinant human laminin-10 (alpha5beta1gamma1). Production, purification, and migration-promoting activity on vascular endothelial cells. J Biol Chem. 2002;277:12741-8.

[150] Mruthyunjaya S, Manchanda R, Godbole R, Pujari R, Shiras A, Shastry P. Laminin-1 induces neurite outgrowth in human mesenchymal stem cells in serum/differentiation factors-free conditions through activation of FAK-MEK/ERK signaling pathways. Biochem Biophys Res Commun. 2010;391:43-8.

[151] Ma W, Tavakoli T, Derby E, Serebryakova Y, Rao MS, Mattson MP. Cell-extracellular matrix interactions regulate neural differentiation of human embryonic stem cells. BMC Dev Biol. 2008;8:90.

[152] Battista S, Guarnieri D, Borselli C, Zeppetelli S, Borzacchiello A, Mayol L, et al. The effect of matrix composition of 3D constructs on embryonic stem cell differentiation. Biomaterials. 2005;26:6194-207.

[153] Discher DE, Janmey P, Wang YL. Tissue cells feel and respond to the stiffness of their substrate. Science. 2005;310:1139-43.

[154] Engler AJ, Sen S, Sweeney HL, Discher DE. Matrix elasticity directs stem cell lineage specification. Cell. 2006;126:677-89.

[155] Pelham RJ, Jr., Wang Y. Cell locomotion and focal adhesions are regulated by substrate flexibility. Proc Natl Acad Sci U S A. 1997;94:13661-5.

[156] Veronese FM, Pasut G. PEGylation, successful approach to drug delivery. Drug Discov Today. 2005;10:1451-8.

[157] Langer R. New methods of drug delivery. Science. 1990;249:1527-33.

[158] Hubbell JA. Bioactive biomaterials. Curr Opin Biotechnol. 1999;10:123-9.

[159] Gonen-Wadmany M, Oss-Ronen L, Seliktar D. Protein-polymer conjugates for forming photopolymerizable biomimetic hydrogels for tissue engineering. Biomaterials. 2007;28:3876-86.

[160] Scott R, Marquardt L, Willits RK. Characterization of poly(ethylene glycol) gels with added collagen for neural tissue engineering. J Biomed Mater Res A. 2010;93:817-23.

[161] Almany L, Seliktar D. Biosynthetic hydrogel scaffolds made from fibrinogen and polyethylene glycol for 3D cell cultures. Biomaterials. 2005;26:2467-77.

[162] Marquardt L, Willits RK. Student award winner in the undergraduate's degree category for the Society for Biomaterials 35th Annual Meeting, Orlando, Florida, April 13-16, 2011. Neurite growth in PEG gels: effect of mechanical stiffness and laminin concentration. J Biomed Mater Res A. 2011;98:1-6.

[163] Seliktar D, Zisch AH, Lutolf MP, Wrana JL, Hubbell JA. MMP-2 sensitive, VEGF-bearing bioactive hydrogels for promotion of vascular healing. J Biomed Mater Res A. 2004;68:704-16.

[164] DeLong SA, Moon JJ, West JL. Covalently immobilized gradients of bFGF on hydrogel scaffolds for directed cell migration. Biomaterials. 2005;26:3227-34.

[165] Gobin AS, West JL. Effects of epidermal growth factor on fibroblast migration through biomimetic hydrogels. Biotechnology progress. 2003;19:1781-5.

[166] Mann BK, Schmedlen RH, West JL. Tethered-TGF-beta increases extracellular matrix production of vascular smooth muscle cells. Biomaterials. 2001;22:439-44.

[167] Shapira-Schweitzer K, Seliktar D. Matrix stiffness affects spontaneous contraction of cardiomyocytes cultured within a PEGylated fibrinogen biomaterial. Acta Biomater. 2007;3:33-41.

[168] Dikovsky D, Bianco-Peled H, Seliktar D. Defining the role of matrix compliance and proteolysis in three-dimensional cell spreading and remodeling. Biophys J. 2008;94:2914-25.

[169] Peyton SR, Kim PD, Ghajar CM, Seliktar D, Putnam AJ. The effects of matrix stiffness and RhoA on the phenotypic plasticity of smooth muscle cells in a 3-D biosynthetic hydrogel system. Biomaterials. 2008;29:2597-607.

[170] Habeeb AF. Chemical evaluation of conformational differences in native and chemically modified proteins. Biochim Biophys Acta. 1966;115:440-54.

[171] Chen J, Baer AE, Paik PY, Yan W, Setton LA. Matrix protein gene expression in intervertebral disc cells subjected to altered osmolarity. Biochem Biophys Res Commun. 2002;293:932-8.

[172] Estes BT, Diekman BO, Guilak F. Monolayer cell expansion conditions affect the chondrogenic potential of adipose-derived stem cells. Biotechnol Bioeng. 2008;99:986-95.

[173] Ferletta M, Kikkawa Y, Yu H, Talts JF, Durbeej M, Sonnenberg A, et al. Opposing roles of integrin alpha6Abeta1 and dystroglycan in laminin-mediated extracellular signal-regulated kinase activation. Mol Biol Cell. 2003;14:2088-103.

[174] Bullock J, Chowdhury S, Severdia A, Sweeney J, Johnston D, Pachla L. Comparison of results of various methods used to determine the extent of modification of methoxy polyethylene glycol 5000-modified bovine cupri-zinc superoxide dismutase. Analytical biochemistry. 1997;254:254-62.

[175] Veronese FM, Mero A. The impact of PEGylation on biological therapies. BioDrugs : clinical immunotherapeutics, biopharmaceuticals and gene therapy. 2008;22:315-29.

[176] Cruise GM, Scharp DS, Hubbell JA. Characterization of permeability and network structure of interfacially photopolymerized poly(ethylene glycol) diacrylate hydrogels. Biomaterials. 1998;19:1287-94.

[177] Yang X, Li X. Nucleus pulposus tissue engineering: a brief review. Eur Spine J. 2009;18:1564-72.

[178] Cloyd JM, Malhotra NR, Weng L, Chen W, Mauck RL, Elliott DM. Material properties in unconfined compression of human nucleus pulposus, injectable hyaluronic acid-based hydrogels and tissue engineering scaffolds. Eur Spine J. 2007;16:1892-8.

[179] Sakai D, Mochida J, Iwashina T, Watanabe T, Nakai T, Ando K, et al. Differentiation of mesenchymal stem cells transplanted to a rabbit degenerative disc model: potential and limitations for stem cell therapy in disc regeneration. Spine (Phila Pa 1976). 2005;30:2379-87.

[180] Kleinman HK, McGarvey ML, Liotta LA, Robey PG, Tryggvason K, Martin GR. Isolation and characterization of type IV procollagen, laminin, and heparan sulfate proteoglycan from the EHS sarcoma. Biochemistry. 1982;21:6188-93.

[181] Iatridis JC, Weidenbaum M, Setton LA, Mow VC. Is the nucleus pulposus a solid or a fluid? Mechanical behaviors of the nucleus pulposus of the human intervertebral disc. Spine (Phila Pa 1976). 1996;21:1174-84.

[182] Gruber HE, Hanley EN, Jr. Human disc cells in monolayer vs 3D culture: cell shape, division and matrix formation. BMC musculoskeletal disorders. 2000;1:1-11.

[183] Iatridis JC, Setton LA, Weidenbaum M, Mow VC. The viscoelastic behavior of the non-degenerate human lumbar nucleus pulposus in shear. Journal of biomechanics. 1997;30:1005-13.

[184] Bibby SR, Jones DA, Ripley RM, Urban JP. Metabolism of the intervertebral disc: effects of low levels of oxygen, glucose, and pH on rates of energy metabolism of bovine nucleus pulposus cells. Spine (Phila Pa 1976). 2005;30:487-96.

[185] Grunhagen T, Wilde G, Soukane DM, Shirazi-Adl SA, Urban JP. Nutrient supply and intervertebral disc metabolism. J Bone Joint Surg Am. 2006;88 Suppl 2:30-5.

[186] Holm S, Maroudas A, Urban JP, Selstam G, Nachemson A. Nutrition of the intervertebral disc: solute transport and metabolism. Connect Tissue Res. 1981;8:101-19.

[187] Nettles DL, Chilkoti A, Setton LA. Early metabolite levels predict long-term matrix accumulation for chondrocytes in elastin-like polypeptide biopolymer scaffolds. Tissue Eng Part A. 2009;15:2113-21.

[188] Leckie SK, Sowa GA, Bechara BP, Hartman RA, Coelho JP, Witt WT, et al. Injection of human umbilical tissue-derived cells into the nucleus pulposus alters the course of intervertebral disc degeneration in vivo. Spine J. 2013;13:263-72.

[189] Revell PA, Damien E, Di Silvio L, Gurav N, Longinotti C, Ambrosio L. Tissue engineered intervertebral disc repair in the pig using injectable polymers. Journal of materials science Materials in medicine. 2007;18:303-8.

[190] Cheng YH, Yang SH, Lin FH. Thermosensitive chitosan-gelatin-glycerol phosphate hydrogel as a controlled release system of ferulic acid for nucleus pulposus regeneration. Biomaterials. 2011;32:6953-61.

[191] Elbert DL, Pratt AB, Lutolf MP, Halstenberg S, Hubbell JA. Protein delivery from materials formed by self-selective conjugate addition reactions. Journal of Controlled Release. 2001;76:11-25.

[192] Pratt AB, Weber FE, Schmoekel HG, Muller R, Hubbell JA. Synthetic extracellular matrices for in situ tissue engineering. Biotechnol Bioeng. 2004;86:27-36.

[193] Salmon P, Trono D. Production and titration of lentiviral vectors. Current protocols in neuroscience / editorial board, Jacqueline N Crawley [et al]. 2006;Chapter 4:Unit 4 21.

[194] Allen KD, Adams SB, Jr., Mata BA, Shamji MF, Gouze E, Jing L, et al. Gait and behavior in an IL1beta-mediated model of rat knee arthritis and effects of an IL1 antagonist. J Orthop Res. 2011;29:694-703.

[195] Boyd LM, Carter AJ. Injectable biomaterials and vertebral endplate treatment for repair and regeneration of the intervertebral disc. Eur Spine J. 2006;15 Suppl 3:S414-21.

[196] Metters A, Hubbell J. Network formation and degradation behavior of hydrogels formed by Michael-type addition reactions. Biomacromolecules. 2005;6:290-301.

[197] Nettles DL, Haider MA, Chilkoti A, Setton LA. Neural network analysis identifies scaffold properties necessary for in vitro chondrogenesis in elastin-like polypeptide biopolymer scaffolds. Tissue Eng Part A. 2010;16:11-20.

[198] Nerurkar NL, Elliott DM, Mauck RL. Mechanics of oriented electrospun nanofibrous scaffolds for annulus fibrosus tissue engineering. J Orthop Res. 2007;25:1018-28.

[199] Chou AI, Nicoll SB. Characterization of photocrosslinked alginate hydrogels for nucleus pulposus cell encapsulation. J Biomed Mater Res A. 2009;91:187-94.

[200] Wang B, Wu Y, Shao Z, Yang S, Che B, Sun C, et al. Functionalized self-assembling peptide nanofiber hydrogel as a scaffold for rabbit nucleus pulposus cells. J Biomed Mater Res A. 2012;100:646-53.

[201] Bron JL, Helder MN, Meisel HJ, Van Royen BJ, Smit TH. Repair, regenerative and supportive therapies of the annulus fibrosus: achievements and challenges. Eur Spine J. 2009;18:301-13.

[202] Leo BM, Li X, Balian G, Anderson DG. In vivo bioluminescent imaging of virus-mediated gene transfer and transduced cell transplantation in the intervertebral disc. Spine (Phila Pa 1976). 2004;29:838-44.

[203] Troy T, Jekic-McMullen D, Sambucetti L, Rice B. Quantitative comparison of the sensitivity of detection of fluorescent and bioluminescent reporters in animal models. Molecular imaging. 2004;3:9-23.

[204] Weiler C, Nerlich AG, Zipperer J, Bachmeier BE, Boos N. 2002 SSE Award Competition in Basic Science: expression of major matrix metalloproteinases is associated with intervertebral disc degradation and resorption. Eur Spine J. 2002;11:308-20.

[205] Bryant SJ, Anseth KS. Controlling the spatial distribution of ECM components in degradable PEG hydrogels for tissue engineering cartilage. J Biomed Mater Res A. 2003;64:70-9.

Biography

Aubrey Therese Francisco was born on September 28, 1985 in Schenectady, NY to Therese and Donald Francisco. Aubrey received her Bachelor of Science degree in Bioengineering from the Department of Biomedical and Chemical Engineering at Syracuse University in May of 2007. As an undergraduate, Aubrey had the good fortune of being offered a research opportunity in the lab of Dr. Julie Hasenwinkel, who introduced her to the field of biomaterials and became a wonderful role model and mentor. Shortly after graduating from Syracuse University, Aubrey relocated to Durham, NC for her graduate studies. During her tenure at Duke, she received an Outstanding Teaching Assistant Award and was awarded honorable mention from the National Science Foundation Graduate Student Fellowship program. Her publications include:

Francisco AT, Hwang PY, Jeong CG, Chen J, Setton LA. Photopolymerizable laminin-functionalized poly(ethylene glycol) hydrogel for intervertebral disc regeneration. (Submitted to Acta Biomaterialia, August 2013).

Jeong CG, Francisco AT, Niu Z, Mancino RJ, Craig SL, Setton LA. Optimized design of hyaluronic acid (HA)-Poly(ethylene glycol) (PEG) composite hydrogels for intervertebral disc regeneration. (In preparation for submission to Acta Biomaterialia, September 2013).

Francisco AT, Mancino RJ, Bowles RD, Brunger JM, Tainter DM, Chen Y, Richardson WM, Guilak F, Setton LA. (2013) Injectable laminin-functionalized hydrogel for nucleus pulposus regeneration. Biomaterials, 34:7381-7388.

Gilchrist CL, Francisco AT, Plopper GE, Chen J, Setton LA. (2011) Nucleus pulposus cell-matrix interactions with laminins. European Cells and Materials Journal, 21:523-532.